

TESTEX Textile Instrument Ltd
Offers a wide range of textile testing equipment with european
quality and chinese price , please kindly contact us for more information.

Web : www.textileinstruments.net
Email : sales@textileinstruments.net

DEVELOPMENT OF AN IMPROVED FABRIC FLAMMABILITY TEST

by

Terry Stephen Fay

A Thesis

Submitted to the Faculty

of the

WORCESTER POLYTECHNIC INSTITUTE

in partial fulfillment of the requirements for the

Degree of Master of Science

in

Fire Protection Engineering

by

May 2002

APPROVED:

Dr. Jonathan R. Barnett, Advisor

Professor David A. Lucht, Director
Center for Firesaftey Studies

Abstract

The Navy Clothing and Textile Research Facility (NCTRF) has been conducting fabric research for many decades. This project is a joint effort in establishing new test methods for evaluating the thermal protection garments provide. As a result of this project a new full scale test facility was constructed and is now operational. In this facility, a new traversing manikin test has been developed and will hopefully become a recognized test standard in the future.

The traversing manikin test is designed to work with current test methods but also to provide a more detailed evaluation of a garment. Incorporated into the facility is the ability to reconfigure the fire source to recreate design fires that resemble those likely to occur onboard naval ships.

While the data gather thus far is limited, it is believed with future testing a large set of data will be available to allow a cross comparison of this test with established test methods.

Preface

I would like to thank my advisor Professor Jonathan Barnett, for introducing me to the field of Fire Protection Engineering and for helping to make this project possible. In addition I would like to thank my reader Professor John Woycheese for taking time to help me with this document.

I would like to thank Alden Research Labs for the help in construction of the test facility especially Dead White and Brian Pierce. In addition, I greatly appreciate the efforts of Bob Taylor and Jim Johnson at WPI for their knowledge and assistance with technical aspects of the construction. And a special thanks to Jay Ierardi for providing insight whenever I needed assistance. And of course, without the student volunteers who have assisted in the operation of the Fire Test Facility, we would not have been able to conduct any of the fire tests.

Table of Contents

1.0	INTRODUCTION & BACKGROUND.....	1
2.0	LITERATURE REVIEW	4
2.1	REVIEW OF CRITICAL TEST PARAMETERS FOR DETERMINING CLOTHING EXPOSURE.....	4
2.1.1	<i>Protective Clothing</i>	6
2.1.2	<i>Current Test Methods.....</i>	9
2.1.3	<i>Clothing Regulations.....</i>	17
2.1.4	<i>Summary of Current Test Standards.....</i>	19
2.2	TYPICAL FIRES EXPECTED ABOARD NAVAL VESSELS	27
2.2.1	<i>Spray/Jet Fires</i>	28
2.2.2	<i>Pool Fires.....</i>	30
2.2.3	<i>Cellulosic Fires.....</i>	34
3.0	METHODOLOGY	37
3.1	NEW LARGE-SCALE MANIKIN TEST.....	37
3.2	ROOM CONSTRUCTION	40
3.2.1	<i>The Square Sand Burner.....</i>	43
3.2.2	<i>Simplified Sprinkler Apparatus.....</i>	44
3.2.3	<i>Tracking System.....</i>	46
3.2.4	<i>Fuel Delivery System</i>	47
3.2.5	<i>Ventilation System.....</i>	49
3.2.6	<i>Gas Detection Systems</i>	50
3.2.7	<i>DAQ System.....</i>	51
3.3	ROOM INSTRUMENTATION.....	52
3.3.1	<i>Schmidt-Boelter Gage.....</i>	52
3.3.2	<i>Thermocouple Jack Panels and Extension.....</i>	52
3.3.3	<i>Thermocouple Arrays.....</i>	53
4.0	DATA ANALYSIS.....	55
4.1	ROOM CONFIGURATION.....	55
4.2	TEMPERATURE PROFILE	56
4.2.1	<i>Maximum – Vertical Left-Right.....</i>	56
4.2.2	<i>Maximum – Vertical (Front to Back).....</i>	59
4.2.3	<i>Maximum Temperature Plan View Profile.....</i>	64
4.2.4	<i>Maximum Temperature Plan View 3D Profile.....</i>	69
4.2.5	<i>Average Temperature Profile.....</i>	73
4.3	FLUX DATA ANALYSIS	75
5.0	CONCLUSIONS.....	79
6.0	REFERENCES	81
APPENDIX A - SAMPLE CALCULATIONS		84
	CONFIGURATION FACTORS	85
	JET/SPRAY FIRE CALCULATIONS	85
	POOL FIRE CALCULATIONS.....	87
	VELOCITY CALCULATIONS USING PITOT TUBE	92
APPENDIX B - DRAWINGS OF TRAVERSING MECHANISMS.....		93
	TRACKING SYSTEM.....	94
APPENDIX C – DIFFERENT BURNER CONFIGURATIONS		100
APPENDIX D – OPERATIONS AND SAFETY GUIDE		102

Table of Figures

FIGURE 2-1: HEAT FLUX EXPOSURES OF VARIOUS FIRE SCENARIOS.....	27
FIGURE 2-2: STEADY STATE HEAT FLUX EXPOSURES FROM JET/SPRAY FIRES	29
FIGURE 2-3: HEAT FLUX TO TARGETS VS. DISTANCE.....	30
FIGURE 2-4: LAYOUT OF THE POOL FIRE SCENARIO.....	31
FIGURE 2-5: HEAT FLUX EXPOSURES OF POOL FIRES.....	32
FIGURE 2-6: RADIATIVE HEAT FLUX TO VERTICAL PLANE 5.5 M FROM JP-4 POOL FIRE (kW/M²)	33
FIGURE 2-7: TARGET FLUX VS. FIRE DIAMETER	34
FIGURE 2-8: HEAT FLUX MEASUREMENTS OF BUNK FIRES	35
FIGURE 3-1: THE ASTM STANDARD TEST CHAMBER.....	37
FIGURE 3-2: NEW TEST CHAMBER ADDITIONS.....	39
FIGURE 3-3: HEAT FLUX VS HEIGHT	42
FIGURE 3-4: SQUARE BURNER HEAT FLUX VS. HEIGHT	43
FIGURE 3-5: DIAGRAM OF BURNER	44
FIGURE 3-6: TOP AND BOTTOM VIEW OF BURNER	44
FIGURE 3-7: (A) FUEL SHED (B) VAPORIZER.....	47
FIGURE 3-8: CONTROLS	47
FIGURE 3-9: THE VAPORIZER	48
FIGURE 3-10: UNION IN DUCTWORK.....	49
FIGURE 3-11: BLOWER.....	49
FIGURE 3-12: GAS DETECTOR	50
FIGURE 3-13: JACK PANEL.....	53
FIGURE 3-14: BARE BEAD THERMOCOUPLE	54
FIGURE 4-1: DIAGRAM OF THE HOLDEN TEST FACILITY	55
FIGURE 4-2: LOCATION OF THE BURNERS WITHIN THE ROOM	56
FIGURE 4-3: VERTICAL LEFT-RIGHT TEMPERATURE PROFILE SLICES	57
FIGURE 4-4: MAXIMUM TEMPERATURE PROFILE OF THE CENTER OF THE BURNER....	58
FIGURE 4-5: MAXIMUM TEMPERATURE PROFILE OF THE FRONT OF THE BURNER	58
FIGURE 4-6: MAXIMUM TEMPERATURE PROFILE OF THE BACK OF THE BURNERS	59

FIGURE 4-7: LOCATION OF THE TEMPERATURE PROFILE SLICES 60

**FIGURE 4-8: MAXIMUM VERTICAL FRONT TO BACK TEMPERATURE PROFILE – 0.86 M
(34 IN) FROM LEFT WALL 60**

**FIGURE 4-9: MAXIMUM VERTICAL FRONT TO BACK TEMPERATURE PROFILE – 0.97 M
(38 IN) FROM LEFT WALL 61**

**FIGURE 4-10: MAXIMUM VERTICAL FRONT TO BACK TEMPERATURE PROFILE – 1.07 M
(42 IN) FROM LEFT WALL 61**

**FIGURE 4-11: MAXIMUM VERTICAL FRONT TO BACK TEMPERATURE PROFILE – 1.17 M
(46 IN) FROM LEFT WALL 62**

**FIGURE 4-12: MAXIMUM VERTICAL FRONT TO BACK TEMPERATURE PROFILE – 1.27 M
(50 IN) FROM LEFT WALL 62**

**FIGURE 4-13: MAXIMUM VERTICAL FRONT TO BACK TEMPERATURE PROFILE – 1.37 M
(54 IN) FROM LEFT WALL 63**

**FIGURE 4-14: MAXIMUM VERTICAL FRONT TO BACK TEMPERATURE PROFILE – 1.47 M
(58 IN) LEFT WALL 63**

**FIGURE 4-15: MAXIMUM VERTICAL FRONT TO BACK TEMPERATURE PROFILE – 1.68 M
(66 IN) FROM LEFT WALL 64**

FIGURE 4-16: LOCATION OF THE TEMPERATURE PROFILE SLICES 64

**FIGURE 4-17: MAXIMUM HORIZONTAL TEMPERATURE PROFILE, 0.46 M (18 IN) ABOVE
THE FLOOR..... 65**

**FIGURE 4-18: MAXIMUM HORIZONTAL TEMPERATURE PROFILE, 0.76 M (30 IN) ABOVE
THE FLOOR..... 66**

**FIGURE 4-19: MAXIMUM HORIZONTAL TEMPERATURE PROFILE, 1.07 M (42 IN) ABOVE
THE FLOOR..... 66**

**FIGURE 4-20: MAXIMUM HORIZONTAL TEMPERATURE PROFILE, 1.37 M (54 IN) ABOVE
THE FLOOR..... 67**

**FIGURE 4-21: MAXIMUM HORIZONTAL TEMPERATURE PROFILE, 1.68 M (66 IN) ABOVE
THE FLOOR..... 67**

**FIGURE 4-22: MAXIMUM HORIZONTAL TEMPERATURE PROFILE, 1.98 M (78 IN) ABOVE
THE FLOOR..... 68**

**FIGURE 4-23: MAXIMUM HORIZONTAL TEMPERATURE PROFILE, 2.29 M (90 IN) ABOVE
THE FLOOR..... 68**

**FIGURE 4-24: MAXIMUM PLAN VIEW 3D-TEMPERATURE PROFILE, 0.46 M (18 IN)
ABOVE THE FLOOR 69**

**FIGURE 4-25: MAXIMUM PLAN VIEW 3D-TEMPERATURE PROFILE, 0.76 M (30 IN)
ABOVE THE FLOOR 70**

**FIGURE 4-26: MAXIMUM PLAN VIEW 3D-TEMPERATURE PROFILE, 1.07 M (42 IN)
ABOVE THE FLOOR 70**

FIGURE 4-27: MAXIMUM PLAN VIEW 3D-TEMPERATURE PROFILE, 1.37 M (54 IN) ABOVE THE FLOOR	71
FIGURE 4-28: MAXIMUM PLAN VIEW 3D-TEMPERATURE PROFILE, 1.68 M (66 IN) ABOVE THE FLOOR	71
FIGURE 4-29: MAXIMUM PLAN VIEW 3D-TEMPERATURE PROFILE, 1.98 M (78 IN) ABOVE THE FLOOR	72
FIGURE 4-30: MAXIMUM PLAN VIEW 3D-TEMPERATURE PROFILE, 2.29 M (90 IN) ABOVE THE FLOOR	72
FIGURE 4-31: AVERAGE TEMPERATURE PROFILE OF THE MIDDLE OF THE BURNERS..	73
FIGURE 4-32: TEMPERATURE PROFILE OF THE AVERAGE TAKEN FROM THE BACK OF THE BURNERS.....	74
FIGURE 4-33: TEMPERATURE PROFILE OF THE AVERAGE TAKEN FROM THE FRONT OF THE BURNERS.....	74
FIGURE 4-34: AVERAGE FLUX MEASUREMENTS COLLECTED WITH STANDARD DEVIATION AS ERROR BARS.....	76
FIGURE 4-35: FLUX AND TEMPERATURE MEASUREMENTS FOR TEST #21 (LOCATION 3)	77
FIGURE 4-36: FLUX AT MIDDLE OF BURNERS TAKEN ON NOVEMBER 27TH	78
FIGURE 4-37: FLUX AT MIDDLE OF BURNERS TAKEN ON NOVEMBER 27TH	78
FIGURE A-1: PREDICTED HEAT RELEASE RATE VS. POOL DIAMETER	89
FIGURE A-2: POOL FIRE MASS BURNING RATE PER UNIT SURFACE AREA	90
FIGURE A-3: POOL FIRE GROWTH TIME TO PEAK HEAT RELEASE RATE	91
FIGURE A-4: POOL FIRE FLAME HEIGHTS.....	91
FIGURE B-1: CARRIAGE MECHANISM FOR TRACK	97
FIGURE B-2: TRACK ILLUSTRATION.....	98
FIGURE B-3: CHAIN TIGHTENING MECHANISM.....	99
FIGURE C-1: DIFFERENT BURNER CONFIGURATIONS	101

Nomenclature

A_f	Surface Area of the Flame (m^2)
A	Area (m^2)
C_p	Specific Heat (kJ/kg-K)
d	Diameter (m)
ϵ	Emissivity (kW/m^2)
g	Gravitational Acceleration Constant ($9.81 m/sec^2$)
H	Height (m)
ΔH_c	Heat of Combustion (kJ/kg)
k	Effective Emission/Absorption Coefficient (m^{-1})
L	Mean Equivalent Beam Length of the Flame (m)
L_f	Flame Length (m)
m''	Mass Burning Rate per unit surface area ($kg/m^2\text{-sec}$)
m_∞''	Asymptotic Mass Burning Rate for large pool fires
\dot{m}	Mass Flow Rate (kg/sec)
Φ	Flame-Element Shape Factor Correction
\dot{Q}	Heat Release Rate (kW or MW)
\dot{Q}^*	non-dimensional Heat Release Rate
\dot{q}_{rad}''	Radiant Heat Flux to Target (kW/m^2)
σ	Stefan-Boltzmann Constant (kW/m^2K^4)
T_f	Flame Temperature (K)
T_a	Ambient Temperature (K)
T_∞	Temperature of Air at STP (K)
τ	Atmospheric Transmissivity
ρ	Fluid Density (kg/m^3)
p_{line}	Absolute Pressure (Pa)
p_{amb}	Ambient Pressure (Pa)
ρ_∞	Density of Air at STP (kg/m^3)
V_s	Volumetric Spill Rate (m^3/sec)
V	Velocity (m/sec)
χ_{ch}	Combustion Efficiency
y	Liquid Pool Fire Regression Rate (m/s)

Subscripts

rad	Radiative
ch	Chemical
f	Flame

1.0 Introduction & Background

The American Burn Association has published data based on the results of the National Health Interview Survey (NHIS) which estimated that over 1 million burn injuries occur per year. Of the burn victims admitted to a burn facility, 46% have a total body surface area (TBSA) burn of 10% or greater with approximately 3,700 resulting in death. [2] While these numbers are significantly less than the previous decade, they are still a concern.

The Navy Clothing and Textile Research Facility (NCTRF) is dedicated to reducing the burn incidents for navy personnel wearing navy clothing. Working with WPI, a project was established (DOD Contract #N00140-00-C-3591) to design and construct a new full scale test with the primary goal of evaluating navy clothing for protection against short duration fire exposures. The project can be broken into two main tasks. Task I is the research and review of ship fires and current test methods and Task II is the design and construction of a test facility.

The current test methods ASTM D 4108, Thermo Protective Performance of Materials for Clothing by Open Flame Method and ASTM F 1930 STM for Evaluation of Flame Resistant Clothing for Protection Against Flash Fire Simulations Using an Instrumented Manikin, uses a static mechanism for testing the clothing's level of protection. The new

design developed under Task II includes a dynamically moving manikin. This new approach provides a more accurate fire exposure to evaluate clothing response to fire.

This project initially began in 1996 with the research of ship fires to develop basic design fire scenarios. LeBlanc outlines three of the most likely scenarios: pool fires, jet/spray fires and cellulosic fire. [18] Based on an analysis of these scenarios the maximum thermal environment was determined to be $2.0 \text{ cal/cm}^2\text{-s}$ (84 kW/m^2). This was followed by the construction of a test facility at Alden Research Labs in Holden, Massachusetts. Full scale calibration tests were conducted to verify that the maximum thermal environment matched the design specification.

Chapter two summarizes the different test methods available for evaluating clothing which range from small scale fabric testing to a full scale garments test with an instrumented manikin. In addition this chapter also provides a detailed review of the thermal criteria selected for this project based on an analysis of several different fire scenarios.

Chapter three introduces the new test design. The water supply, ventilation system and fuel delivery system along with all the major equipment needed to run and operate this facility are described. The instrumentation used to record the data in the room is also outlined in this chapter along with the layout of the data acquisition (DAQ) equipment.

Chapter four presents the findings from this project and the data collected at this facility. The chapter ends with suggestions for future testing.

Chapter five is a final review of the project and summarizes the work completed. In addition a brief list of equipment which would enable more precise control of the test facility is outlined.

Finally the appendix contains a copy of the current Operations and Safety manual for the facility that gives instructions on how to safely operate the onsite equipment. In addition procedural checklists are included to aid in the operations of this equipment.

2.0 Literature Review

2.1 Review of Critical Test Parameters for Determining Clothing Exposure

Before any evaluation of current test methods are performed, it is important to understanding the different parameters needed to predict the level of protection a garment may provide in a fire scenario. The following section briefly covers the parameters used in this evaluation. Leblanc provides a more detailed discussion of these variables in his work. [18]

The critical test parameters for determining clothing exposure can be broken down into three groups: the duration of exposure, fire intensity and the type of heat transfer involved. The duration of exposure is a difficult variable to analyze since the behavior of people is difficult to predict. The time after which a fabric no longer needs to provide protection from a fire, is known as time to failure. Using this parameter instead of exposure time for a fabric is useful as the time to failure is a constant value for a given scenario while the exposure time can vary. Knowing the time to failure of a fabric in various scenarios allows for a good comparison of how different fabrics perform. In different fire scenarios, the time to failure can vary significantly. For example, a fabric may have a higher resistance to flame impingement than to radiant heat transfer and as such the time to failure would be greater in the test by flame impingement.

It is important to define the range of different fire scenarios to which a fabric or garment might be exposed. This range of fires can then be evaluated to determine a reasonable

fire configuration in which the garment's performance can be evaluated. Exposing a garment to a fire scenario that is beyond the range of plausible fire environments does not seem an appropriate use of resources, as the garment is being tested beyond its intended use.

Convective and radiative heat transfer also plays a significant role in evaluating a fabric's performance as these two methods of heat transfer are the most likely exposure to be faced from a fire. It is also plausible that a fire that cannot be seen could be significant enough to cause thermal exposure to an individual nearby or in an adjacent corridor. However, accurately predicting the modes of heat transfer from a fire to a target is difficult to accomplish as small changes in the orientation of clothing, type of fuel burning, or the ventilation in a room could have significant impact on the heat transfer [18].

Some other considerations which should be acknowledged in a comparative analysis includes the fit of the garment, dirt and moisture content, sweat concentration, and the fatigue of the fabric. These factors could have a significant impact on a test's results and thus care should be taken to make sure these factors are the same in a comparative analysis. Comparing a fabric that is soaking wet to one that is dry would provide inconsistent results.

2.1.1 Protective Clothing

All clothing apparel provides some level of protection from the rain, sun, and wind. To measure the level of protection against fire and extreme heat, several performance test methods are available which give a comparative analysis of a fabric's performance. This section examines the fabric test methods that are in use today, and compares their strengths and weaknesses.

2.1.1.1 Flame and Heat Resistance

Evaluating current test methods requires some distinctions to be made between different types of garments. It would not be appropriate to evaluate a fire fighter's turn out gear against a daily wear uniform, thus different classifications are used to describe a garment's level of protection. These classifications are: Primary, Secondary, and Tertiary concerns. These categories group garments by the fire scenarios they are likely to be exposed to.

Primary Concern

The greatest level of protection is demanded from garments worn by individuals who actively fight fires. The primary concerns for these garments are their response to both the fire itself and the heat flux from the fire. The temperatures in a compartment fire can be in the range of several hundred degrees Celsius with isolated and limited heat fluxes in the flames approaching 100 kW/m^2 . It is a common occurrence for a firefighter to be in these harsh fire conditions for a period of time greater than a few seconds. Therefore

garments that would fall into a primary concern must be able to maintain their protective properties longer than those garments which fall into a secondary concern category.

Secondary Concerns

This category of garments does not require the heavy heat and flame resistance that the firefighter's gear requires, but a high level of protection is still needed. Individuals who need this level of protection usually consist of uniformed professionals who work in an environment with a possible fire scenario.

The potentials for fire events during the jobs these people perform are greater than most average professionals. While these people would not face the same exposure to heat conditions as a firefighter, their clothing still needs to protect them from possible short fire exposures.

Tertiary Concerns

This level of concern accounts for garments with a basic level of flame resistance and the majority of garments worn by the average person falls into this category. This basic level is meant to provide some standard that would prevent an accidental encounter with a flame source that could be hazardous [17]. However, these garments should not be worn in a hazardous environment. All textiles should have this basic level of protection and any garment that does not meet this level should be considered unsafe.

2.1.1.2 Test Methods

Flammability test methods can be divided into two general subdivisions. Small-scale testing (or bench scale testing) involves using a small section of the garment while large-scale testing uses the entire garment in the test.

Small-Scale

Small-scale tests are performed on a bench top and are usually not very complicated. Fabric properties are the general concern in these tests. A small section of fabric is cut away from a large roll of fabric or a garment. Its behavior is considered to be an indication of the performance of the entire system. Small-scale tests are generally preferred since they are simplistic and inexpensive to run compared to their full-scale counterparts.

Large-scale

Large-scale testing is more complicated than the bench top tests and involve the use of the entire fabric system, or the whole garment. This type of testing generally provides a more detailed analysis of a fabric's performance, at a price greater than small-scale tests. This type of testing is advantageous because the entire system is tested instead of just a sample. The behavior of the garment depends upon the configuration as well as the materials in a fire scenario.

2.1.2 Current Test Methods

There are an assortment of clothing flammability and related tests. These test methods attempt to determine how flame-resistant, heat resistant, or injury-resistant a particular fabric and/or garment is. Below is brief summary of each test method to describe how a fabric or garment is tested.

2.1.2.1 Small-scale

Small-scale testing is the backbone of research, as it provides the most cost efficient method to compare different specimens amongst one another. However, protective clothing small-scale test methods provide only a limited analysis of a fabric's performance in a specific scenario; thus several different tests may be required to get a general understanding of a fabric's performance. This section contains a generalized summary of the available small-scale test methods.

The small-scale test methods for fabric flammability may be divided into two general categories based on the make up of the test. The first category of tests involves subjecting the sample of clothing to an ignition or pilot flame. The post-pilot time that the material burns and the char lengths are the usual results sought in these tests. The second category of tests involves subjecting the material to a known heat flux or temperature and measuring the heat flux or temperature on the opposite side of the material. Usually the heat flux or temperature measured is correlated to burn data to determine the extent of burns human skin might experience under the test conditions.

Flaming Exposure Test Methods

The first category of test methods may be referred to as flaming exposure test methods; typically a flame is impinged on the fabric and subsequent flame spread time is measured along with the total distance of charring. These methods are generally inexpensive and easy to run, leading to a high level of repeatability that adds to their advantages. Generally, the test setups are simple and the apparatuses are easily attainable.

2.1.2.1.1 CFR 16 Part 1610

In this standard, “Standard for the Flammability of Clothing Textiles”, a 2 in by 6 in (50 mm by 150 mm) sample of cloth, mounted at a 45° angle, is exposed to a butane flame for one second. The time that the flame propagates 5 in (127 mm) is recorded. If that time is less than 4 seconds, it fails. [3, 11] This standard was designed to prevent serious burn injuries by restricting the textiles used in clothing manufacturing. [17]

2.1.2.1.2 CFR 16 Parts 1615 and 1616

The “Standard for Flammability of Children’s Sleepwear” is meant to protect children and is therefore more stringent than CFR 1610. A conditioned specimen 3.5 in by 10 in (8.9 mm by 254 mm) is suspended vertically in a closed container; a small burner is located beneath the suspended garment and is supplied with at least 97% pure methane. Once the specimen is in place within the test apparatus, the burner is ignited and placed so that the flame impinges on the bottom edge of the specimen for 3 ± 0.2 seconds. The subsequent flaming period after the burner is turned off is measured, to the nearest

second. Also, the char length is measured. The garment fails the test if the flaming period lasts more than 10 seconds and/or the char length is 7 in (17.8 cm) or greater. [15]

2.1.2.1.3 ASTM D 1230-94

This test method, “Standard Test Method for the Flammability of Clothing Textiles” is similar to CFR 1610. A sample is mounted inside of a chamber at a 45° angle and subjected to a pilot flame. After the pilot flame is extinguished, the time it takes for the flame to spread 5 inches is recorded.

2.1.2.1.4 ASTM F 1358-95

“Standard Test Method for Effects of Flame Impingement on Materials Used in Protective Clothing Not Designed Primarily for Flame Resistance” is a test method developed to measure the ease of ignition and the burning behavior. In this method, a conditioned specimen is folded over a holder with the fabric surface suspended over a gas flame and is then exposed to a standardized flame for a period of 3 seconds. If ignition does not occur, the sample is exposed for an additional 12 seconds. After the exposure, the post-pilot burning time, afterglow time and burn distance are measured and recorded. Observations of the burning behavior are also recorded. [6]

2.1.2.1.5 FTMS 5903.1

Federal Test Method 5903.1, “Standard Test Method for Flame Resistance of Cloth; Vertical” is very similar to ASTM F 1358-95, except that the sample is in a vertical position within the cabinet and the exposure time to a methane flame is 12 seconds. After the exposure, the post-pilot burning time, afterglow and the length of char are measured and recorded. [18]

2.1.2.1.6 NFPA 701

“Standard Test Method of Fire Tests for Flame-Resistant Textiles and Films” is divided into two tests, test 1 is for textiles and test 2 is for films or fabrics with a density greater than 21 oz/yd² (700 g/m²). The fabrics are tested inside of a test chamber by a flame that is at least 97% methane. Test 1 consists of taking a weighted specimen that is 5.90 in x 15.75 in (150 mm x 400 mm) in size. The specimen is hung vertically over a flame and exposed to a standardized gas flame with a height of 4 in (100 mm), for a period of 45 seconds. The flame is withdrawn and the after burn time is recorded. Upon self-extinguishment, the specimen is weighed and compared with the initial weight to calculate a percentage of weight loss. Also an observation of the specimen’s burning behavior is recorded.

Test 2 consists of taking a weighted specimen that is 47.25 in (1.2 m) in length and exposing it to a gas flame of 280 mm ± 12 mm in height for a period of 2 minutes. Observations of flaming combustion, after-burn, and afterglow times are recorded. [21]

These test methods expose the sample to an open flame in an attempt to ignite the fabric. The reactions of the sample material is then measured and noted. The measurements are made with relatively crude instruments such as, stopwatches, rulers, and scales. Comparison of fabric performance in the specified fire scenario can be made; however no analysis can be done to determine how a garment constructed from the test fabric will perform.

Thermal Exposure Test Methods

In the thermal exposure tests, a heat source is used to measure the thermal properties of the material rather than applying a flame to the material and allowing the material to ignite. These tests tend to be more expensive and more involved than the flaming exposure tests.

The current thermal exposure test methods incorporate a copper slug calorimeter as a heat flux-measuring device. Four J-type thermocouples are connected to a 1.57 in (40 mm) diameter copper disk sunken into an insulating material so that the faces of each are completely flush. Knowing the average temperature rise of the thermocouples along with the time-change, the thermal properties of copper and the area, the heat flux may be calculated [4]. This heat flux is used to predict if a second-degree burn would have occurred. This is done by using tables providing correlations between second-degree skin burn data and heat flux [4]. The difference between these thermal exposure tests lies in the heat source.

2.1.2.1.7 ASTM D 4108-87

The “Standard Test Method for Thermal Protective Performance of Materials for Clothing by Open-Flame Method” uses an open flame to supply $2.0 \text{ cal/cm}^2\text{-s}$ (84 kW/m^2) to the sample in a static, faced-down position. The temperature and the time are then recorded. This test method incorporates mainly convective heat transfer along with some radiation to the material tested from the source flame. [1, 9]

2.1.2.1.8 ASTM F 1060-87

The “Standard Test Method for Thermal Protective Performance of Materials for Protective Clothing for Hot Surface Contact”, also known as the TPP test, measures the performance of insulating materials in contact with a hot surface based on human tissue response as simulated by a copper calorimeter, to the conducted heat. Each material is measured under a contact pressure of 0.5 psi (3 kPa). A 4 inch by 6 inch (100 mm by $150 \pm \text{ mm}$) specimen is sandwiched between a hot plate capable of maintaining $600 \text{ }^\circ\text{F}$ ($300 \text{ }^\circ\text{C}$) and a copper calorimeter/steel block assembly supplying the pressure and recording the measurements. Although this test method does not incorporate a flame, it is important for fire testing purposes, as the evaluation of the thermal protection is an important parameter in determining the level of protection provided by a garment [5].

2.1.2.1.9 Radiative Protection Performance Test Method

The “Radiative Protection Performance” (RPP) test method uses a quartz lamp to provide a heat flux of $0.5 \text{ cal/cm}^2\text{-s}$ (21 kW/m^2) to the sample. Unlike the TPP test methods, the

RPP test method places the sample in a horizontal fashion. This test method is designed to prevent flame impingement and thus evaluates only the radiative portion of the heat source. [22, 23]

All three thermal exposure test methods create a heat transfer network to test for thermal properties of the sample material. The copper calorimeter is described in the standards; however any number of sensors may be used. Unlike the flaming exposure tests, the thermal exposure tests usually require data acquisition systems and can correlate the heat flux data to an equivalent burn on human skin tissue.

2.1.2.2 Large-scale

Currently the large-scale test method for clothing flammability uses a fully dressed manikin to represent a person. This manikin is then subjected to a fire environment and an evaluation of the entire garment assembly is made rather than just a small sample of textiles from the small-scale test methods.

2.1.2.2.1 Instrumented Manikin Tests

The instrumented manikin test was developed for garment testing in the 1960's. [18] Typically, the manikin is subjected to a flash fire scenario where eight jets of fire, in four corners of a small room, engulf the manikin for anywhere from 2.5 to 10 seconds at a time. The surrounding eight propane jets expose the manikin to a heat flux of 2.0

cal/cm²-s (84 kW/m²). [10] This type of instrumented manikin test has been developed into the standard ASTM 1930.

The standard outlines the distribution of 100 instruments to measure the heat flux. Typically, the temperature is measured at these 100 positions by thermocouples and recorded using a data acquisition system. [7] Knowing the temperature rise of the thermocouple, the elapsed time, and the thermal inertia of the thermocouple bead, the heat flux may be determined. The relationship between the temperature and the heat flux is given as [18]:

$$q = \frac{T - T_{in}}{2\sqrt{t}} (\pi k \rho c)^{1/2} \quad (2-1)$$

Where

- T – is the temperature (K)
- T_{in} – is the initial temperature (K)
- q – is the heat flux (W/m²)
- t – is the time elapse (s)
- $k\rho c$ – is the thermal inertia of the thermocouple (J²/m⁴-K²-s)

The temperature data is transformed into energy data. This energy data is then used to determine the extent of burn injuries that would occur. [12]

The important feature of this test method is that the garment is tested, as a human would wear it. The thermal small-scale tests use a copper slug calorimeter sensor that represents human skin, but this cannot provide an overall account of how the garment performs. A detailed map of a person may be generated after a large-scale test showing the degree of

the burn faced by each section of the body using the correlated data for second-degree skin burns.

The Navy Clothing and Textile Research Facility (NCTRF) has modified the instrumented manikin by placing the manikin on a boom and dynamically moving the manikin through a fire. This modification is called a Manikin Pit Test. [8] The thermal exposure is an n-heptane pool fire that is capable of up to $2.0 \text{ cal/cm}^2\text{-s}$ (84 kW/m^2). The manikin is first lowered and moved to an initial exposure to the fire and is then moved through the fire and away from the fire in a certain amount of time to better simulate the exposure one might face aboard a vessel. It is important to note that this modification is not considered a standard, and there is only limited documentation on this test method.

2.1.3 Clothing Regulations

Clothing regulations exist that tie these test methods together. These regulations are for firefighter clothing, both turnout gear and office-wear. In order to be approved by these regulations garments must pass certain flammability tests. The following clothing standards were developed by the National Fire Protection Association. These guides and standards serve as models for local government regulations.

2.1.3.1 NFPA 1971

NFPA Standard number 1971 provides a test procedure for testing protective ensembles for the structural firefighter, a primary concern garment [24]. Structural fire fighting is

described as “the activities of rescue, fire suppression, and property conservation in buildings, enclosed structures, vehicles, marine vessels, or like properties that are involved in a fire emergency situation”. [24] This standard calls for both the FTMS method 5903.1 test and the TPP open flame test method along with other flame resistance testing with boots, helmets, and gloves in mind. In order for structural fire fighting clothing to meet this guide, the clothing must pass all of the bench scale testing. [24]

2.1.3.2 NFPA 1975

NFPA 1975 provides a test procedure for the station/work uniforms for firefighters, a secondary concern garment.[25] Since the office uniform of a firefighter does not need to protect against fire as much as the turnout gear in actual firefighting, the regulations are more relaxed in terms of flame resistance. This guide requires the clothing only to pass the FTMS method 5903.1 test to be suitable in this standard. [25]

2.1.3.3 NFPA 1976

NFPA 1976 provides test procedure for the protective clothing for proximity fire fighting. [22] Proximity fire fighting builds off of structural fire fighting to include fires that include extremely high levels of conductive, convective, and radiative heat. Such fires include aircraft fire, bulk flammable gas fires, and bulk flammable liquid fires. This guide requires the clothing to pass the RPP test in order to meet the regulation. [22]

2.1.3.4 NFPA 1977

NFPA 1977 provides test procedure for the protective clothing and equipment for wildland fire fighting. [23] Wildland fire fighting is essentially forest fire-fighting. As with NFPA 1976, this guide requires the clothing to pass the RPP test in order to meet the regulation. Also, the clothing must pass the FTMS methods 5903.1 to meet this regulation. [23]

These clothing regulations along with government standards like CFR 16 Parts 1610, 1615, and 1616 protect the consumer from fire injury. These regulations address the fabrics that could be hazardous in a fire scenario and provide test procedures that can be used to validate a fabric's level of safety. A test method can determine the level of safety in an article of clothing, however the government standards make meeting those criteria a law.

2.1.4 Summary of Current Test Standards

The scope of all possible fire scenarios is too broad to warrant a comparative analysis of a fabric performance thus the range of possible fires was confined to those mostly likely to occur on a navy vessel. Pool fire and spray fires are the most plausible shipboard fires thus these are primary concern for evaluating a test protocol.

The small-scale test methods, the flaming exposure test methods and the thermal exposure test methods, were found to lack in their ability to accurately model the heat flux distribution from a real fire. Since the primary mode of failure for a garment while

its ability to prevent convective and radiative heat transfer to the wearer of the garment, these small-scale tests cannot be used to accurately describe the level of protection a garment can provide. These tests can be used to evaluate the ease of ignition of a fabric under a given test condition. The use of several small-scale tests can also be used to determine the level of flammability and as part of the methodology in determining a garments level of protection.

The thermal exposure test methods are more telling of how an article of clothing might behave in a fire environment, than the flaming exposure test methods. These methods attempt to determine if an article of clothing will allow a second-degree burn or not. Care has to be taken into account when performing these tests as air-gaps have the potential to change the results. Perhaps a standard needs to be developed to test loose clothing, but with the current test methods, air-gaps cannot exist. The conductive TPP (ASTM F1060-87) test also needs some further examination into the effects of pressure on burn data. A study should be conducted on the differences between copper slug calorimeters and calorimeters that more closely simulate human skin. Also further research is needed into the topic of skin burns.

The most drastic change is needed in the instrumented manikin large-scale test method. Instead of positing the manikin in a fully engulfing fire, the manikin should move through the fire environment to simulate a person running through the fire scenario. The Navy's Manikin Pit Test needs to be evaluated further so that the new methods used can be critiqued.

2.1.4.1 Shortcomings of the Current Test Methods

The test methods mention above, do not provide real fire scenarios and as such the results need to be evaluated before data can be obtained. The characteristics of burning human skin can vary with temperature, heat flux, and blood flow. With these limitations, only best fit approximation curves are available for determining the response of skin tissue to applied heat fluxes. [28] For this reason, these test methods have an inherent error that must be considered in any fabric or garment analysis.

2.1.4.1.1 Small-scale Tests

Small-scale testing is important in assessing the level of protection provided by fabrics as it offers an inexpensive means of fabric testing. However the drawback of these small scale tests is that the level of protection offered by a garment constructed from these fabrics cannot be determined. The results from these small-scale tests can only be used to evaluate the performance of fabrics in the tested fire scenario and no application to a real fire can be accurately extrapolated. Also the construction of the testing apparatus and the orientations of the test fabrics are not indicative of the normal application of the fabrics. In each of these small-scale tests, the material is tested in a static, dry fashion and the test is not an accurate depiction of a real fire scenario. Both the fatigue of movement and the amount of perspiration in a garment can affect the performance of the garment and these factors are not accounted for these small-scale fabric tests. [27]

However, these small-scale can be used as part of a methodology in determining a garments level of protection.

Since the performance of a garment cannot be directly extrapolated from the information obtained from these tests, it is difficult to determine which of the parameters of clothing exposure can be accurately determined. In the case of direct exposure to a flame, the ease of ignition can be determined for the fabrics, however a more likely scenario would be the radiative and convective penetration of the garment, which could result in severe burns of the wearer of the garment.

2.1.4.1.2 Flaming Exposure Test Methods

The flaming exposure test methods are the easiest and simplest test methods available. However, they only provide a limited amount of data. These tests expose a sample of a textile to a flame and allow the material to burn. The results from these test methods provide information that has limited applicability to fire scenarios other than the test environment. This data can only be used to compare a fabric response with another fabric in the same exact conditions. Any change in the fire scenario would require retesting of all fabrics involved. [18] With such a limited scope of applicability, the results of these tests can not be used to predict the performance of the garment in a real fire situation.

An example of these tests limited applicability could be a wire-mesh outfit. The wire-mesh could pass each of the flaming exposure test methods, yet in a real fire the person would face considerable injuries because the garment offered no protection from the heat transfer of the fire.

Essentially, these test methods predict the performance of clothing in an unrealistic fire scenario. The results of these tests cannot be used alone to accurately predict the level of protection a garment can provide. These test methods are based on an idea that clothing should hinder the spread of fire, not protect the wearer from the heat of a nearby fire. These test methods may be used to test how easily an article of clothing ignites and perhaps some flame spread properties, but the effects on a person wearing a garment constructed of these fabrics can not be determined from the data obtained.

2.1.4.1.3 Thermal Exposure Test Methods

The thermal exposure test methods, unlike the flaming exposure test methods provide a more detailed account of fabric performance in a fire scenario. These test methods predict the amount of heat the person would feel and thus give some level of performance in a fire event. However, it is important to know that an air gap can have a significant role in the heat transfer circuit of these test methods. If the material is not properly attached to the copper slug calorimeter, then some bunching of the material can result, and within the bunches exists the air-gaps. [27, 28] Also, the material may be attached to the calorimeter in such a manner to simulate loose clothing; this too could play a significant role in the heat transfer circuit. [18]

Another problem with the thermal exposure test methods lies with the copper slug calorimeter. The calorimeter has been in existence for a long time and is generally considered the benchmark in heat flux sensors for clothing. [9] However, testing can be

slowed because the calorimeter needs to cool between testing. [9] The copper calorimeters also lacks durability and can frequently break. Other sensors exist, however most are not durable, and only the water-cooled sensors can be used successively without cooling between tests. [9] Another shortcoming of the copper slug calorimeters is its dissimilarities to skin. [28] Skin is a complex medium with multiple layers unlike the rigid copper. It is not known how a sensor closer to that of human skin in material properties, would change results of these tests. [28]

The copper slug calorimeter correlates skin burns to energy, heat flux times time. [28] Each of the three thermal exposure test methods use a table to determine burn severity based on total heat. The severity of the burn is based on Stoll's data, which was measured with respect to skin temperature. [1, 4, 5, 22, 23] The copper or other material is not at the same temperature for a given heat flux as human skin, the temperature findings from the correlations for skin temperature were translated into energy data and is then compared to the energy received by the sensor. According to Wieczorek, this method is not suggested and can have erroneous results. [28] This data does not consider heating effects after the exposure. [8] Whether this is an accurate method or not is not known, therefore this technique could produce erroneous results.

Large-scale Tests

The current instrumented manikin test method involves a fully dressed manikin placed within a small enclosure with eight propane torches surrounding it. The torches are

activated and more than 100 sensors on the inside of the clothing measure the internal heat flux.

The problems that exist with this test method begin with the sensor issues. The heat flux sensors range from temperature sensitive tape [8] to complex water-cooled sensors, [9] but the sensors are used to measure heat flux and then correlate that to the burn data. [7] Research has been conducted on the how temperature affects skin burn; however, there has not been any significant research on skin burns cause from a heat flux. Thus the heat flux to the skin needs to be correlated to a temperature on the skin and a comparable burn is found using skin burn table. This calculation is used to predict skin burn based on heat flux. This approach of correlated heat flux data to skin burn data has not been proven accurate. [28]

It is apparent that a single test scenario cannot be used to develop an accurate description of a garment performance in any fire scenario. In order to develop a decent description of a garment performance in a given scenario, that scenario must be recreated in the test environment.

Another shortcoming of this test procedure is the environment to which the manikin is faced. The manikin is subjected to four banks of flames, impinging on the clothing, from all sides. A more realistic scenario is needed where the manikin is upright and moving through a fire environment. The clothing fatigue and the movement of the manikin would closer resemble a real fire scenario. The Navy's Manikin test moved the manikin through

the fire, but the actual movements are not documented, and therefore the specifics of the test cannot be critiqued.

2.2 Typical Fires Expected Aboard Naval Vessels

The following section is a synopsis of the plausible fire scenarios expected onboard navy vessels and describes the heat flux associated with these types of fire scenarios. This section is based on the work by LeBlanc [18]. Three basic types of fire scenarios were selected: jet/spray fires, pool fires, and cellulosic fires (the primary type of material that furniture items such as bunks, tables, and chairs are made from). The fires described are representatives of typical fires on board ships. The heat flux curves for these scenarios are shown in Figure 2-1 below. [18]

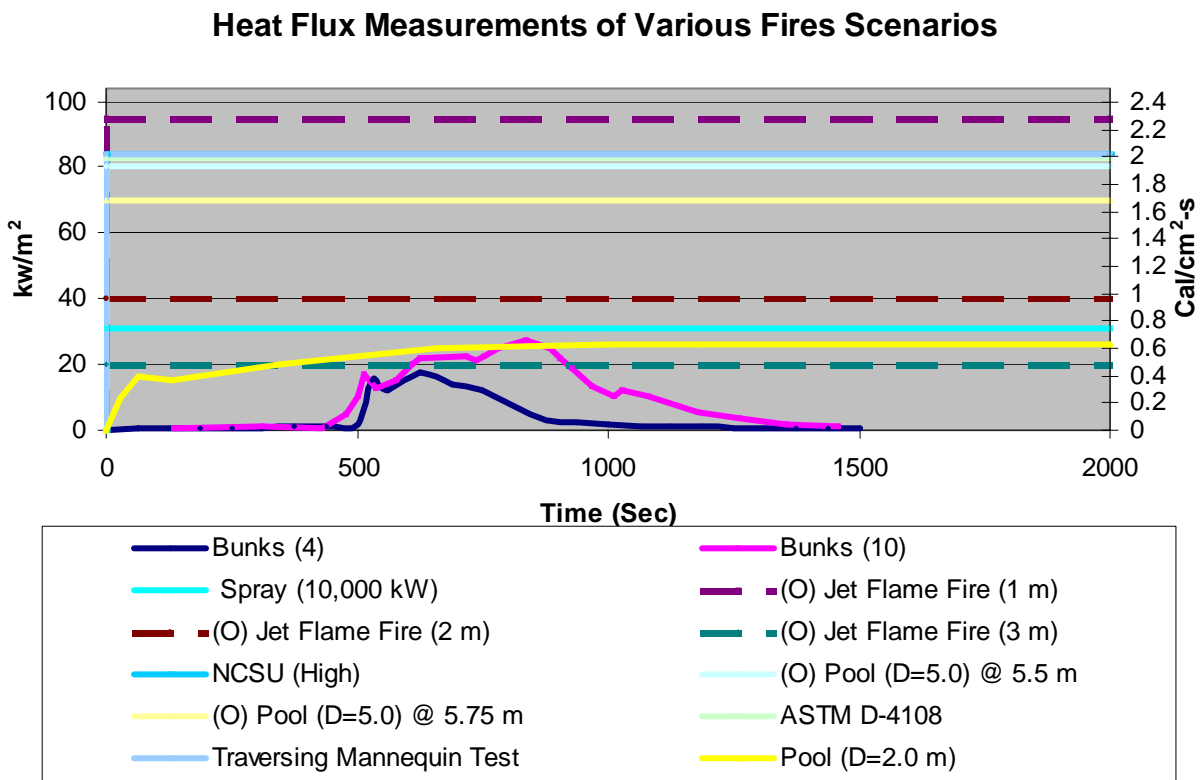


Figure 2-1: Heat Flux Exposures of various Fire Scenarios

2.2.1 Spray/Jet Fires

The spray fire scenarios evaluated are divided into two categories. The first is a fire occurring in an open area, such that the effect of a compartment can be ignored. The second type of fire occurs in smaller compartments, where the compartment effects must be taken into account. Spray fires are likely to occur where high-pressure lines are located such as on a deck or in an engine room. The most likely occurrence is due to failure of a hydraulic oil line, which can occur in either an open area or within an enclosed compartment.

The heat flux from fires in an open space is expected to range from $0.4 \text{ cal/cm}^2\text{-s}$ (20 kW/m^2) to over $2.2 \text{ cal/cm}^2\text{-s}$ (95 kW/m^2). For fires within a compartment, the heat flux is expected to be about $0.8 \text{ cal/cm}^2\text{-s}$ (35 kW/m^2). Figure 2-2 graphs heat flux versus time for these steady state fire exposures. This steady state approximation is a conservative scenario, since the heat release rate decays as the pressure within a hydraulic line decreases over time. [18]

Heat Flux Measurements of Jet/Spray Fires

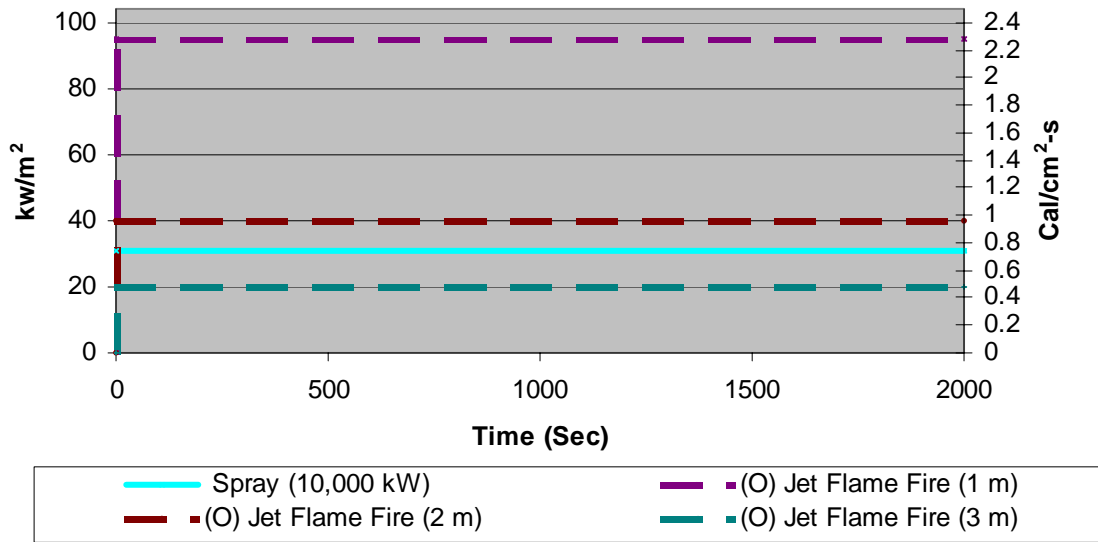


Figure 2-2: Steady State Heat Flux Exposures From Jet/Spray Fires

2.2.1.1 The Spray Fire in an Open Area

The fire scenario investigated is a 5 cm (1.95 in) rupture in a standard hydraulic oil hose at a pressure of 7000 kPa (1015 psi). The heat release rate is approximately 30 MW. The primary focus of this investigation is to predict the heat flux from the fire to a target (person) at a variable distance from the source. Figure 2-3 compares the heat flux to a target vs. the distance from the fire source. For distances less than 0.5 meters, the target is located within the fire and thus direct impingement by the flame occurs and the convective heat transfer by the flame becomes an important issue. At a distance less than 0.5 meters, the heat flux is greater than 200 kW/m² (4.76 cal/cm²-s) and the probability of survival for such an exposure is not likely. The heat flux measurements at 1, 2, and 3

meters from the centerline of the fire, plotted in Figure 2-3, show a plausible range of exposures one faces when encountering such fires.

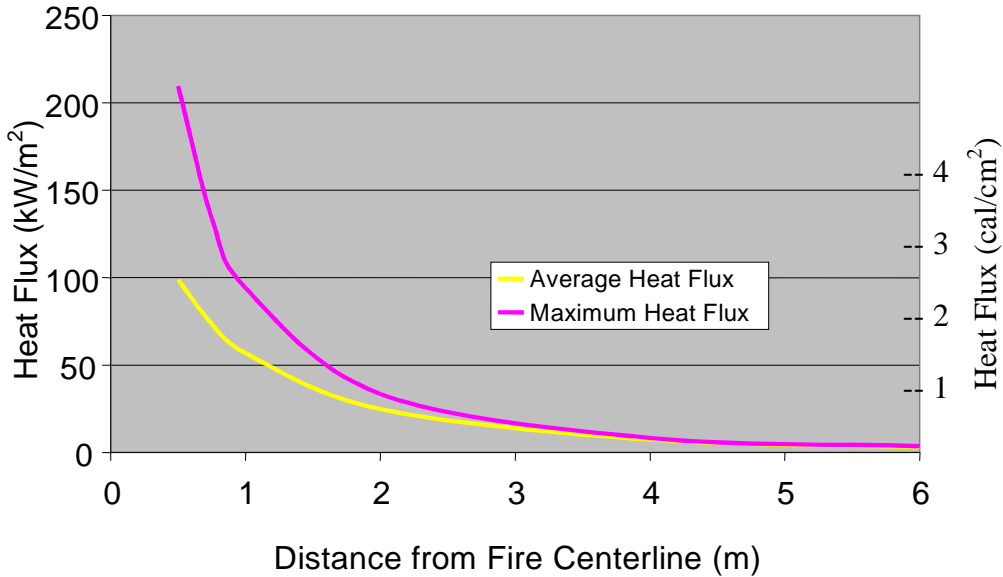


Figure 2-3: Heat Flux to Targets vs. Distance

2.2.1.2 The Spray Fire within a Compartment

To investigate the effect within a compartment, a standard hydraulic oil spray fire with a constant heat release rate of 10, MW (2390 kg-cal/sec) was studied to determine the heat flux generated. This is an arbitrary value, in terms of the pipe diameter and pressure, as several combinations of these variables could produce the given heat release rate. The heat flux from this scenario is plotted in Figure 2-1 and Figure 2-2.

2.2.2 Pool Fires

Pool fires are classified as either unconfined or confined. It is assumed that unconfined pool fires occur in large open areas (where the compartment effects can be neglected). If

an unconfined fire did occur within a compartment, the heat flux within the compartment would be too large for survival. Only confined fires will be evaluated within compartments.

The heat flux is calculated to a vertical target located a given distance from the centerline of the pool fire. Figure 2-4, illustrates the layout of the target and the pool fire used for these calculations.

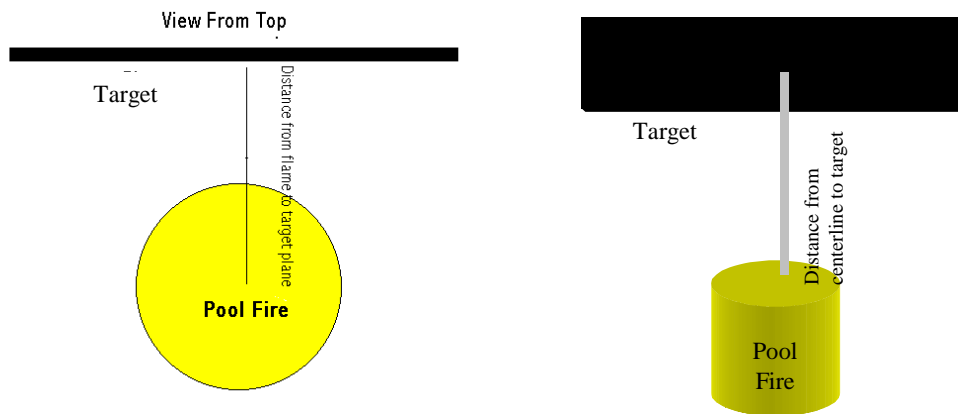


Figure 2-4: Layout of the Pool Fire Scenario

The heat flux from pool fires in an open space are expected to range from 1.7 cal/cm²-s (70 kW/m²) to about 1.9 cal/cm²-s (80 kW/m²), while the heat flux within a compartment is expected to vary with time until it reaches a steady state value of about 0.6 cal/cm²-s (35 kW/m²). Figure 2-5 shows a pool fire's heat flux on the same scale as the jet/spray fires illustrated in Figure 2-1. [18]

Heat Flux Measurements of Pool Fires

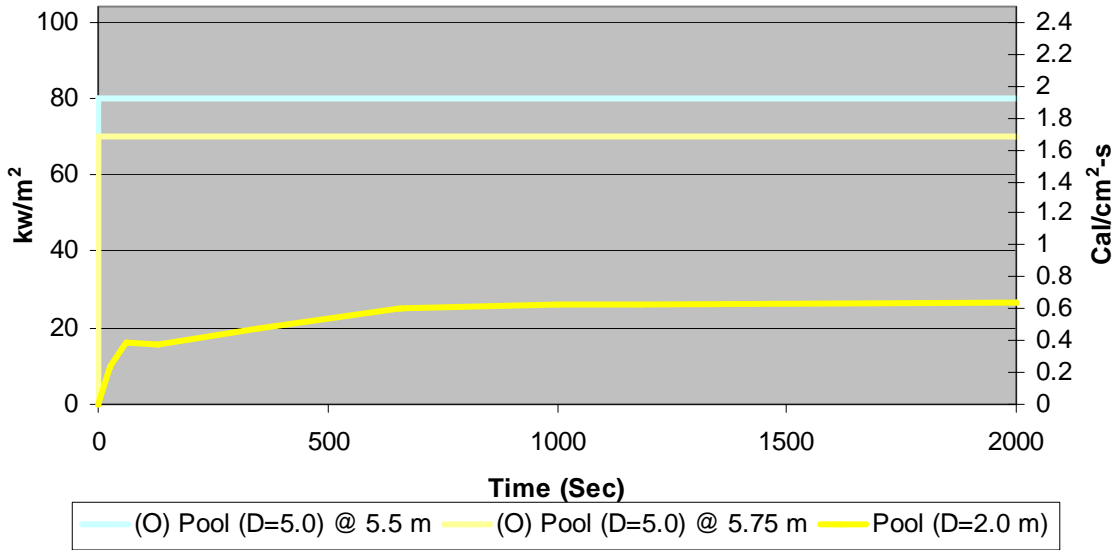


Figure 2-5: Heat Flux Exposures of Pool Fires

2.2.2.1 The Pool Fire in an Open Area

A JP-4 pool fire with a diameter of 5.0 meters (16.4 feet) located in an open area with a steady state heat release rate of 40 MW is modeled to determine the heat flux to a target at given distances from the centerline of the fire. The maximum heat flux at 5.5 meters (18 feet) and 5.75 meters (18.9 feet) are plotted in Figure 2-6.

On a technical note, the heat flux distribution over the wall is not a constant flux, Figure 2-6 shows the flux distribution expected at 5.5 meters from the centerline of the given fire source. However for the most reasonable worst-case scenario, the highest flux is

assumed constant over the entire target. Again this is a conservative approach used for design purpose. This maximum flux is the value plotted on the graph in Figure 2-1.

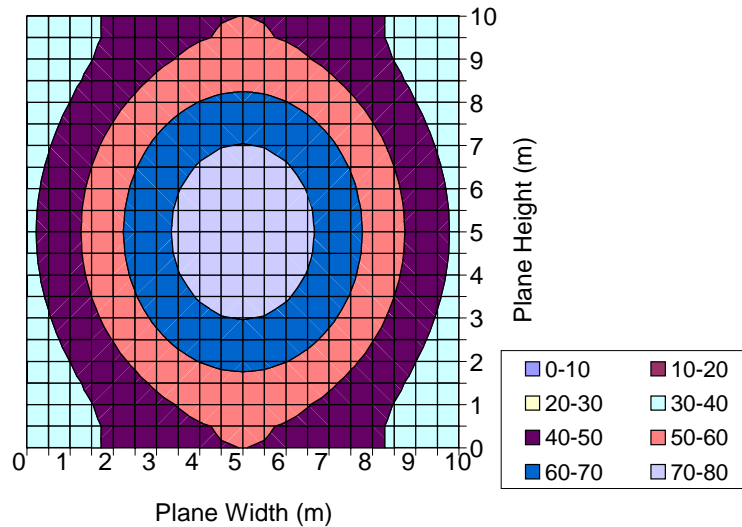


Figure 2-6: Radiative Heat Flux to Vertical Plane 5.5 m From JP-4 Pool Fire (kW/m²)

2.2.2.2 The Pool Fire within a Compartment

The second pool fire scenario is a 2.0 meter (6.5 ft) diameter kerosene pool fire in a 10 x 10 x 3 meter enclosure (32.8 x 32.8 x 9.84 ft). The heat release rate for this scenario was about 5.5 MW. Figure 2-7 illustrates the maximum heat flux generated at steady state conditions for different diameter kerosene pool fires. The data from the 2.0m fire was plotted in Figure 2-5.

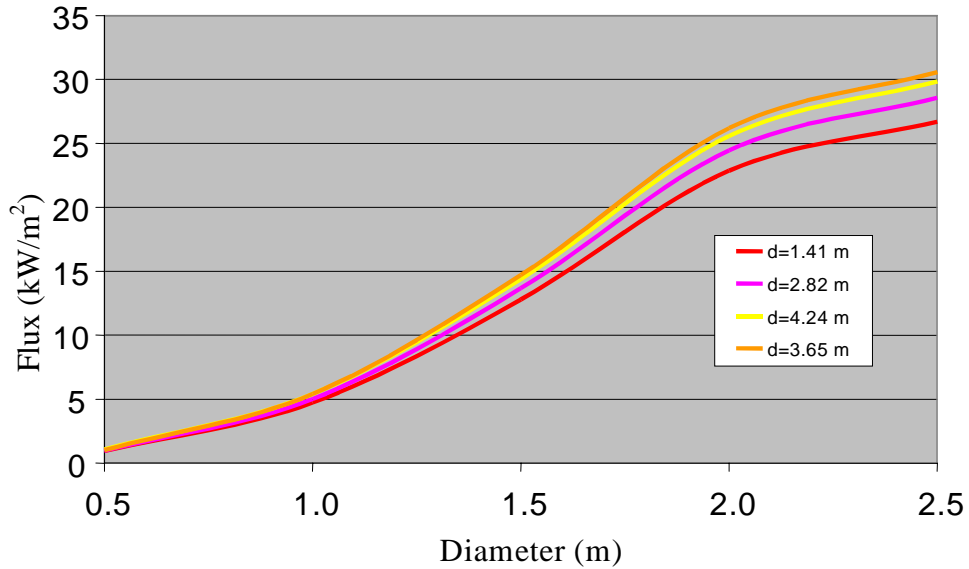


Figure 2-7: Target Flux vs. Fire Diameter

2.2.3 Cellulosic Fires

Cellulosic fires will most likely occur within the sleeping quarters. These fires are usually started by arson or careless behavior. In terms of magnitude of the heat flux, these fires are much smaller than the previous two scenarios; however they can still result in serious injury to someone who is not adequately protected.

The heat flux from the fire in an open space varied with time with a maximum of about $0.6 \text{ cal/cm}^2\text{-s}$ (25 kW/m^2) and the heat flux within a compartment varied in time with a maximum of about $0.4 \text{ cal/cm}^2\text{-s}$ (20 kW/m^2). Figure 2-8, shows illustrative bunk fire heat flux curves on the same scale as Figure 2-1. [18]

Heat Flux Measurements of Bunk Fires

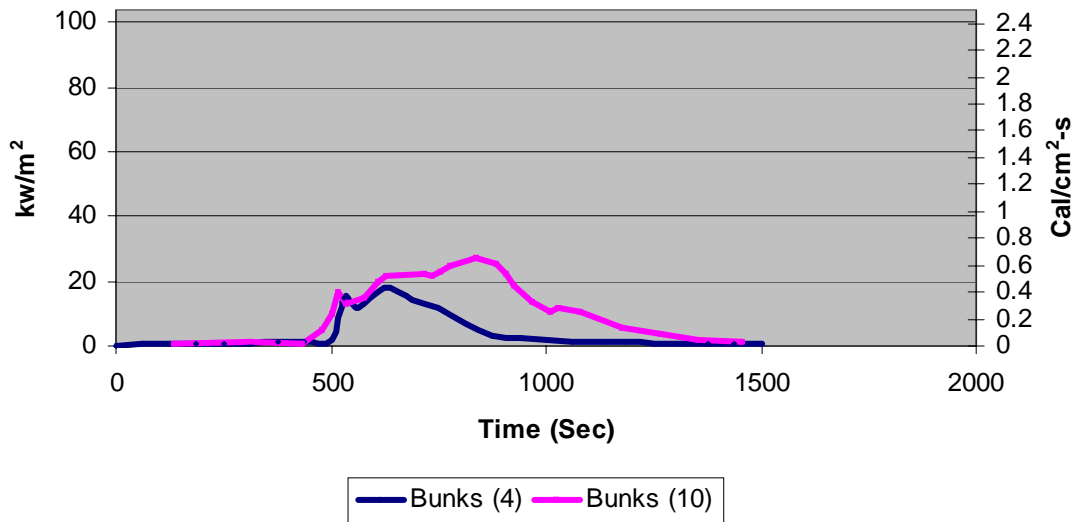


Figure 2-8: Heat Flux Measurements of Bunk Fires

The Four (4) Bunk Fire

This scenario has four bunks where the first bunk is ignited at time=0 and one additional bunk is ignited every 60 seconds thereafter. The compartment size is 33 x 33 x 10 feet (10x10x3 meters) and two vents, a door of approximately 3 x 7 feet (0.91 x 2 meters) and a ceiling vent of about 2 x 2 feet (0.5 x 0.5 meters). The predicted peak heat release rate is about 5.9 MW. [18]

The Ten (10) Bunk Fire

This scenario uses the same enclosure but ten bunk beds and the first bunk is ignited at time=0 with one additional bunk ignited every 50 seconds thereafter. The peak heat release rate for this scenario is about 7.8 MW. [18]

2.2.4 Summary

The heat flux from these scenarios varies dramatically, as shown in Figure 2-1, and can not be accounted for by a single thermal exposure commonly used in current test methods. The new test facility, described in the following chapter, was created with the ability to simulate a wide variety of fire scenarios and would allow for the scenarios listed here to be recreated within a controlled environment. The goal is to improve the methods used in evaluating the level of thermal protection offered by different types of clothing.

3.0 Methodology

The Fire Test Facility located in building 11 of Alden Research Labs in Holden, MA was designed and constructed during the course of this project. The following sections describe the criteria for the new manikin test and outline the specification of the equipment and apparatus used in conjunction with this facility. Also included is a summary of the safety devices that are in place for the protection of both life and property.

3.1 New Large-scale Manikin Test

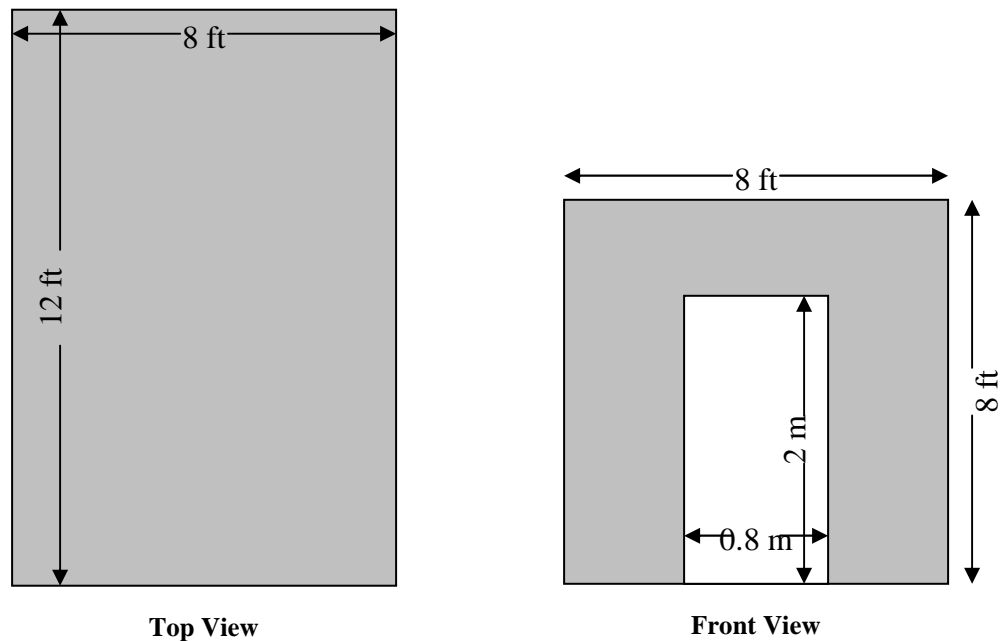


Figure 3-1: The ASTM Standard Test Chamber

The new test consists of using a test chamber with the same dimension of an ASTM room (see Figure 3-1) with the addition of eight square burners as shown in Figure 3-2. The manikin enters the test chamber using a straight overhead track and proceeds through a second door on the opposite side.

The objective of the new test is far broader than a test such as ASTM F1930-99, as it can be used to evaluate garment flammability for routine daily wear as well as fire fighting needs. This is done in the new test by moving burners and by turning them on and off. Thus different fire scenarios can be modeled using the same test apparatus.

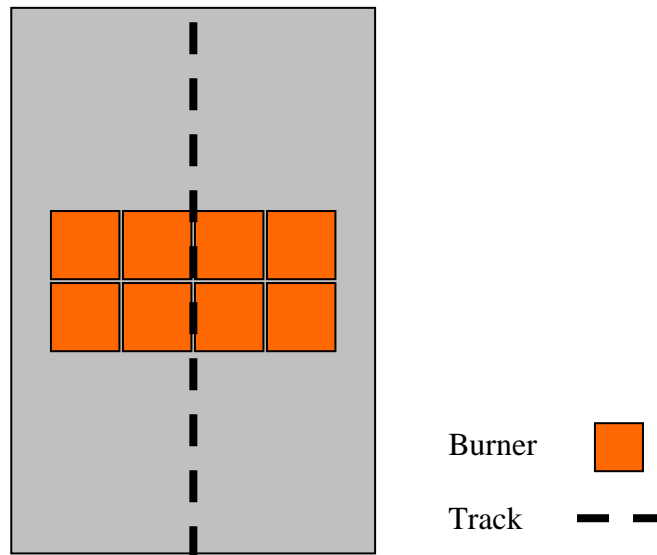


Figure 3-2: New Test Chamber Additions

Therefore the test simply consists of setting the burning configuration to the desired heat flux setting then having the manikin enter the room for a preset amount of time (the actual exposure time is controlled by the speed at which the manikin is moving). Thus a fully scalable thermal environment has been created.

This new test method incorporates the positive features from both the instrumented manikin test and the Navy's pit test while addressing the weaknesses that include: unrealistic fire scenario, effects of joint movement, effects of moisture in the clothing, and affects of the manikin's bulk movement through the scenario. The current facility is able to simulate the thermal environment outlined in Chapter two of this report. However, the effects of a mechanized manikin with moving joints and the effect of perspiration in clothing are beyond the scope of the current project are mentioned to keep the reader

aware that future research should consider these factors. The current test facility was designed for use with the mechanized when it becomes available.

In addition, considerations of a variable heat flux distribution are incorporated into the design to allow for variations in the type of fires to which the manikin can be exposed. The idea of a single design fire to evaluate several types of garment performance does not seem plausible; however this test facility allows for a variation in the fire environment and enables testing with different design fires. This test facility can be used for testing a range of different garments in different thermal settings.

3.2 Room Construction

Fuel Arrangement

A typical ASTM room includes a 100 lb propane tank at a pressure of about 109 psi (751,528 Pa) with a ½ inch (0.0127 m) diameter hose connecting the tank to a one foot (0.3048 m) square burner. With this setup, the maximum heat release rate is about 200 kilowatts. The following tables contain the fuel related properties used to calculate the heat flux associated with different fuels that are often used in the ASTM room.

Table 3-3: Properties of Selected Fuels (Table 3-4.16 SFPE HB)

Fuel	Composition	Molecular Weight (g/mol)	ΔH_T (MJ/kg)	ρ_{liquid} * (kg/L)
Propylene (SI)	C3H6	42	46.4	0.5139
Propane (SI)	C3H8	44	46.0	0.5005

Table 3-3: Heat of Combustions for the selected fuels (Table 3-4.11 SFPE HB)

Fuel	ΔH_T (MJ/kg)	ΔH_{CH} (MJ/kg)	ΔH_{CON} (MJ/kg)	ΔH_{RAD} (MJ/kg)	χ_{CH}	χ_{RAD}
Propylene (SI)	46.4	40.5	25.6	14.9	0.873	0.321
Propane (SI)	46.0	43.7	31.2	12.5	0.950	0.272

For a cylindrical flame, the heat flux associated with the fire varies with respect to the height of the flame. Figure 3-3 shows the theoretical heat flux with respect to height for a heat release rate of 200 kW on a one foot (0.3048 m) square burner. The solid horizontal line is the theoretical flame height using the Heskestad's correlation [13] (see Appendix A for a sample calculation). The four curves illustrate the heat flux at varying distances (0.5, 1.0, 1.5, 2.0 ft). It is apparent from this figure, that the standard propane setup described, is not adequate to produce the heat fluxes needed to simulate the desired thermal environments of 84 kw/m² specified in section 2.2.

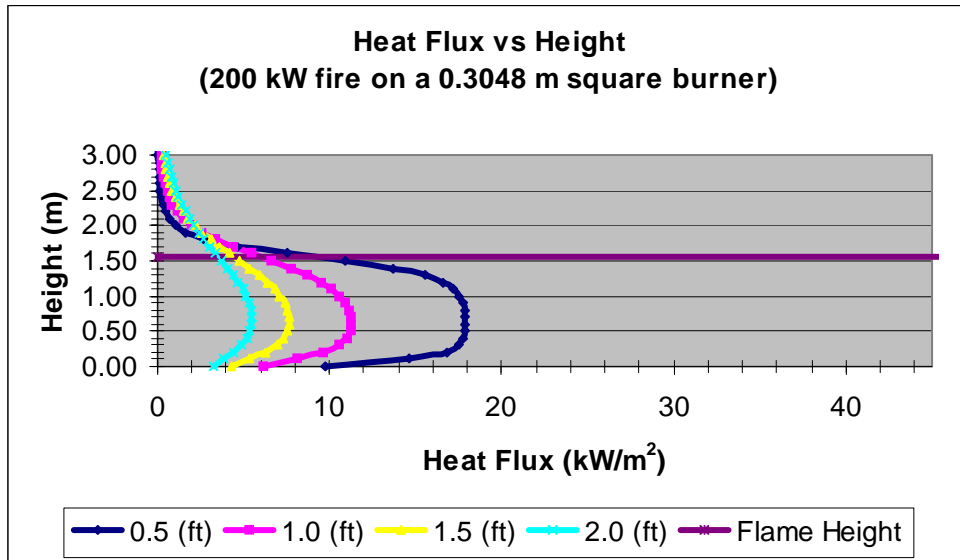


Figure 3-3: Heat Flux vs Height

Modifications of the ASTM room

As discussed, the standard room's burner has a maximum heat release rate of about 200 kilowatts. However, with the addition of a fuel vaporizer which can supply the fuel at a steady state and pressure, the heat release rate can be greatly increased. In the Fire Science Laboratory at WPI, the Ely Energy TF-100 fuel vaporizer is capable of producing short duration fires on the order of two to three megawatts. It is not expected that a heat release rate above 500 kilowatts will be required for each individual burner, as at this heat release rate the flame length approaches the ceiling for a 1 ft square burner, using the Heskestad's flame height correlation. [13]

Theoretical evaluations of the 500 kW propane burner, shows that heat fluxes range from 16 to 30 kW/m² (0.40 to 0.75 cal/cm²) at a distance of 0.5 ft, while at 1.0 ft, the heat flux

is reduced to 10 to 19 kW/m² (0.25 to 0.48 cal/cm²), as illustrated in Figure 3-4. Clearly, a single 500 kW square burner cannot provide enough heat flux. Both a radiant panel and an array of burners were investigated to determine how to create the desired flux in a controlled environment. Due to budget constraints the radiant panel was quickly removed as a viable option and the array of burners were selected as the most cost efficient way to produce the fire environment.

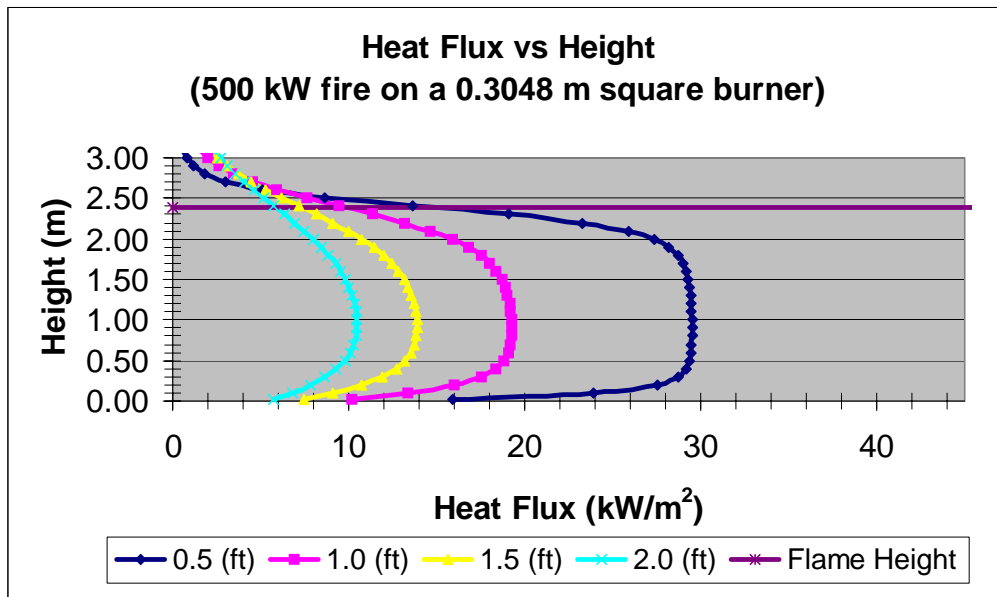


Figure 3-4: Square Burner Heat Flux vs. Height

3.2.1 The Square Sand Burner

The eight burners were fabricated from ¼ in hot rolled steel. The inside dimensions are 12 in square. The sand for the burners was taken from a local gravel yard. The sand was sifted with wire mesh screens to get the appropriate particle sizes as prescribed by ISO 9705. The lower portion of the burner was limited to sand particle size of 2.8 mm to 4.0 mm and the upper portion of the burner was limited to sand particle size of 1.4 mm to 2.0 mm.

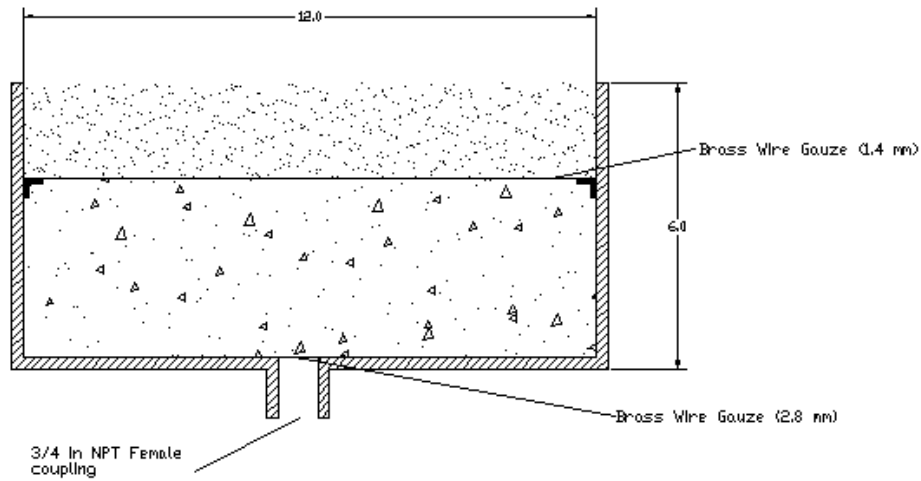


Figure 3-5: Diagram of Burner



Figure 3-6: Top and Bottom View of Burner

3.2.2 Simplified Sprinkler Apparatus

As an added precaution a series of sprinkler heads were design to work as part of the apparatus. The seven sprinkler heads are located directly above the test room. The sprinklers are Standard Response 160°F (k=5.65) brass upright sprinklers, Firematic

Model "U". The system also includes a 2" Model C-700 Positive Displacement flow meter by ABB.

The system is designed to only be charged during testing and the operations manual in the appendix has the procedures for charging and discharging the system.

3.2.3 Tracking System

The manikin travels along a system that is specifically designed for use in this application. This track is a 40 ft. long overhead conveyor system. It consists of a carbon steel single strand ANSI roller chain, a motor to drive the chain, an enclosure to shield the chain from the heat of the room, and hangers to carry the manikin and the attached thermocouple wires. (Appendix B, Figures 1 and 2)

Technical Specifications for motor	
Manufacturer	Leeson (from MSC)
Type	Series Parallel Shaft Gearmotor
Model	P1100 Series
Horse Power	1/3
Volts	Single Phase, 115/230 VAC, 60 HZ
Amps	6.2 DC
RPM	288
Frame	P1102-48

The protective enclosure is 40 feet of channel beam (C4X5.4, made of ASTM A36 structural steel), divided into three sections of 9 ft., 11 ft., and 20 ft. The 20-foot section is used for the tracking system inside the room, while the 9-foot section is on the outside of the room and holds the motor. The 11-foot section of C-beam is attached to the opposite end of the 20-foot section and is the area where the manikin is prepared for each test. The three sections of track are mounted flush to one another with mounting brackets at the top and bottom of the adjoining beam ends. The track is covered with Kaowool inside the room to provide an added level of thermal protection.

Using a stopwatch, the time it took for the mannequin to travel from one end of the 12 ft. room to the other end was recorded. This was done multiple times. In each case, it took 5.2 seconds for the mannequin to move from one end of the room to the other. Dividing the 12 ft. by 5.2 seconds, the maximum speed of the manikin is 2.31 ft./sec. The speed

can be reduced as necessary by cutting the power to the motor with a variable speed transformer.

3.2.4 Fuel Delivery System

The fuel delivery system is composed of several elements. The fuel source is four 100 lb tanks of liquefied propane gas (LPG) stored in a gas storage shed located outside the facility. The four tanks are connected through a manifold and fed through the wall into the TF200 ThermoFlo Vaporizer. There is also a pressure gage located in the propane manifold used to evaluate the status of the propane tanks. Figure 3-7a is the fuel shed . Figure 3-7b shows the TF 200 vaporizer.



Figure 3-7: (a) Fuel Shed



(b) Vaporizer

The $\frac{3}{4}$ in SS hose (silver) connects the propane tank manifold to the vaporizer and the 1 in hose (black) connects the vaporizer to the control station manifold. This manifold separates the propane gas into eight channels corresponding to each burner. Each one of



Figure 3-8: Controls

these eight channels is then split into two sub channels that have both a needle valve and a ball valve on the front side of the control station. These sub channels are then rejoined after the valves and then connected to the burners. Figure 3-8 shows the controls for one of the burners. The needle valve on the ignition line is set at minimal flow rate to allow for ignition. This setup allows the operator to safely control the flow while a flame is lit within the room. Once ignition is obtained on all eight burners, the test valve can be used to control the flame during testing.



Technical Specifications for Vaporizer	
Manufacturer	Ely Energy
Type	ThermoFlo Vaporizer
Model	TF 200
Fuel Capacity	120 Gal / hr
Water Capacity	47 gal
Inlet Dimension	¾ in
Outlet Dimension	1 ¼ in
Dry Weight	663 lbs

Figure 3-9: The Vaporizer

3.2.4.1 Nitrogen System

The nitrogen system works in conjunction with the fuel delivery stem and acts as the purging agent for the system. The nitrogen tank has five outlets, four of which go to each propane tank and the fifth line is connected to the pressure relief line of the vaporizer. This can be used to make sure the pressure relief line is operating correctly before turning on the vaporizer. The operations and safety manual details the procedure for using Nitrogen to purge the system.

3.2.5 Ventilation System

The ventilation system is comprised of two 10 ft square exhaust hoods located above each door of the test room. The ductwork for the ventilation system is all 24 gauge and is 16 in diameter from the hood to the union and 22 in diameter from the union to the blower. Figure 3-10 shows the union of the two hoods and the differences in duct sizes.



Figure 3-10: Union in Ductwork

The ventilation system is powered by a Buffalo Forge centrifugal blower which is on loan from ARL. This blower has five power settings that are: closed, 25%, 50%, 75%, and fully open. These setting correspond to the position of the exit vents of the centrifugal blower. The complete specifications are in Figure 3-11.



Figure 3-11: Blower

Technical Specifications for Blower	
Manufacturer	Buffalo Forge Company
Type	Centrifugal Blower
Model	Westinghouse Lifeline T
Horse Power	15
Volts	230/460, 3 Ph
Amps	38.6/19.3
RPM	1170
Frame	284T

Initial testing was done to determine the flow rates of the blower at both room temperature and during actual fire testing. To determine the flow rates, a pitot tube was placed in the center of the airflow of the 22 in diameter duct and a water displacement was recorded. At ambient conditions with the blower at fully open, a water displacement

of 2.4 in was recorded. However, all the fire tests are run at the 75% power setting and at this setting the displacement is 1.8 in of water. The airflow of the centrifugal blower at 75% open when no fire tests are being performed is roughly 14,000 cfm, giving each hood a velocity of 7,000 cfm.

During the fire test, the blower was set at 75% power and the lowest the displacement dropped was to 1.15 in and the airflow varied from 13,300 cfm to 13,700 cfm. The table on the right shows the temperature and the flow

ROOM TEMP	EXHAUST TEMP	AIRFLOW	
		m ³ /s	Cfm
°C	°C		
20	136	6.32	13,387
20	146	6.40	13,550
20	154	6.46	13,678

Table 3: Airflow Rates

rates of the exhaust gases through the centrifugal blower during the fire tests.

3.2.6 Gas Detection Systems

The Fire Test Facility has a MSA Ultima Gas Monitor system designed to detect a propane gas leak. It consists of a remote propane sensor, a relay module to provide a local light and horn alarm, and gas monitor module which will display the propane concentration in percentage of the Lower Explosive Limit (% LEL). If the LEL for a gas was 10% in



Figure 3-12: Gas Detector

air and the monitor displayed 50% LEL, then the concentration would be 0.50 x 0.10 or 5% of the gas in air. It is important to note the gas monitor reading is not the total concentration of the gas in the environment. The system also has an AC to DC power converter module to provide the necessary 12 Volts DC need to operate the gas monitor and relay modules.

In addition to the MSA system, a localized hand held gas detector is used in conjunction with soapy water to spot check for leaks in the fittings used in the gas delivery system as well as the burners.

An ADT alarm system was also installed which allows the continual monitoring of the facility when personnel are not present. This system consists of smoke and heat detectors placed within the facility. Details on the operations and maintenance of this system are in the Operations & Safety Guide.

3.2.7 DAQ System

The Data Acquisition (DAQ) system is a limited system used to recorded properties of the room for calibration purposes. It was not designed to handle sensors from the manikin and as such the system is only setup up to handle 64 separate data channels. All the room instrumentation listed in Section 4.3 was connected to this system. The hardware is from National Instruments and the components are listed below:

- Qty. (1) SCXI-1000 4-slot chassis (Donated)
- Qty. (1) SCXI-1200 12 Bit DAQ Module (#776783-00)
- Qty. (2) SCXI-1102C 32-channel amplifier (#776572-02C)
- Qty. (2) SCXI-1303 32-channel isothermal terminal blocks (#777687-03)

The Virtual Instrument (VI) is the interface that allows the data from the instruments to be recorded. The VI used for calibration of the room varied during initial testing and the current VI is described in the Operations & Safety guide. This guide will describe the VI along with its intended use.

3.3 Room Instrumentation

3.3.1 Schmidt-Boelter Gage

A Schmidt-Boelter gage was acquired for heat flux testing and used as the primary source for data gathering.

A Schmidt-Boelter gage is a water cooled instrument used to record the incident flux to a target. It is comprised of a thermopile (a series of differential thermocouples) which operates on the same principles of a regular thermocouple. However the thermopile is wired to have the hot junction on the exposure side of the gage and the cold junction is located next to the water flow. [16] This allows the gage to provide a continuous differential reading instead of a time based differential.

The Schmidt-Boelter gage's major drawbacks are the constant water supply needed and the relative cost associated with purchase and maintenance of the device.

3.3.2 Thermocouple Jack Panels and Extension

A type K 40-channel thermocouple jack panel was purchased from Omega Engineering, Inc. (Model No. 19UJP-4-40-K). This jack panel accepts both miniature and standard-size male thermocouple connectors, and can be mounted in industry standard 19-inch racking. A separate custom wooden enclosure was built to house this jack panel. This

enclosure was designed so that it is possible to position the panel at a separate location in the lab from the actual DAQ system, making the required length of the thermocouple probe shorter. The custom wooden enclosure was designed using a “toolbox” locking mechanism so that future enclosures could be added and stacked on top of one another and latched together making a single unit if so desired.

Figure 3-13 is a front-view of the jack panel and its custom enclosure and a rear view of the jack panel and enclosure. Note the strain relief mechanism. The yellow wires are 30 gage thermocouple extensions that connect the jack panel to the National Instruments terminal blocks. These extensions are made of Omega Engineering’s 20 gauge extension grade polyvinyl insulated twisted electro-magnetically shielded thermocouple wire (Model Number EXPP-K-20-TWSH).

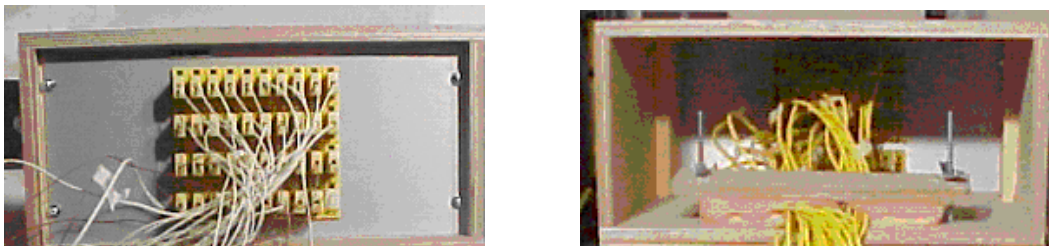


Figure 3-13: Jack Panel

3.3.3 Thermocouple Arrays

Thermocouple arrays were used to measure temperature profiles within the test room at different locations. These arrays are commonly referred to as *rakes* or *trees* throughout this report. Each rake consisted of a vertical array of 24 thermocouples spaced at ten-centimeter intervals from floor to ceiling. The top thermocouple was positioned

approximately five centimeters below the ceiling. These thermocouples were formed from Omega Engineering's high temperature glass insulated 24 gauge Type K thermocouple wire (Model Number HH-K-24). A Hot Spot II spot welder by DCC Corporation was used to form bare bead thermocouples. A close-up of a typical thermocouple is shown below in Figure 3-14.

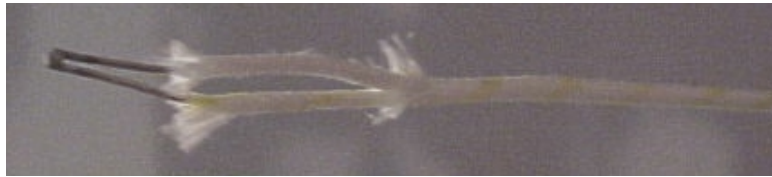


Figure 3-14: Bare Bead Thermocouple

The thermocouples were held in place by drilling holes through a one-inch diameter steel pipe and feeding the wires through these holes. Each thermocouple junction extended approximately six inches from the steel pipe to minimize radiation- blocking effects. The rake was position horizontal in the room to give a temperature profile from the right wall to the left wall. The rake was moved into one of 7 preset positions to take readings at 1 foot intervals above the burner. With this method, 168 temperature readings were taken in the plane above the burner. This same procedure was done at the front and rear of the burners to give a total of 504 temperature readings over the region of the burners. With these points a thermal map of the plane can be developed giving a profile of the heat distribution at the centerline of the room.

4.0 Data Analysis

4.1 Room Configuration

The following diagram of the test facility provides the reference points for data collected. Figure 4-2 shows the actual physical location of each of the eight burners. The color codes were used to uniquely identify the burners during actual testing. Figure 4-1 illustrates this color and numbering scheme.

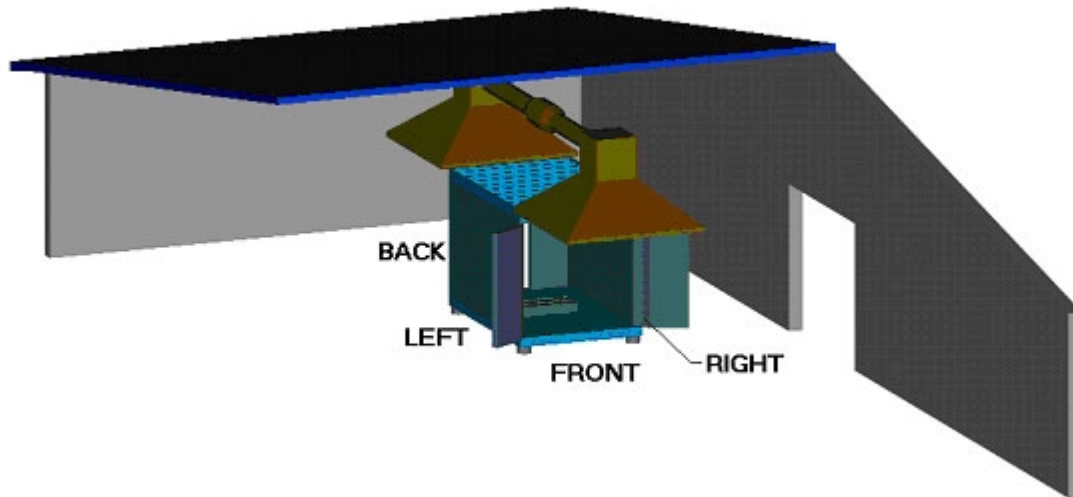


Figure 4-1: Diagram of the Holden Test Facility

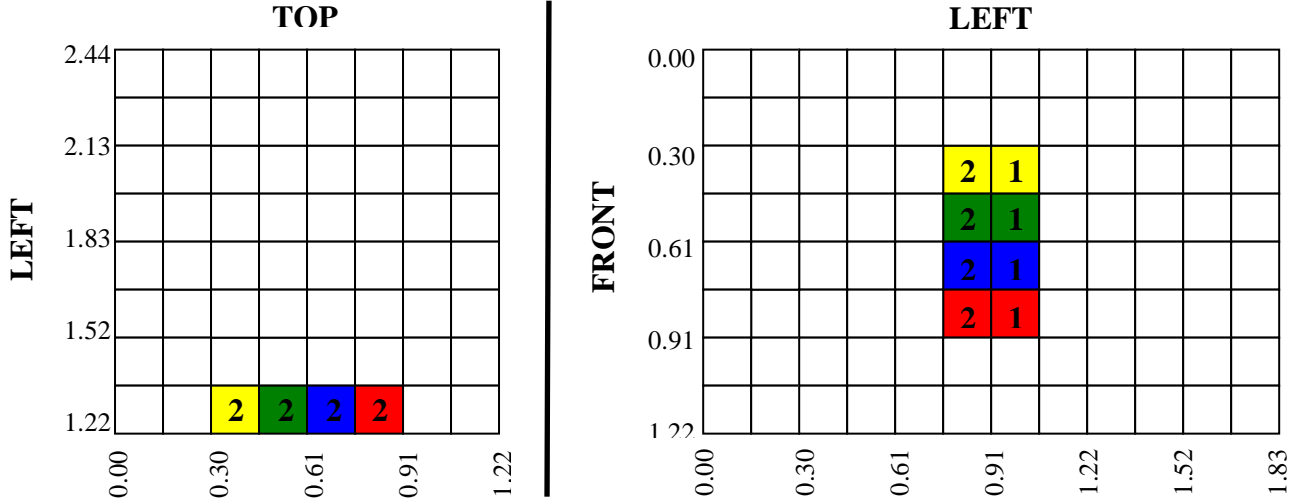


Figure 4-2: Location of the Burners within the Room

4.2 Temperature Profile

The temperature rake apparatus described in section 3.3.3 was used to collect the data discussed in this section. Of the 24 thermocouples on the rake, three of them were defective and did not collect data. The three locations at 1.57 m, 1.98 m, and 2.29 m from the edge of the rake are accounted for by taking an average of the temperature recorded on each side of the defective thermocouple.

4.2.1 Maximum – Vertical Left-Right

The data discussed in this section is based on the maximum temperature recorded. It appears the burners are hotter at the base of the right side of the room and the upper portion of the flames are leaning toward the left wall as shown in the temperature profile

slices in Figure 4-4. This phenomenon is likely caused by the entrainment of the air flow from the open overhead door causing a more complete combustion at the base of the flame (with a higher temperature) while at the same time pushing the flame towards the left wall. However the changes in the temperature profile is consistent over the center two burners. This region is more important than the outside burners because the traversing manikin will be exposed to the region directly above the two center burners. Figure 4-5 and Figure 4-6 show the temperature profile slices at the front and back of the burners. It is cooler in the front of the burners than in the back of the burners. Figure 4-3 shows the location of these temperature profile slices within the room.

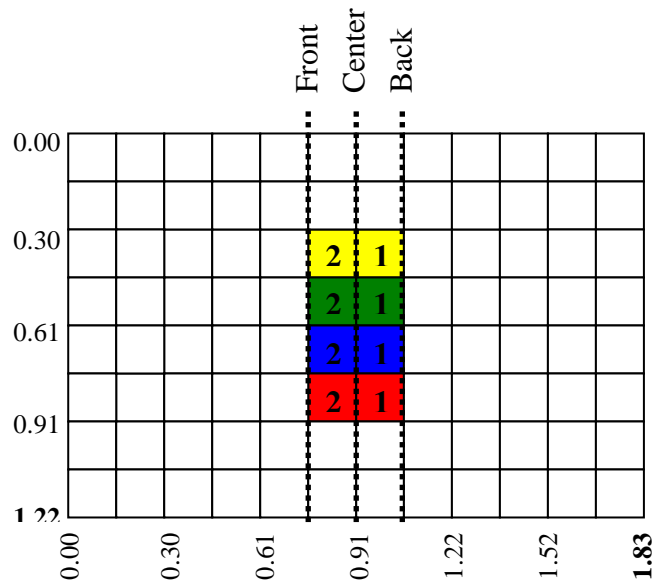


Figure 4-3: Vertical Left-Right Temperature Profile Slices

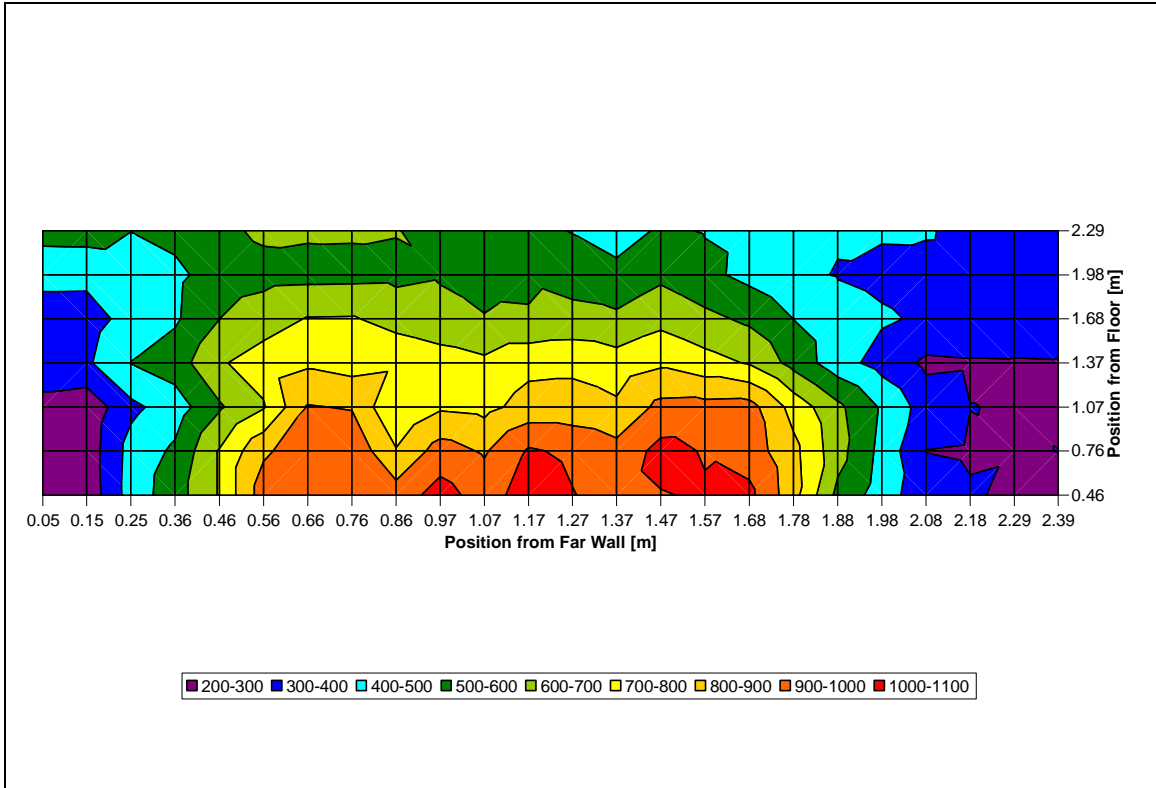


Figure 4-4: Maximum Temperature Profile of the Center of the Burner

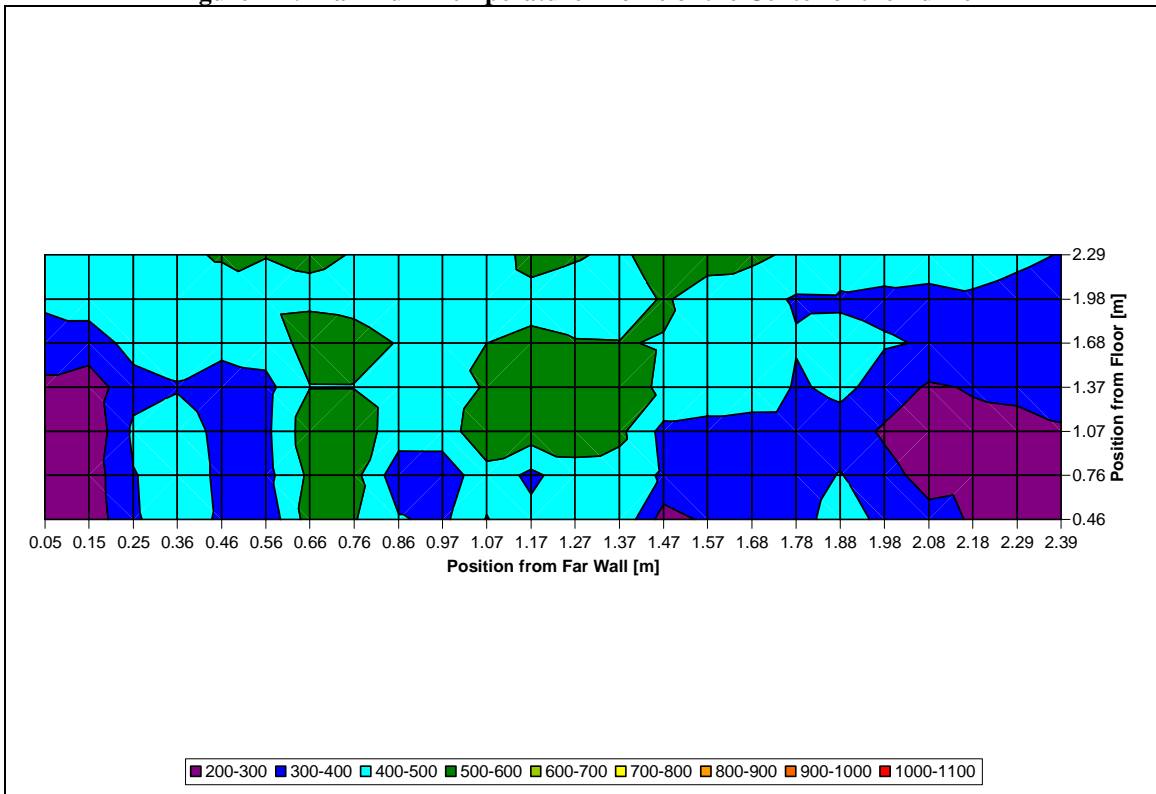


Figure 4-5: Maximum Temperature Profile of the Front of the Burner

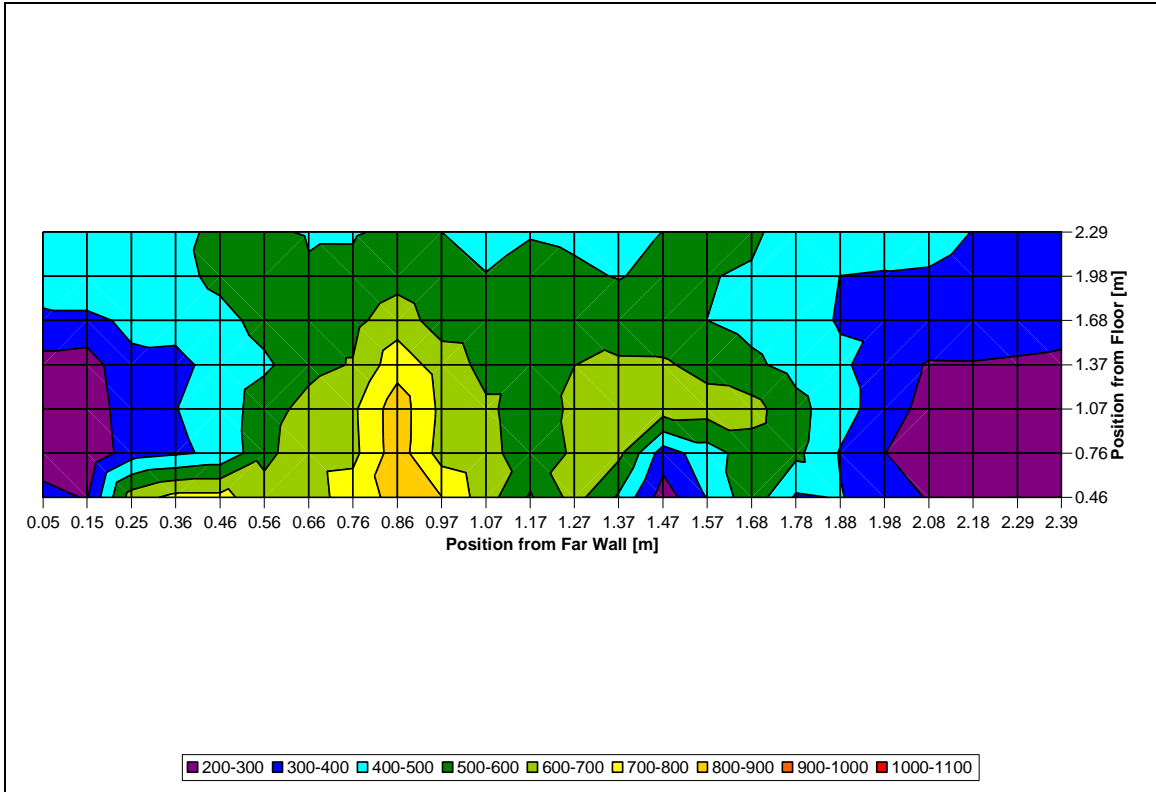


Figure 4-6: Maximum Temperature Profile of the Back of the Burners

4.2.2 Maximum – Vertical (Front to Back)

Figure 4-8 to Figure 4-15 are vertical (front to back) slices of the surface temperature profile over the burners. Figure 4-7 shows the position of these slices within the room. The centerline of the burners is located at 1.83 m (72 in) from the front wall. The temperature profiles show that the back of the burners are hotter than the front of the burners. The most likely cause of this is the open overhang door located at the right-front corner of the room. Thus the air flow from the front causes the flames to lean slightly towards the back of the room.

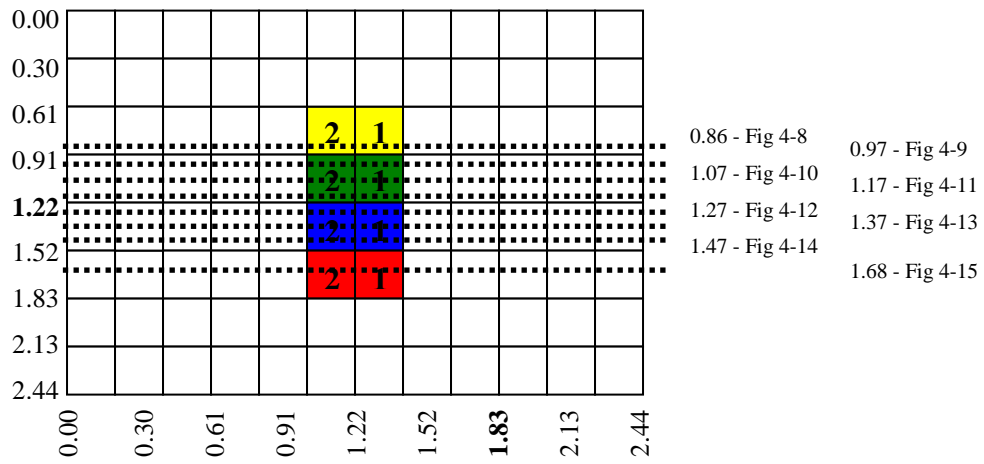


Figure 4-7: Location of the Temperature Profile Slices

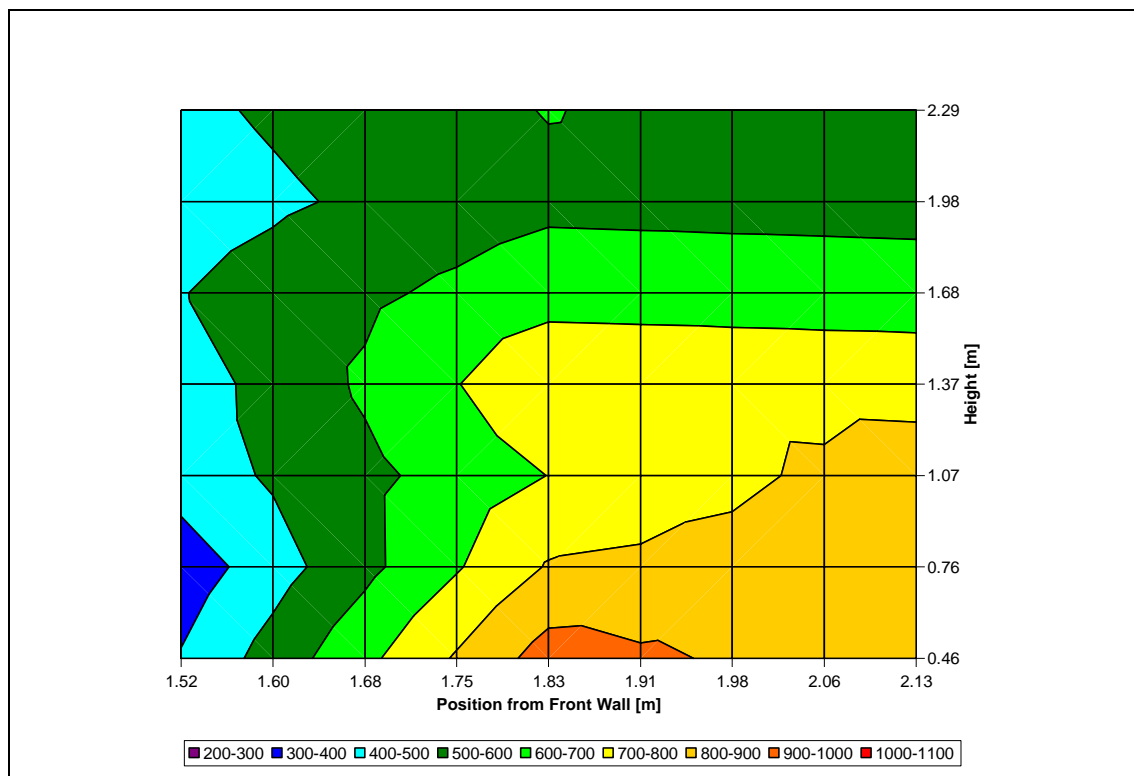


Figure 4-8: Maximum Vertical Front to Back Temperature Profile - 0.86 M (34 in) From Left Wall

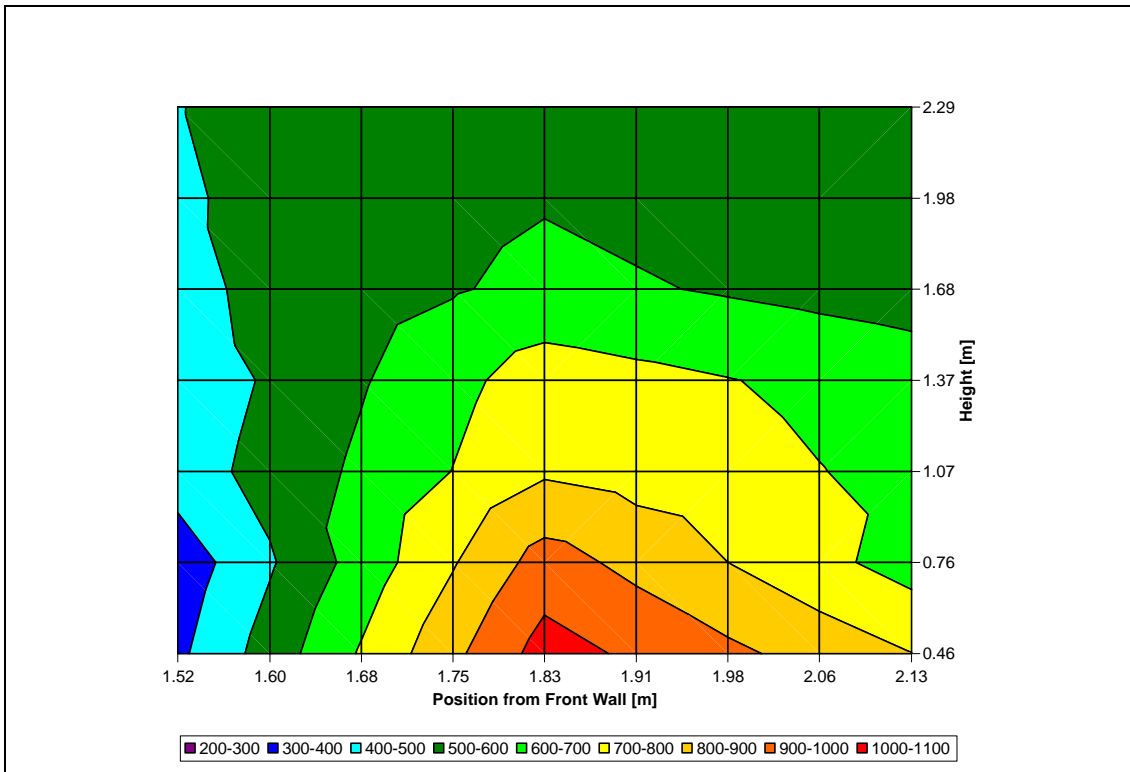


Figure 4-9: Maximum Vertical Front to Back Temperature Profile – 0.97 M (38 in) From Left Wall

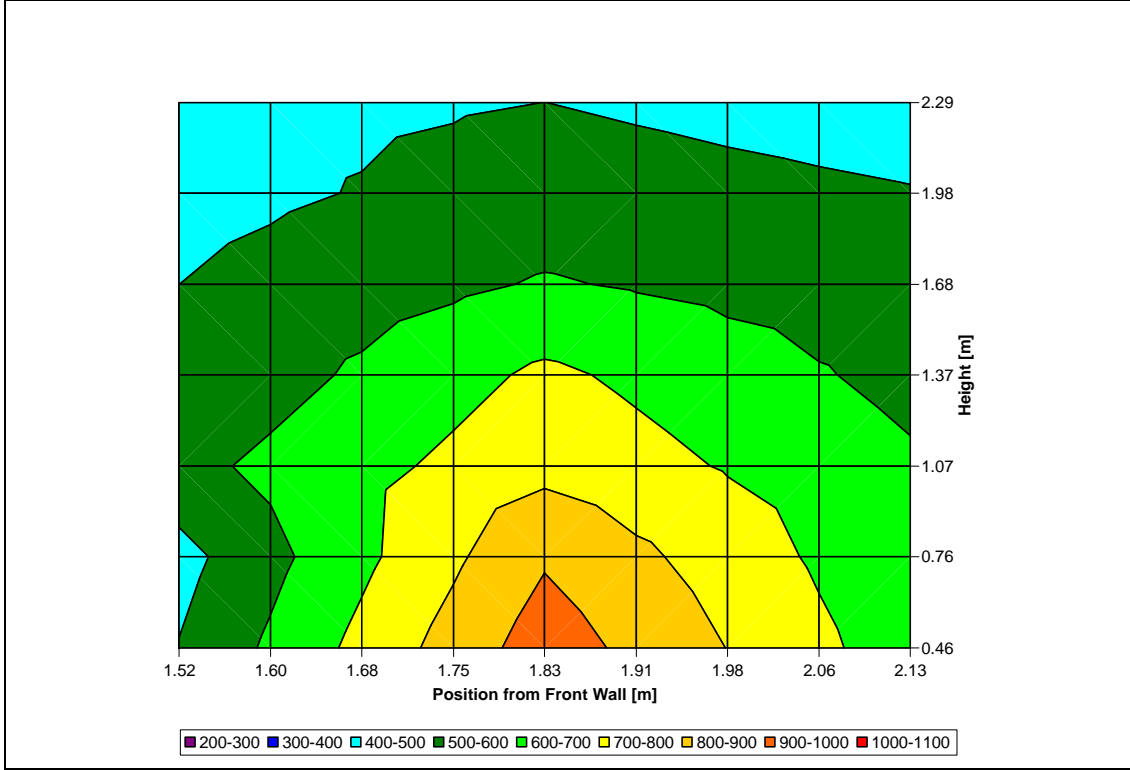


Figure 4-10: Maximum Vertical Front to Back Temperature Profile – 1.07 M (42 in) From Left Wall

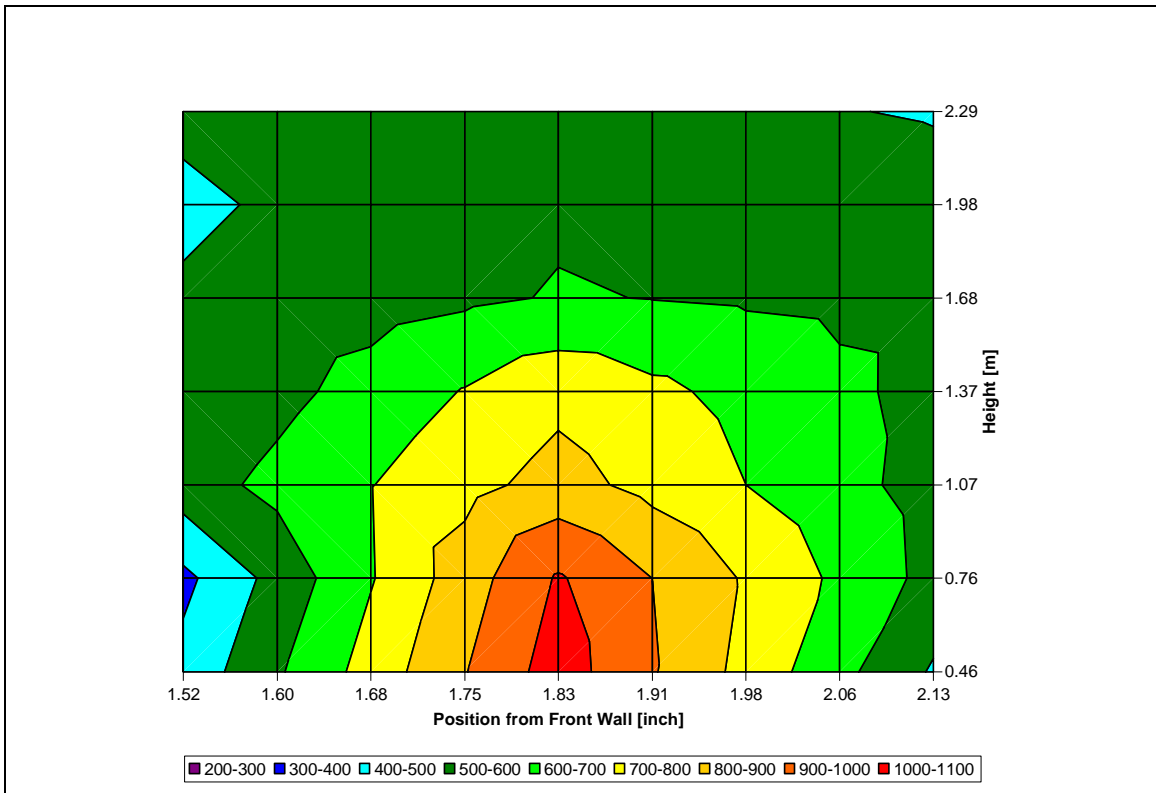


Figure 4-11: Maximum Vertical Front to Back Temperature Profile – 1.17 M (46 in) From Left Wall

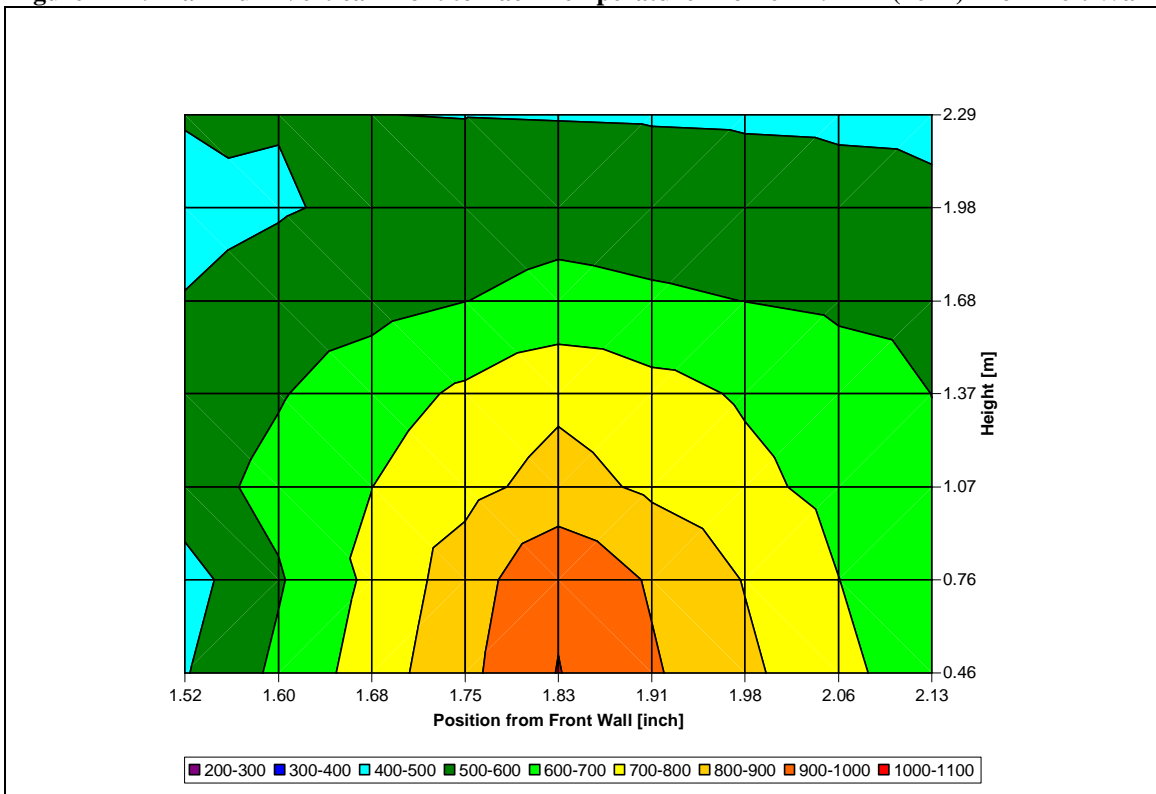


Figure 4-12: Maximum Vertical Front to Back Temperature Profile – 1.27 M (50 in) From Left Wall

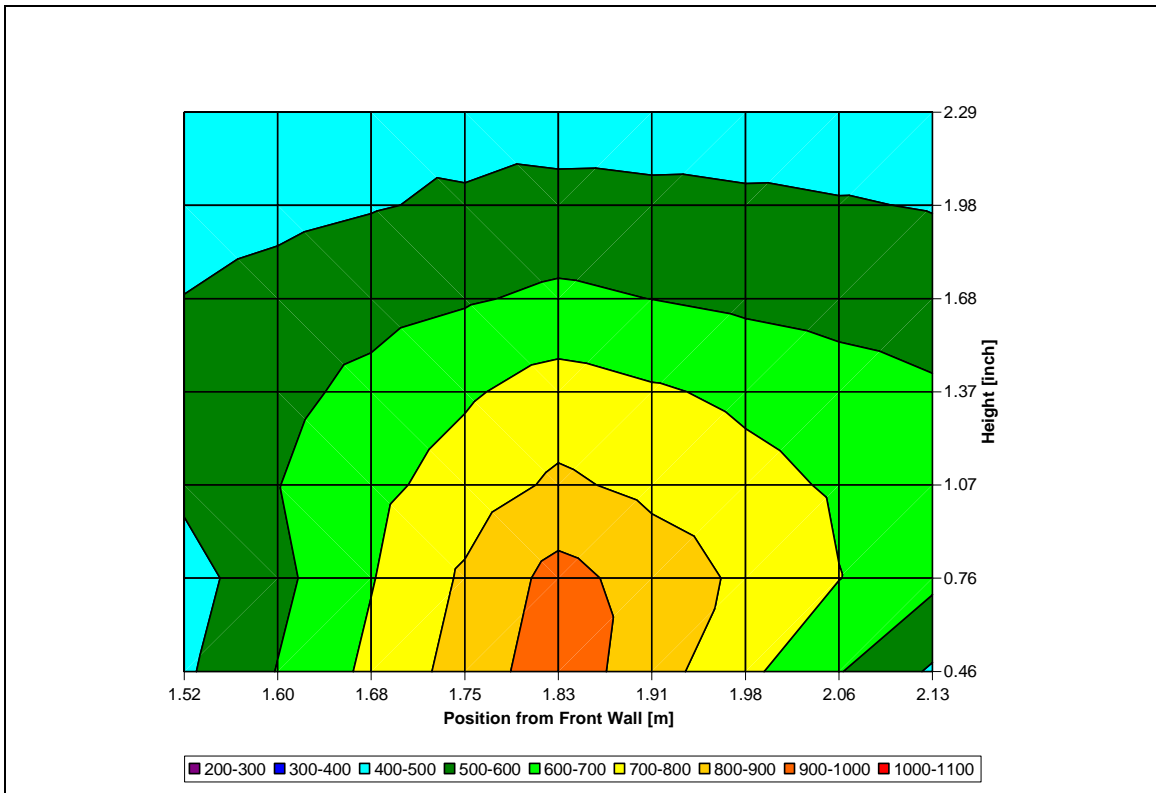


Figure 4-13: Maximum Vertical Front to Back Temperature Profile – 1.37 M (54 in) From Left Wall

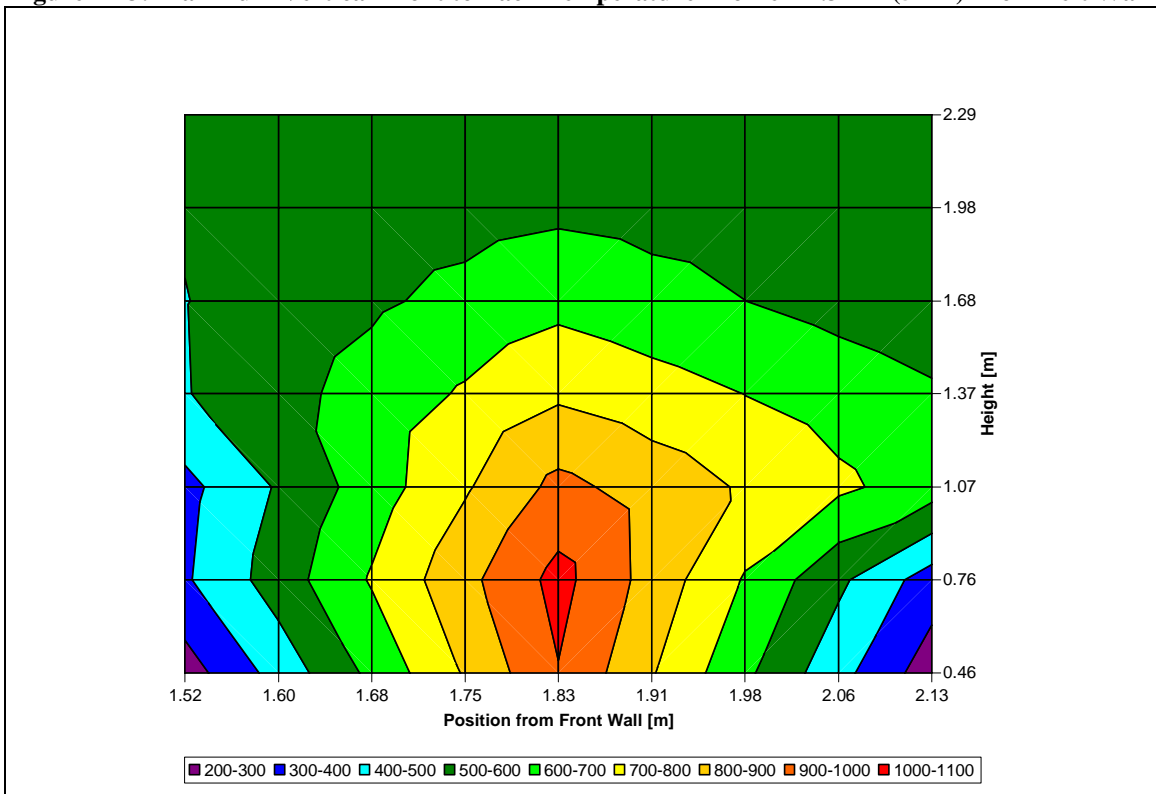


Figure 4-14: Maximum Vertical Front to Back Temperature Profile – 1.47 M (58 in) Left Wall

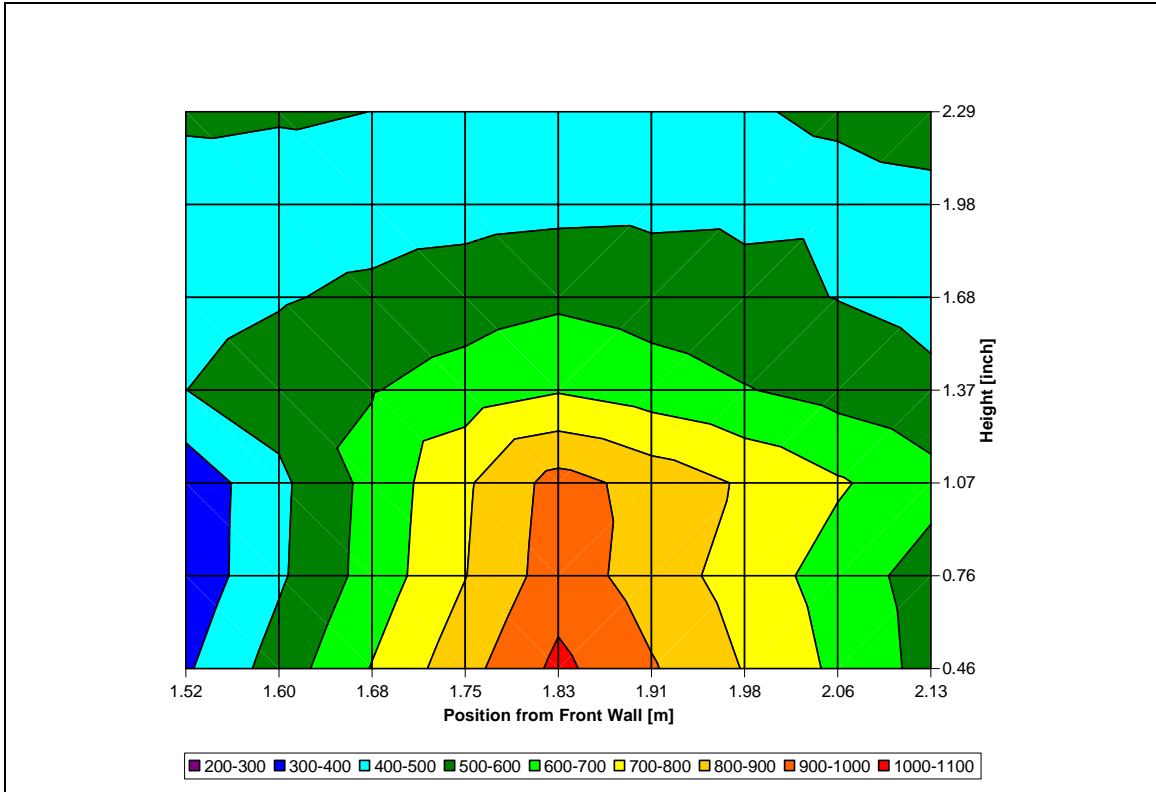


Figure 4-15: Maximum Vertical Front to Back Temperature Profile – 1.68 M (66 in) From Left Wall

4.2.3 Maximum Temperature Plan View Profile

Figure 4-17 to Figure 4-23 are horizontal (left to right) slices of the surface temperature profile above the burners. This would be the temperature profile as if the burners were being observed from the ceiling. The burner is located from 0.61 to 1.83 m (24 to 72 in) from the left wall and 1.52 to 2.13 m (60 to 84 in) from the front wall. The temperature profile

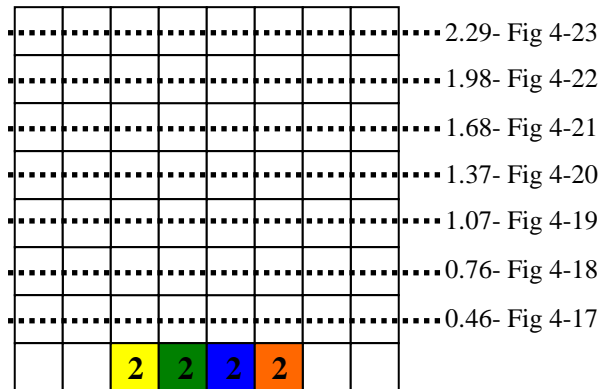


Figure 4-16: Location of the Temperature Profile Slices

shows that the back edge of the burners is hotter than the front edge. Figure 4-16 illustrates the position of these surface plot slices within the room.

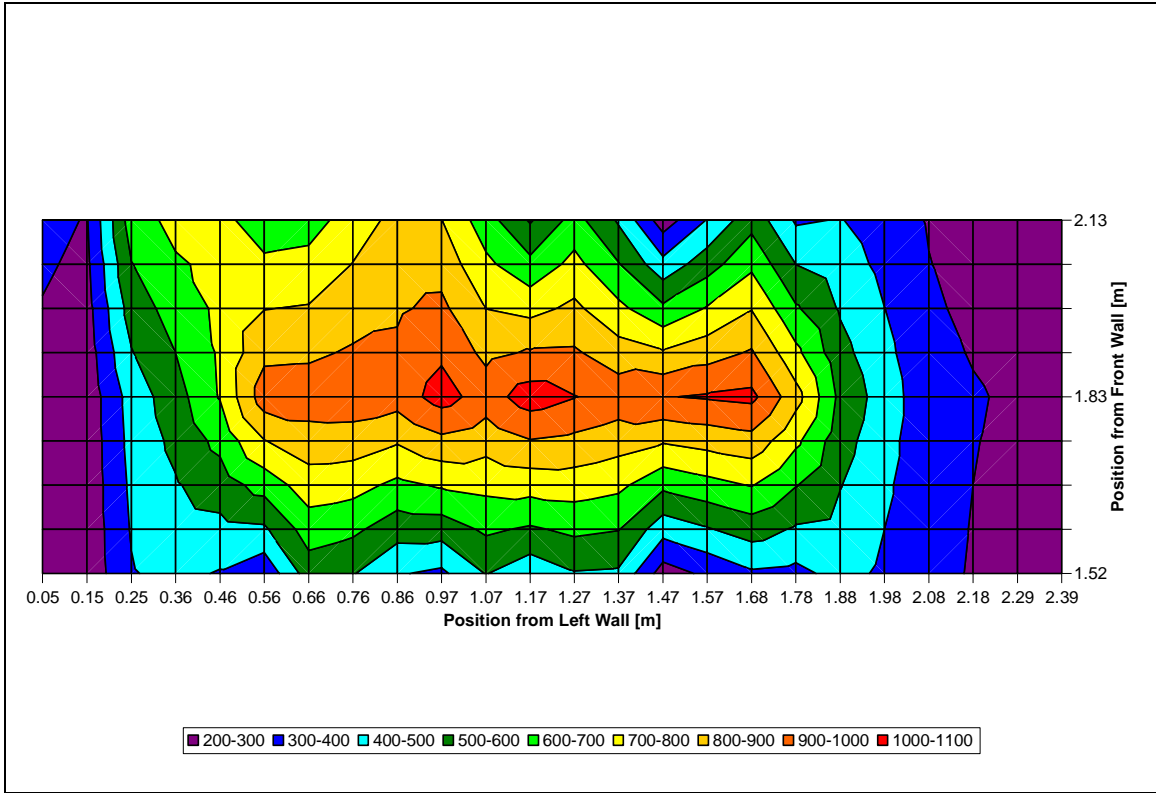
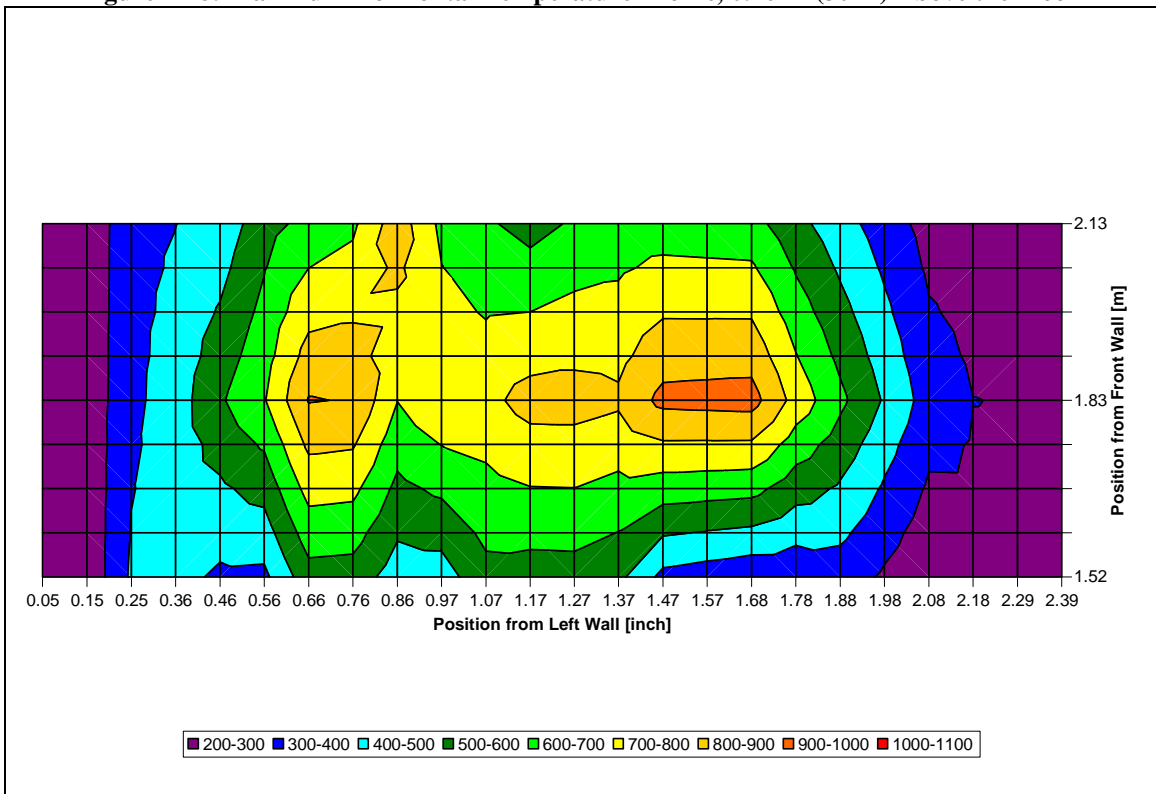
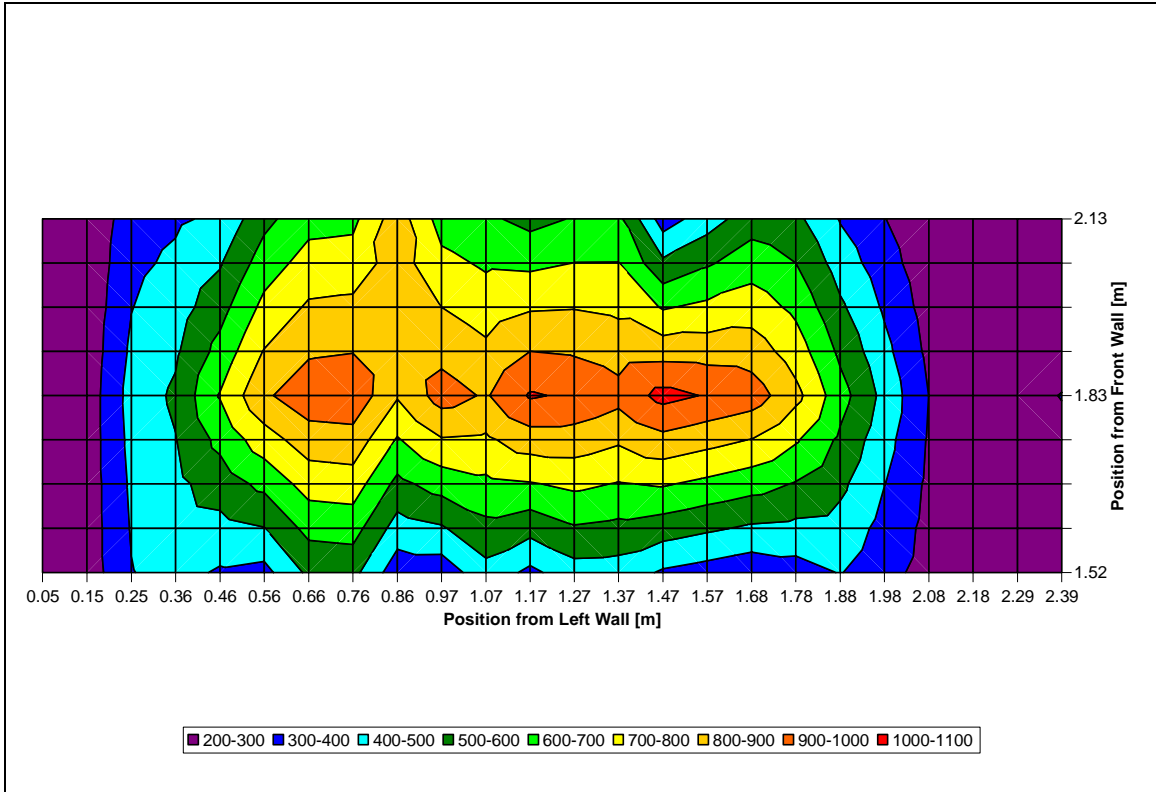


Figure 4-17: Maximum Horizontal Temperature Profile, 0.46 M (18 in) Above the Floor



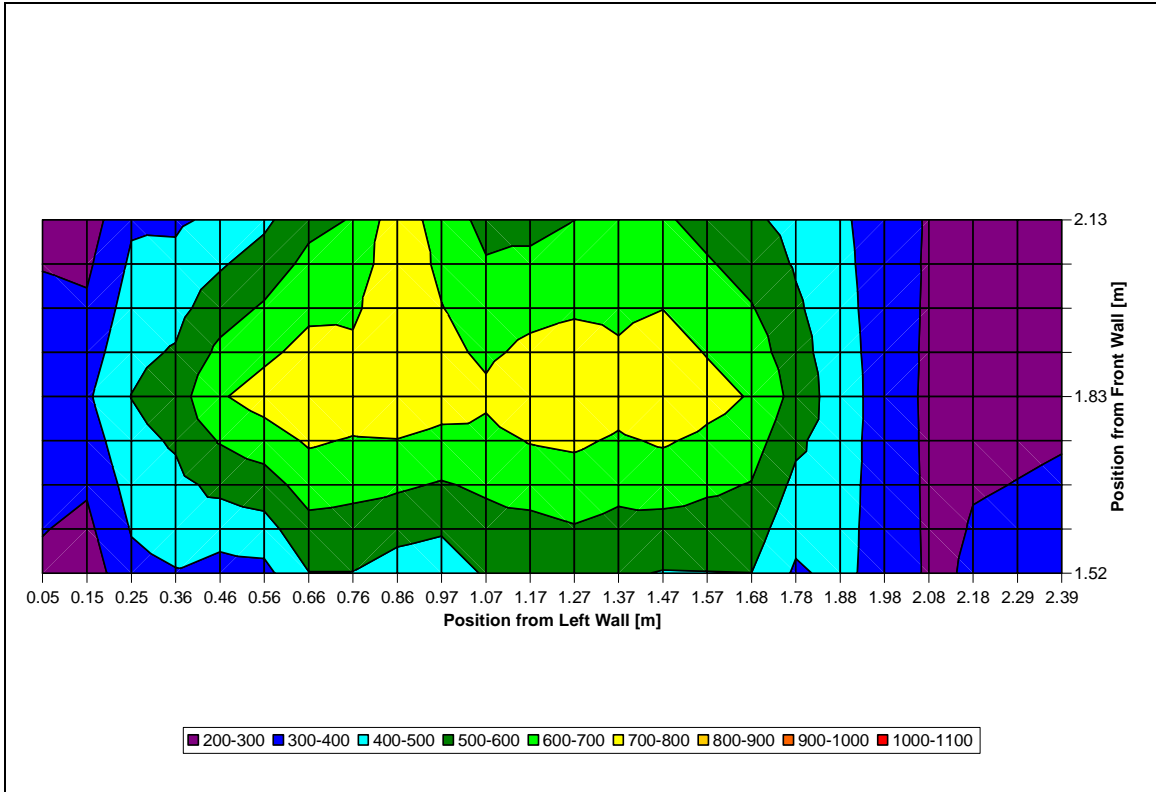


Figure 4-20: Maximum Horizontal Temperature Profile, 1.37 M (54 in) Above the Floor

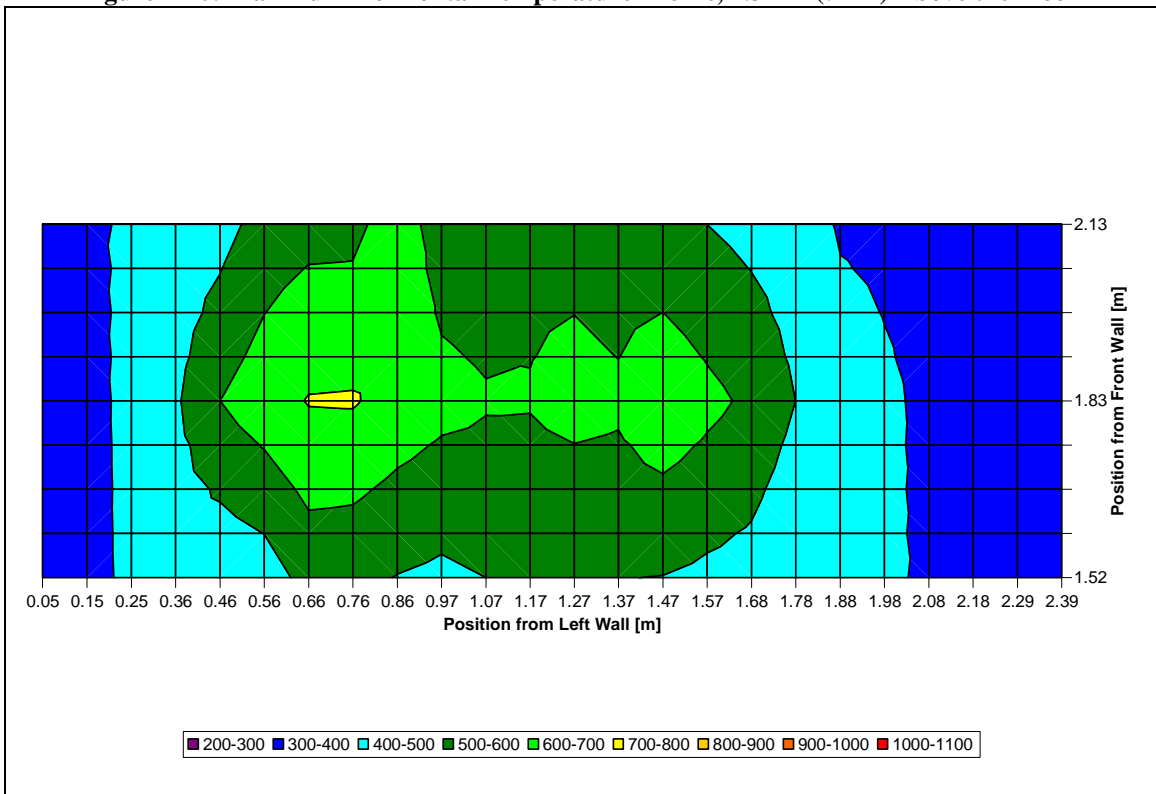
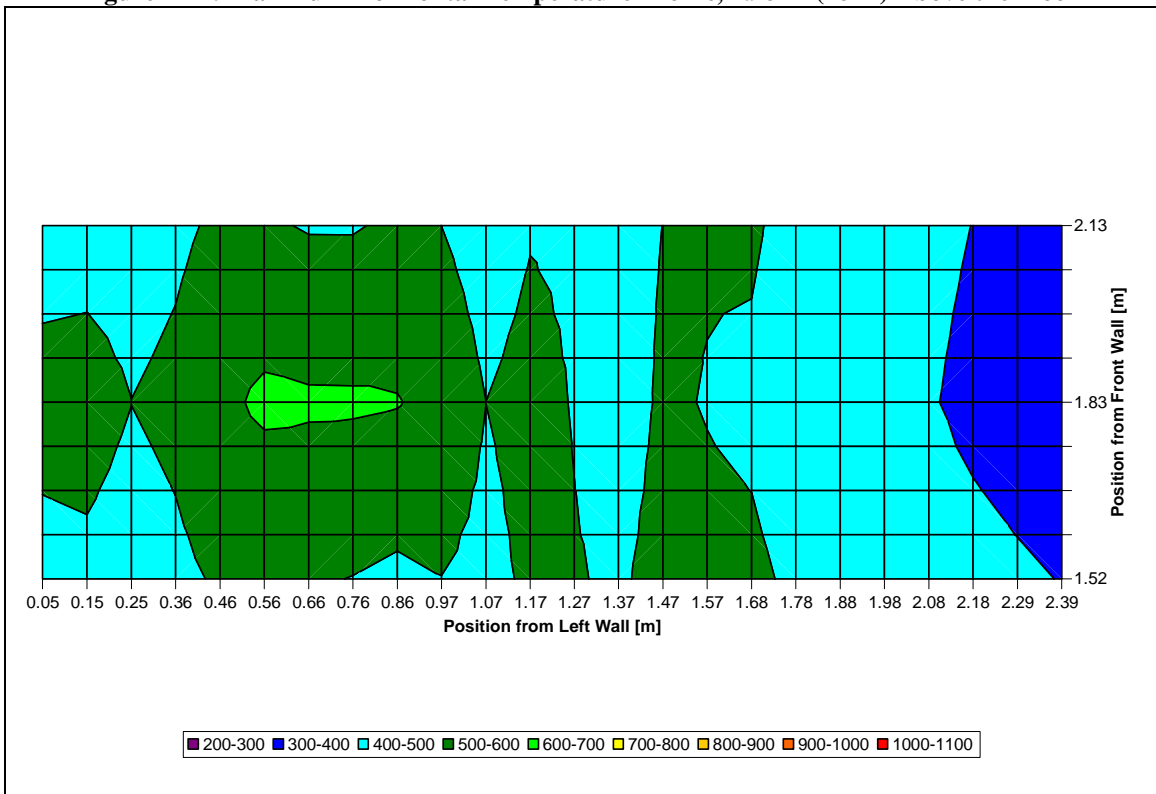
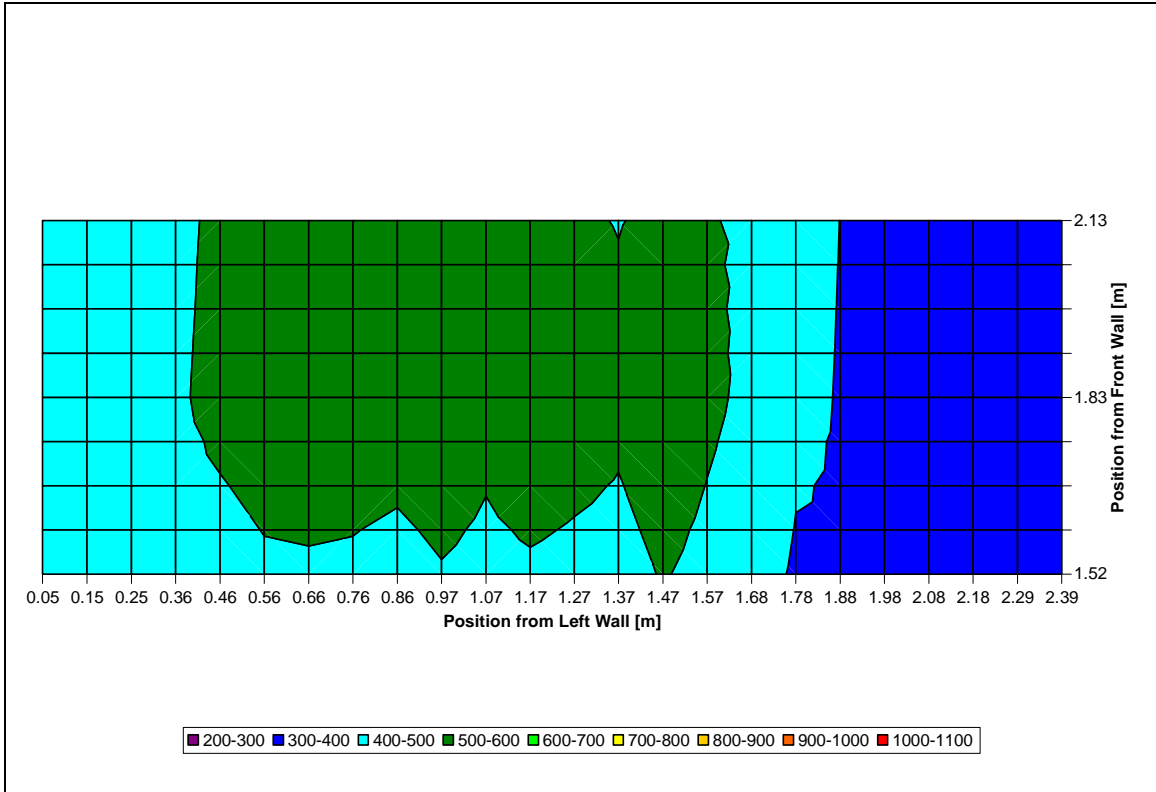


Figure 4-21: Maximum Horizontal Temperature Profile, 1.68 M (66 in) Above the Floor



4.2.4 Maximum Temperature Plan View 3D Profile

Figure 4-24 to Figure 4-30 are 3D plots of the same data in section 4.2.3. They help to illustrate the temperature gradients at each of the seven locations.

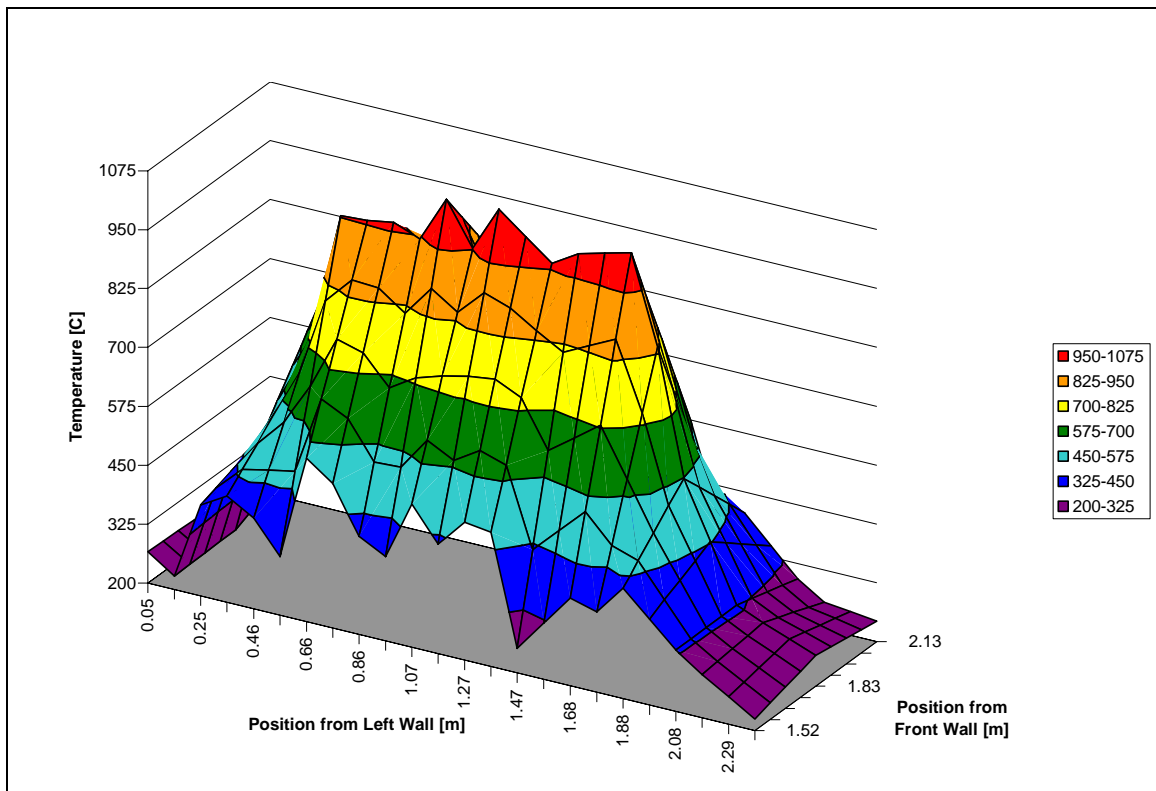


Figure 4-24: Maximum Plan View 3D-Temperature Profile, 0.46 M (18 in) Above the Floor

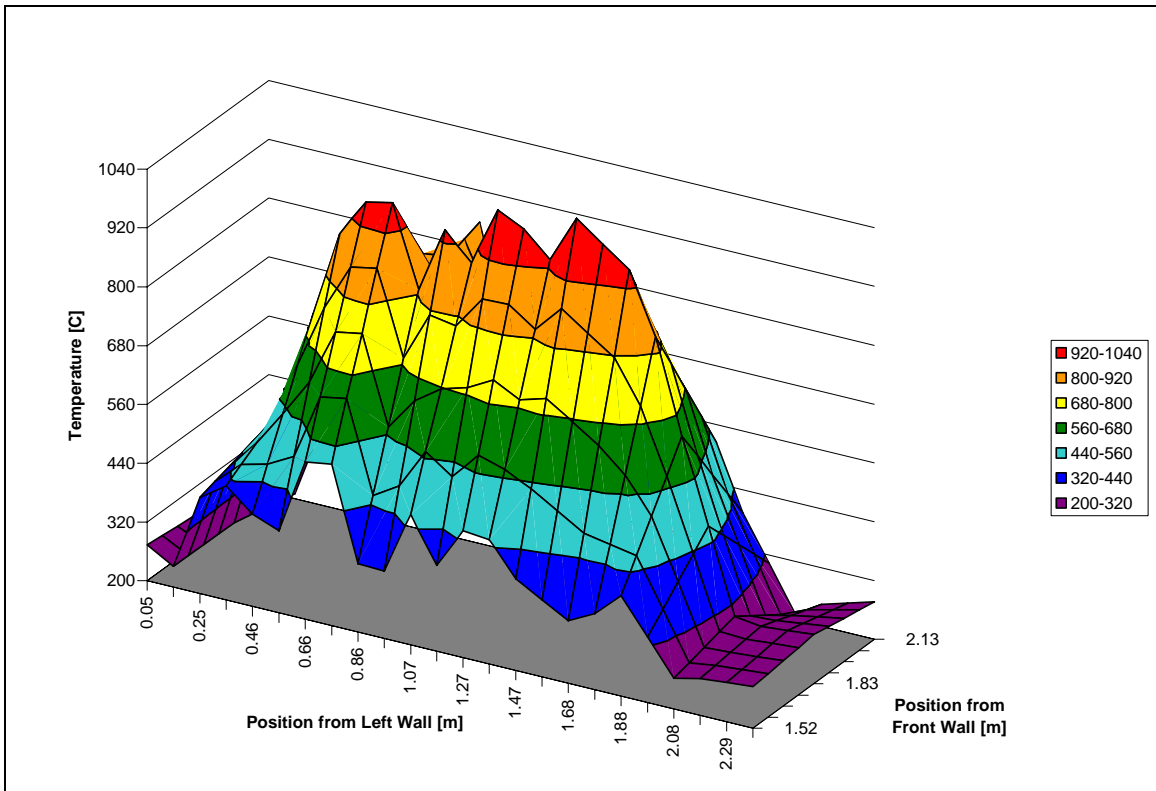


Figure 4-25: Maximum Plan View 3D-Temperature Profile, 0.76 M (30 in) Above the Floor

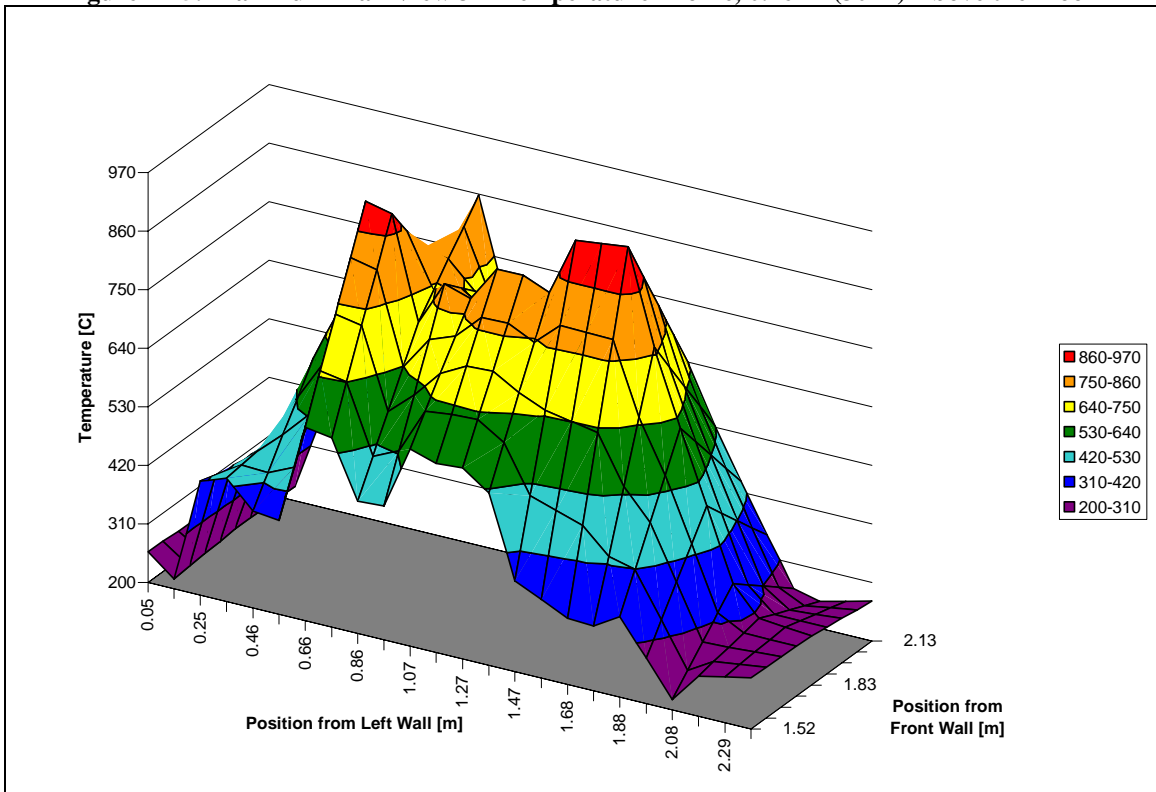


Figure 4-26: Maximum Plan View 3D-Temperature Profile, 1.07 M (42 in) Above the Floor

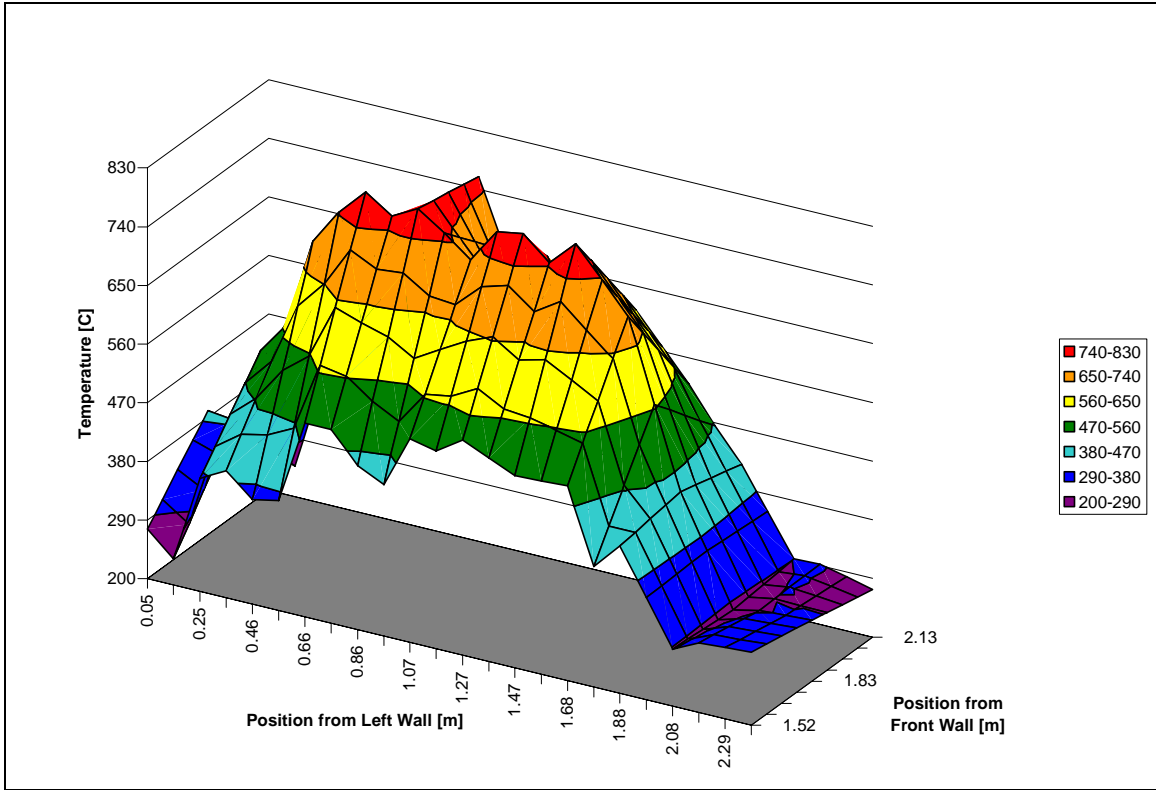


Figure 4-27: Maximum Plan View 3D-Temperature Profile, 1.37 M (54 in) Above the Floor

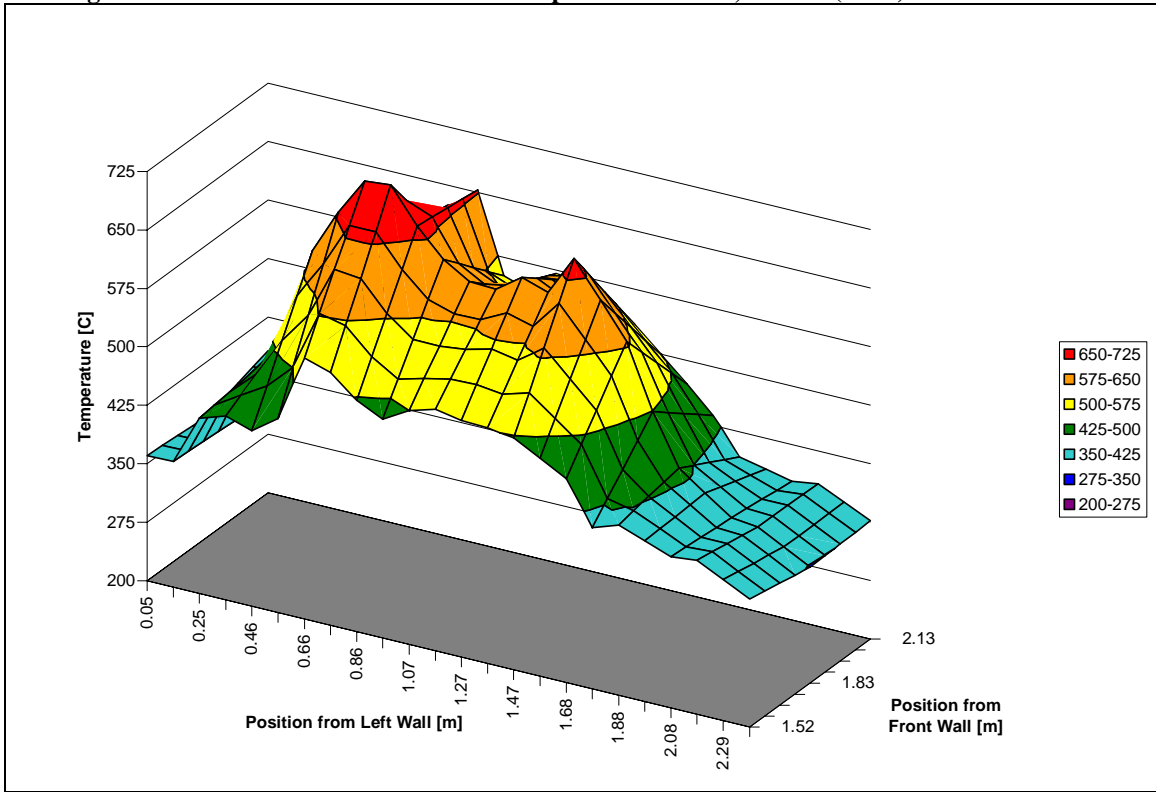


Figure 4-28: Maximum Plan View 3D-Temperature Profile, 1.68 M (66 in) Above the Floor

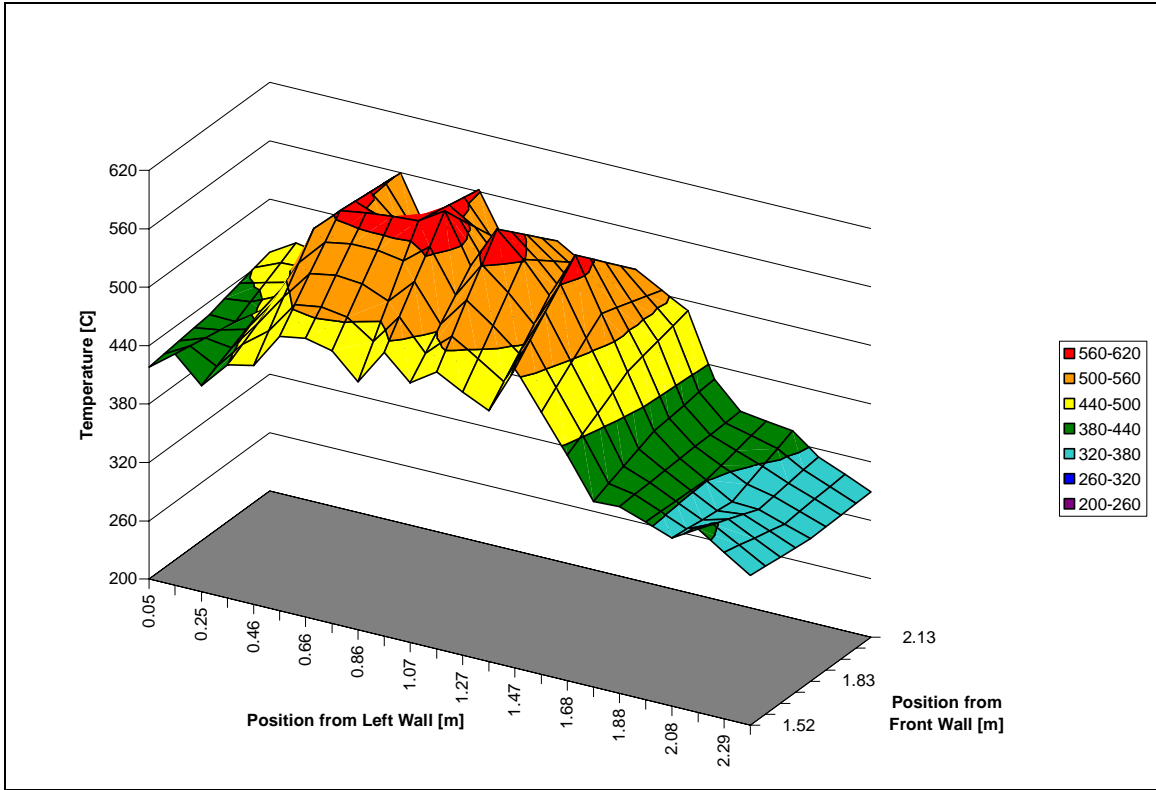


Figure 4-29: Maximum Plan View 3D-Temperature Profile, 1.98 M (78 in) Above the Floor

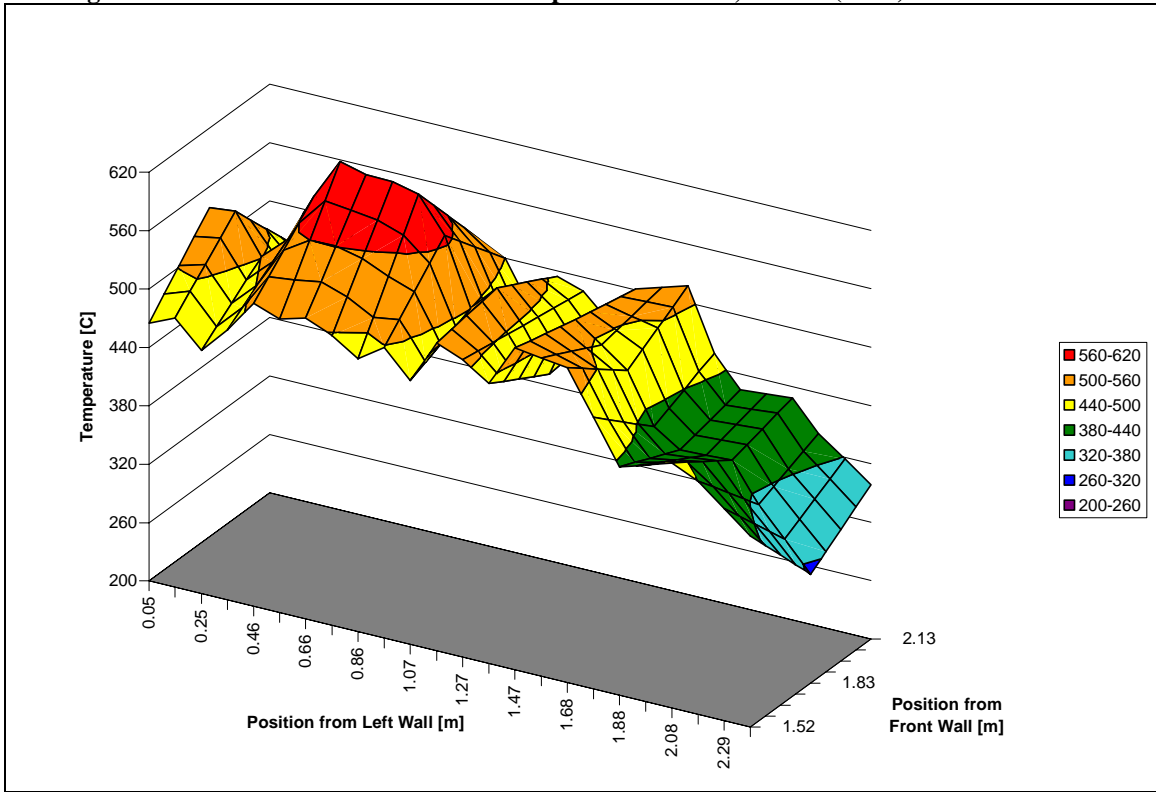


Figure 4-30: Maximum Plan View 3D-Temperature Profile, 2.29 M (90 in) Above the Floor

4.2.5 Average Temperature Profile

The average was based on removing any temperature measurements that were below 200°C. The value of 200°C was selected because the data showed that the room temperature rapidly increased above this value during heating and quickly decreased below this temperature during cooling. The average was then calculated based on all the measurements that were collected above this value. This average data gave similar temperature profiles to the maximum temperature shown in section 4.2.3.

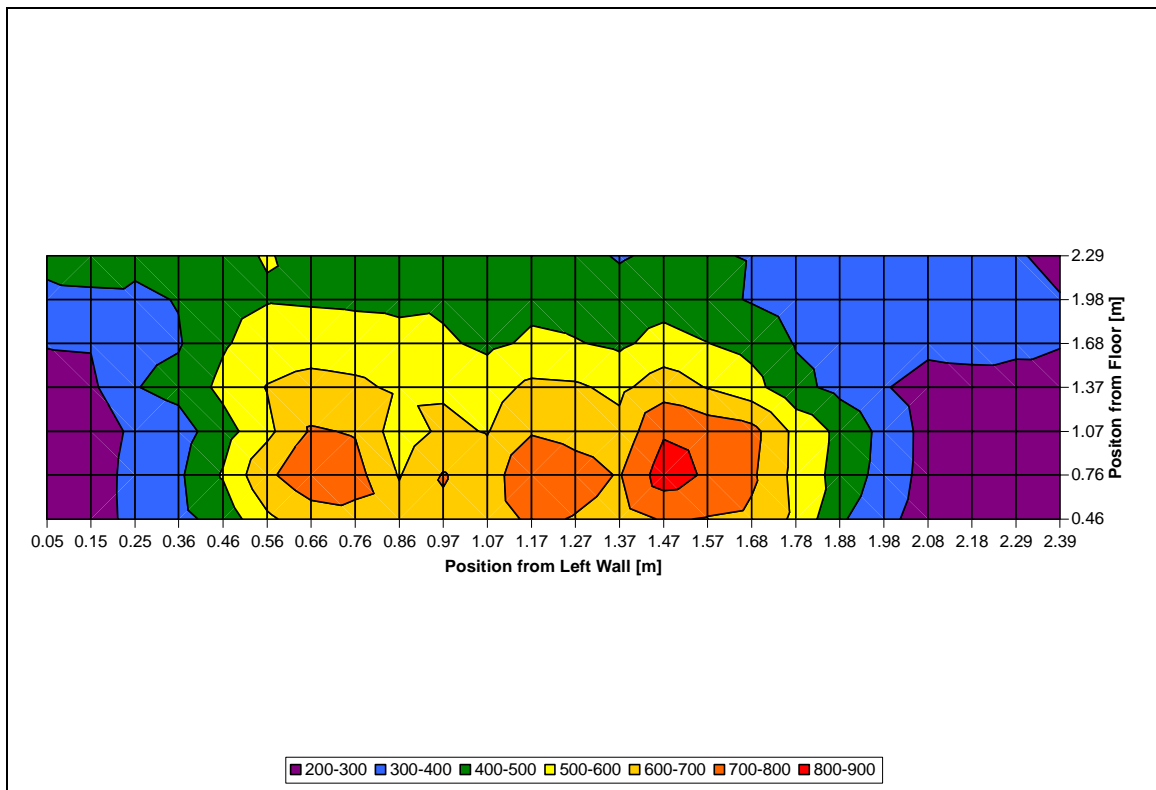


Figure 4-31: Average Temperature Profile of the Middle of the Burners.

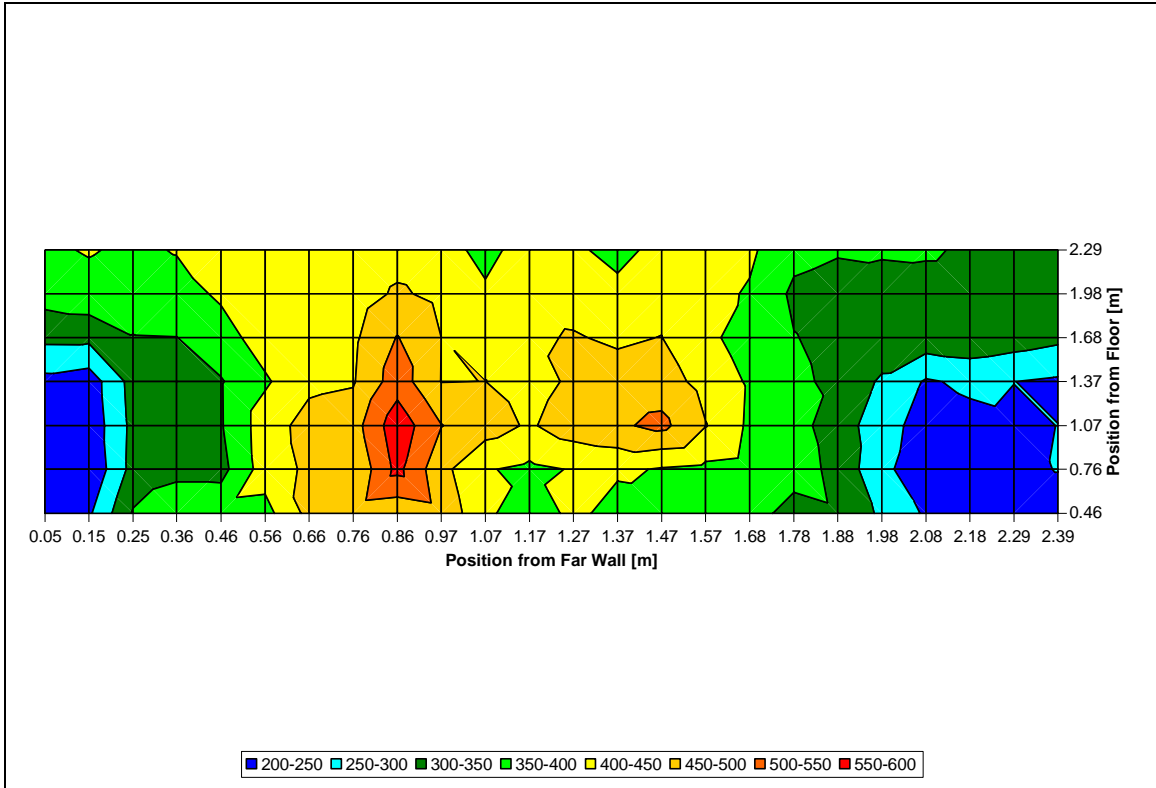


Figure 4-32: Temperature Profile of the Average Taken From the Back of the Burners

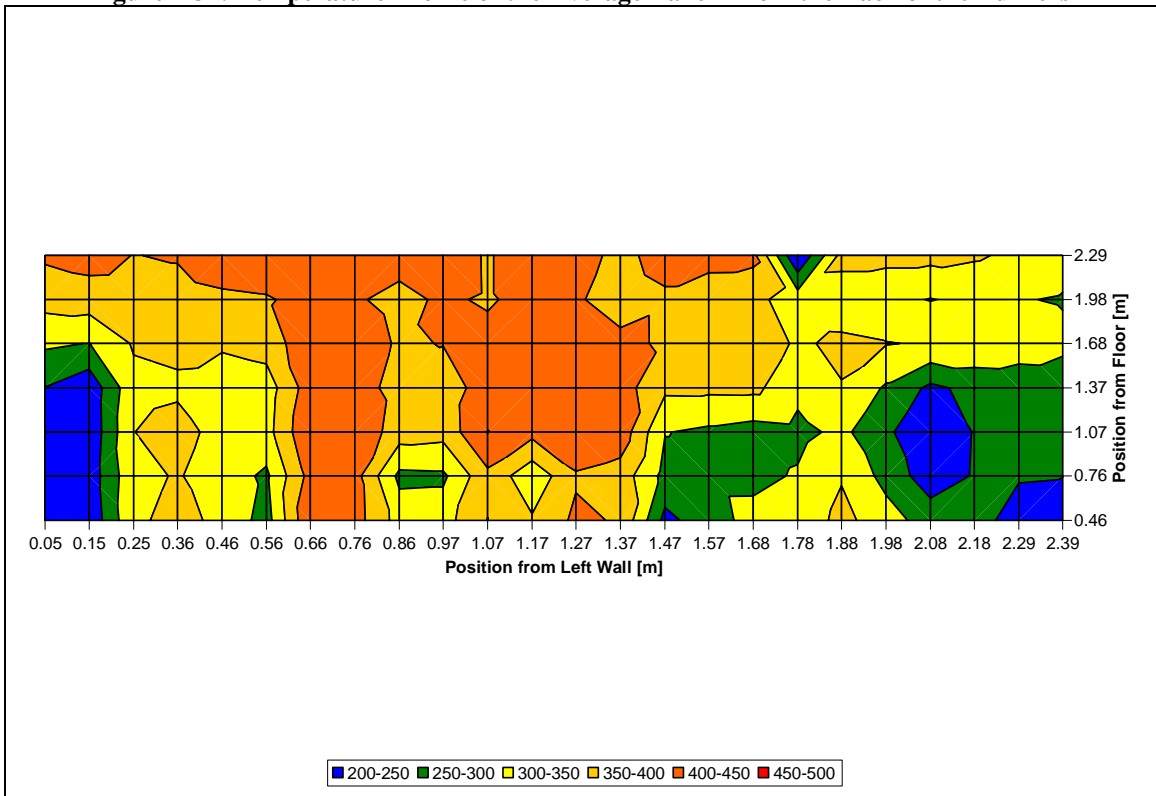


Figure 4-33: Temperature Profile of the Average Taken From the Front of the Burners

4.3 Flux Data Analysis

There were several heat flux measurements at five different elevations which are summarized in Table 4-1 and Table 4-2. Figure 4-34 is the average flux recorded for each measurement at different elevations. The average is calculated from a continuous data set that was recorded while the room was near a constant temperature. The standard deviation ranged from 4.8 to 20.2. High elevations of the flux gage resulted in greater fluctuation in values. This was due to the pulsing of the flame at higher elevations, and the inconsistent flame insult on the flux gage. A graph was created for each test that included the flux, temperature at the ceiling, and temperature in the duct of the blower. Figure 4-35 is an example of one of these individual tests. Figure 4-36 and Figure 4-37 show the centerline heat flux that was recorded on November 27th, 2001. The flux in this graph shows that it is in the design region of 84 kw/m² from about 0.71 m to about 1.1 m above the floor. However above 1.32 m, the heat flux fell sharply. This is most likely due to the fact that the flame is intermittent at this height. This can be corrected by slightly increasing the output of the burners to increase the flame height and stabilizing the flame at the ceiling of the room.

Location #	Position (Front-Back)
1	Left-Right
2	Left-Middle
3	Left-Left
4	Middle-Middle
5	Right-Right
6	Right-Middle
7	Right-Left

Table 4-1: Flux Locations (Horizontal)

Location #	Position (Bottom to Top)
1	0.41 m
2	0.71 m
3	1.02 m
4	1.32 m
5	1.62 m

Table 4-2: Flux Locations (Vertical)

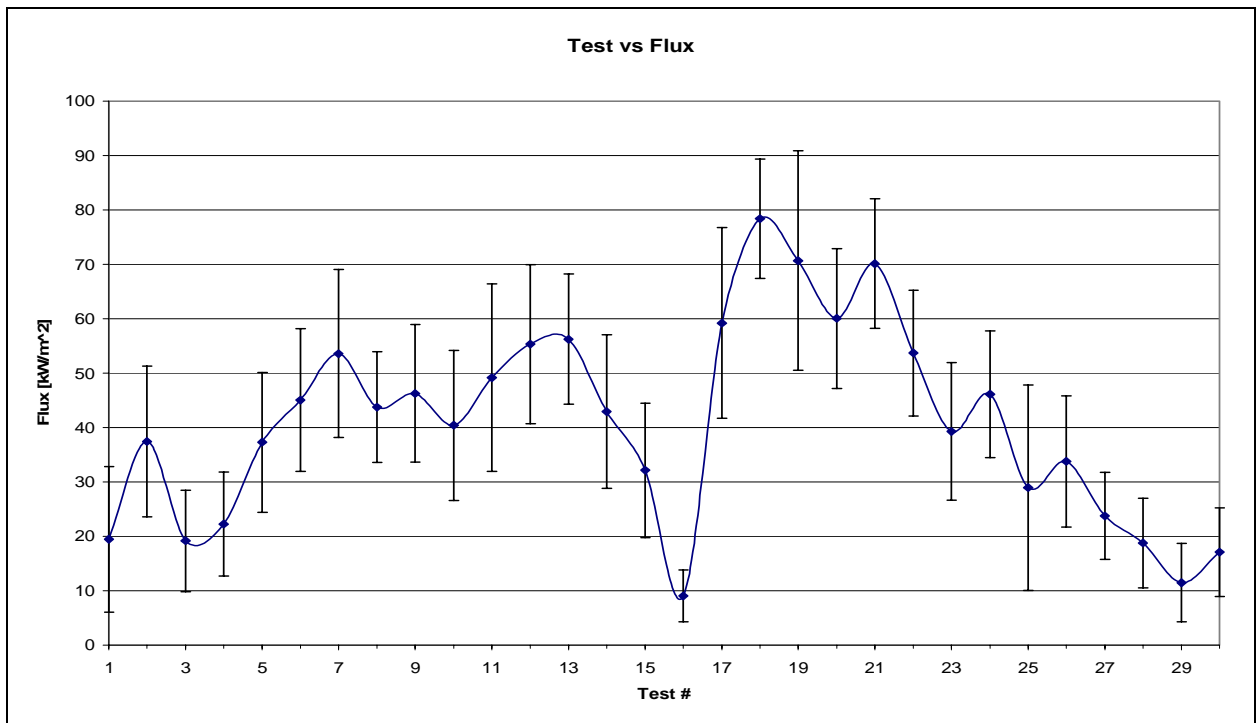


Figure 4-34: Average Flux Measurements Collected With Standard Deviation as Error Bars

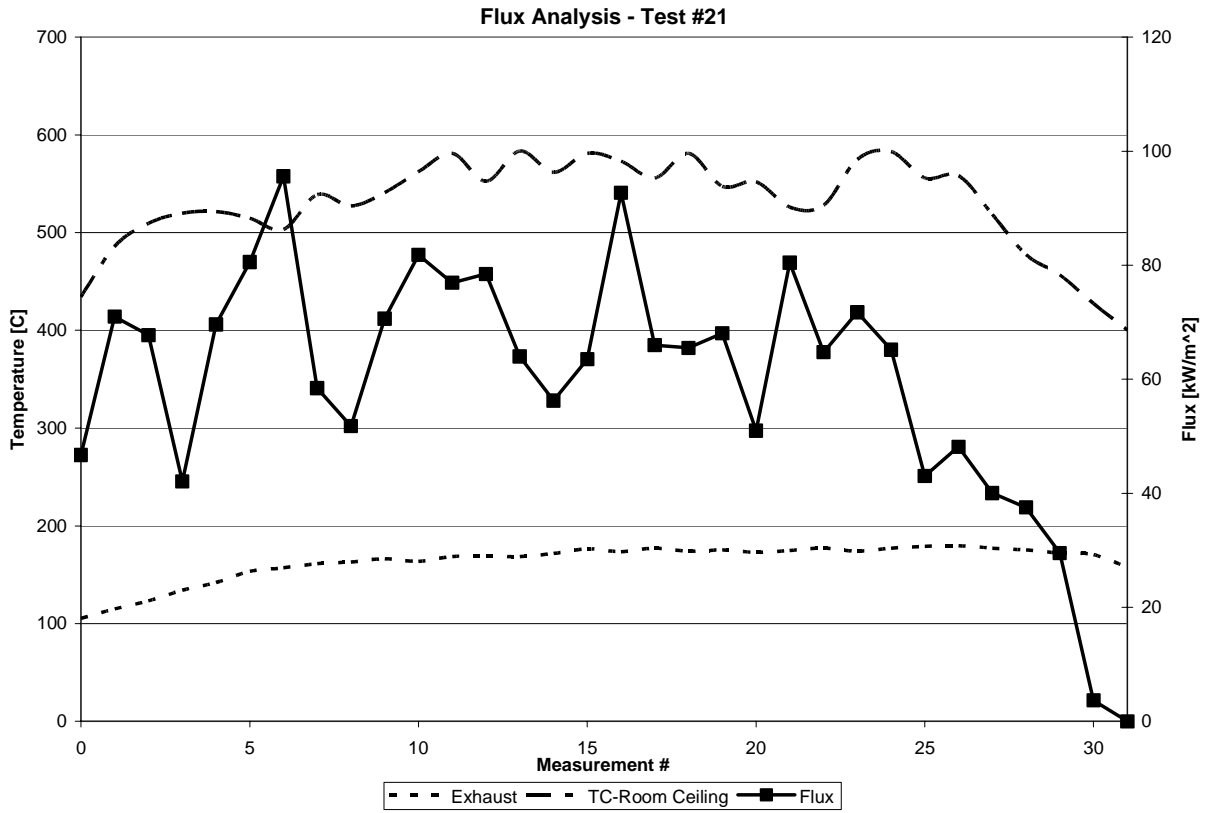


Figure 4-35: Flux and Temperature Measurements for Test #21 (Location 3)

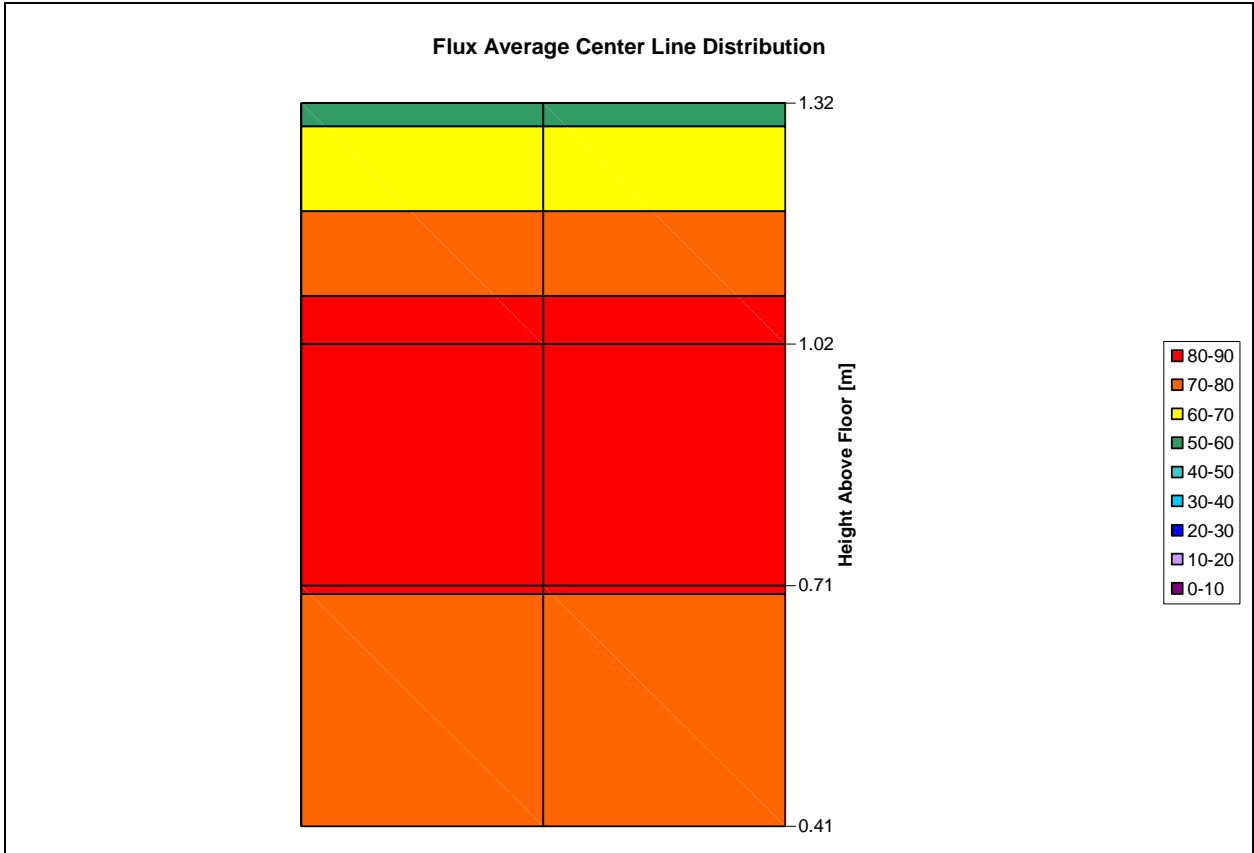


Figure 4-36: Flux at Middle of Burners Taken on November 27th

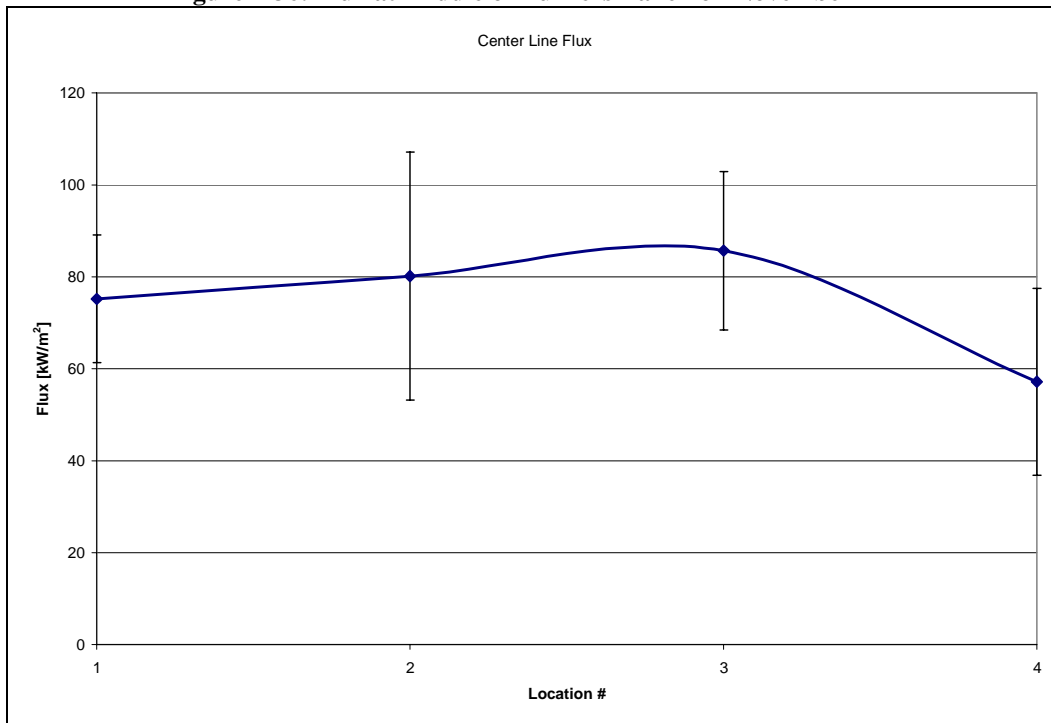


Figure 4-37: Flux at Middle of Burners Taken on November 27th

5.0 Conclusions

The initial data collected gives very positive results. The desired heat flux exposure of 84 kW/m² was obtained in the majority of the region to which the manikin was exposed. In the upper region of the room, the flame height was not consistent and the average heat flux was much less when compared with the lower portion of the room. The heat release rate was less than a megawatt for the initial testing; however the system is capable of delivering over a two megawatt fire. It is only a minor adjustment to increase the HRR and produce a constant flame height from the floor to the ceiling which would also increase the heat flux in the upper region of the room.

Additional Equipment

It is strongly suggested that a means to accurately measure the HRR be acquired to help insure reproducibility from test to test. The most desirable equipment to get is eight electronic flow meters than can be controlled from within the Lab View software. This would allow the entire test procedure to be pre-programmed and controlled using a computer. The estimated cost for the eight flow controllers and the equipment needed to run it, is approximately \$35,000. An alternative is to purchase a single flow controller and attach it to the main inlet thus being able to control the total input. This setup would reduce the cost significantly; however, it would also limit the configurations of the eight burners via the flow controllers. This would cost approximately \$7,000. The third alternative is to have an orifice plate to restrict the flow to a certain flow rate. This

option does not allow for any feedback in the system and a new orifice plate would be required for each desired setting. It would cost less than \$2,000 for the plate and the additional fittings.

It is also felt that a few Schmidt-Boelter or Gardon gages would prove more useful than thin skin calorimeters for measuring the flux. These gages could be placed at the centerline of the room to measure the flux to the wall and thus provide test to test comparisons of the heat flux to the walls. These water cooled gages cost about \$1,500 each to purchase and calibrate.

Possible Room Configurations

In addition to increasing the heat release rate of the burners, it is believed that a different burner configuration would provide valuable in evaluating the level of protection of a garment. The suggested burner configurations are discussed in more detail in appendix C of this report.

Conclusion

This work will hopefully lead to the development of a completely new test standard which will enable clothing to be more accurately evaluated when determining the level of protection they may provide against thermal exposures. The majority of test standard for clothing do not account for different fire scenarios or the effect that movement may have on the test performance. These benefits are the basis of the new test and it is hoped that a comparative analysis with the current standards can be done in the near future.

6.0 References

- [1] Air Standard 61/81 Tests for Protective Capacity of Fire Resistant Clothing Materials (Washington, D. C.: United States Air Force, Air Standardization Coordinating Committee, 1990).
- [2] American Burn Association. "Burn Incidence and Treatment in the US: 2000 Fact Sheet". <http://www.ameriburn.org/pub/factsheet.htm>, 3/31/02.
- [3] ASTM D 1230-94 Standard Test Method for Flammability of Apparel Textiles, (Philadelphia, PA: American Society for Testing and Materials, 1994).
- [4] ASTM D 4108-87 Standard Test Method for Thermal Protective Performance of Materials for Clothing by Open-Flame Method, (Philadelphia, PA: American Society for Testing and Materials, 1987).
- [5] ASTM F 1060-87 Standard Method for Thermal Protective Performance of Materials for Protective Clothing for Hot Surface Contact, (Philadelphia, PA: American Society for Testing and Materials, 1987).
- [6] ASTM F 1358-95 Standard Method for Effects of Flame Impingement on Materials Used in Protective Clothing Not Designed Primarily for Flame Resistance, (Philadelphia, PA: American Society for Testing and Materials, 1995).
- [7] ASTM F 1930-99 Standard Test Method for Evaluation of Flame Resistant Clothing for Protection Against Flash Fire Simulations Using an Instrumented Manikin (American Society for Testing and Materials, 1999).
- [8] Audet, Norman F. and Spindola, Kenneth J., "U. S. Navy Protective Clothing Program," *Performance of Protective Clothing, ASTM STP 900* (1986).
- [9] Baker, Roger L. et al, Review and Evaluation of Thermal Sensors for use in Testing Firefighters Protective Clothing NIST GCR 99-772 (Gaithersburg, MD: National Institute of Standards and Technology, 1999).
- [10] Behnke, Wallace P. et al, "Thermo-Man® and Thermo-Leg: Large Scale Test Methods for Evaluating Thermal Protective Performance," *Performance of Protective Clothing: Fourth Volume, ASTM STP 1133*, (1992).

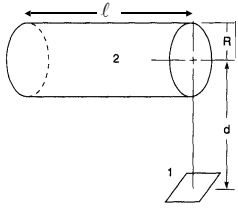
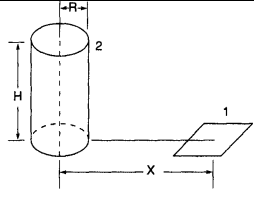
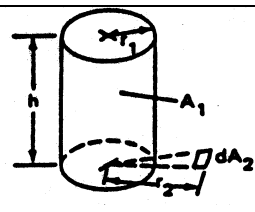
- [11] *CFR 16 Part 1610 – Standard for the Flammability of Clothing Textiles* (United States Government, Office of the Federal Registrar, 1995).
- [12] Dale, James D. et al, “Instrumented Manikin Evaluation of Thermal Protective Clothing,” *Performance of Protective Clothing: Fourth Volume, ASTM STP 1133*, (1992).
- [13] DiNenno, Philip. SFPE Handbook of Fire Protection Engineering – Second Edition. National Fire Protection Association; Quincy, MA. 1995.
- [14] Drysdale, Dougal. An Introduction to Fire Dynamics – Second Edition. John Wiley & Sons; Chichester: 1998.
- [15] Hilado, Carlos J., *Flammability Test Methods Handbook* (Westport, Connecticut: Technomic Publishing Co., Inc., 1973).
- [16] Kidd, C. T., and C. G. Nelson, How the Schmidt-Boelter Gage Really Works; 41st Intn'l Instruments Symp, May 1995, Denver, Colo.
- [17] Lantz, Renee V., *Ignition Index – An Engineering Based Methodology for Fabric Flammability Testing*, (M.S. Thesis, Worcester Polytechnic Institute, 1994).
- [18] Leblanc, Dave *Fire Environments Typical of Navy Ships, Draft No. 3*, (M.S. Thesis, Worcester Polytechnic Institute, 1998).
- [19] Mills, A. F. Heat Transfer – Second Edition. Prentice Hill; Upper Saddle River, NJ: 1999.
- [20] Munson, Bruce R., Donald F. Young & Theodore H. Okiishi. Fundamentals of Fluid Mechanics – Third Edition Update. John Wiley & Sons, Inc; New York: 1998.
- [21] “NFPA 701,” *1998 National Fire Codes*, (Quincy, MA: National Fire Protection Association, 1998).
- [22] “NFPA 1976,” *1998 National Fire Codes*, (Quincy, MA: National Fire Protection Association, 1998).
- [23] “NFPA 1977,” *1998 National Fire Codes*, (Quincy, MA: National Fire Protection Association, 1998).
- [24] “NFPA 1971,” *1998 National Fire Codes*, (Quincy, MA: National Fire Protection Association, 1998).

- [25] “NFPA 1975,” *1998 National Fire Codes*, (Quincy, MA: National Fire Protection Association, 1998).
- [26] Sonntag, Richard E., Claus Borgnakke & Gordon J. Van Wylen. Fundamentals of Thermodynamics – Fifth Edition. John Wiley & Sons, Inc; New York: 1998.
- [27] Torvi, David A. and Dale, J. Douglas, “Heat Transfer in Protective Fabrics Under Flash Fire Conditions”
- [28] Christopher J. Wieczorek and Nicholas A. Dembsey, “Engineering Guide for Predicting 1st and 2nd Degree Skin Burns From Thermal Radiation,” (Society of Fire Protection Engineers, SFPE Engineering Task Group on Engineering Practices, Thermal Radiation Hazards, 1998).
- [29] Bradbury, Laura, Cardina, Jason and Daelhousen, Matthew. “Traversing Mechanism for Clothing Flammability Test” (MQP, Worcester Polytechnic Institute, 2001).

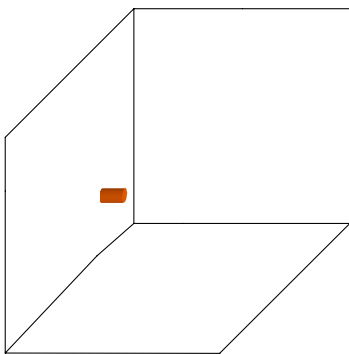
Appendix A - Sample Calculations

Configuration Factors

Table A-1: Cylindrical Burner Configuration Factors (Appendix D – SFPE HB)

No	View	Shape Factor
1		$D = \frac{d}{r} \quad L = \frac{l}{r} \quad A = (D+1)^2 + L^2 \quad B = (D-1)^2 + L^2$ $F_{12} = \frac{1}{\pi D} \tan^{-1} \left(\frac{L}{\sqrt{D^2 - 1}} \right) + \frac{L}{\pi} \left[\frac{A - 2D}{D\sqrt{AB}} \tan^{-1} \sqrt{\frac{A(D-1)}{B(D+1)}} - \frac{1}{D} \tan^{-1} \sqrt{\frac{D-1}{D+1}} \right]$
2		$X' = \frac{X}{H} \quad R' = \frac{R}{H}$ $F_{12} = \frac{1}{\pi} \left[\tan^{-1} \left(\sqrt{\frac{X' + R'}{X' - R'}} \right) - \frac{(1.0 + X'^2 - R'^2)}{(1.0 + X'^2 + R'^2)} \tan^{-1} \sqrt{\frac{X' - R'}{X' + R'}} \right]$
3		$L = \frac{h}{r_2} \quad R = \frac{r_1}{r_2} \quad X = \sqrt{(1 + L^2 + R^2) - 4R^2}$ $F_{12} = \frac{1}{2\pi} \cos^{-1}(R) + \frac{1}{\pi} \left\{ \tan^{-1} \left(\frac{R}{\sqrt{1 - R^2}} \right) - \frac{1 + L^2 - R^2}{X} \tan^{-1} \left[\frac{X \tan(0.5 \cos^{-1}(R))}{1 + L^2 + R^2 - 2R} \right] \right\}$

Jet/Spray Fire Calculations



In order to determine the radiative heat flux from a jet/spray fire to a target, several variables must first be determined. The required variables are the heat release rate of the burner, the net heat of combustion of the fuel, the mass flow rate of the fuel source, the surface area of the flame, and the view factor of the flame to a target.

Table A-3 has the equation used to determine the heat flux to a target while table A-1 has the configuration factors for the simplified cylindrical approximation of the flame.

Table A-2: The Heat Flux Equations for a Jet /Spray Fire

Equation	The Terms	No	Ref
$\dot{q}_{rad}'' = E_f \Phi \tau$	\dot{q}_{rad}'' is the radiant heat flux to the target (kW/m ²) E_f is the flame emissive power (kW/m ²) Φ is the flame-element shape factor correction τ is the atmospheric transmissivity (taken as 1)	(0.1)	13
$E_f = \frac{Q_{rad}}{A_f}$	Q_{rad} is the radiant heat release (kW) A_f is the surface area of the flame (m ²)	(0.2)	
$\dot{Q}_{ch} = \dot{m} \Delta H_c \chi_{ch}$	\dot{Q}_{ch} is the chemical heat release rate (kW) \dot{m} is the mass flow rate (kg/sec) ΔH_c is the net heat of combustion (kJ/kg) χ_{ch} is the combustion efficiency	(0.3)	13
$\dot{m} = V_{exit} A_{exit} \rho$	\dot{m} is the mass flow rate (kg/sec) V_{exit} is the exit velocity of the flammable liquid (m/sec) A_{exit} is the discharge area (m ²) ρ is the fluid density (kg/m ³)	(0.4)	
$V_{exit} = \sqrt{\frac{2 \left(\frac{p_{amb}}{\rho} - \frac{p_{line}}{\rho} \right)}{\frac{A_{inlet}^2}{A_{exit}^2} - 1}}$	V_{inlet} is the fluid velocity at the inlet to the nozzle (m/sec) V_{exit} is the fluid velocity at the exit of the nozzle (m/sec) p_{line} is the absolute pressure measured in the line (Pa) p_{amb} is the ambient pressure (Pa) A_{inlet} is the area of the hose at the inlet to the nozzle (m ²) A_{exit} is the area of the discharge orifice of the nozzle (m ²) g is the acceleration due to gravity (9.81 m/sec ²) ρ is the fluid density (kg/m ³)	(0.5)	13
$L_f = 0.578 Q^{0.824} + 0.42$	L_f is the flame length (m) Q is the heat release rate (MW)	(0.6)	
$\frac{H}{D} = 3.7 \dot{Q}^{*2/5} - 1.02$	H is the flame height (m) \dot{Q}^* is the ND heat release rate	(0.7)	13
$\dot{Q}^* = \frac{\dot{Q}}{\rho_{\infty} C_p T_{\infty} \sqrt{g D D^2}}$	\dot{Q}^* is the ND heat release rate (ND) \dot{Q} is the heat release rate (kW) ρ_{∞} is the density of air at STP (kg/m ³) C_p is the specific heat of air (kJ/kg-K) T_{∞} is the temperature of air at STP (K) g is the gravitational constant (m/s) D is the diameter of the flame (m)	(0.8)	13

Since

$$\dot{Q} = \dot{m} \Delta H_c x$$

$$\dot{m} = V_{exit} A_{exit} \rho$$

Thus for a 10,000 kilowatt hydraulic oil fire, (where the combustion efficiency is 0.84), and the density of the liquid is 760 kg/m³.

$$10,000 \text{ kw} = \dot{m} \left(46.4 \frac{\text{kJ}}{\text{kg}} \right) (0.84)$$

The mass flow rate can be calculated

$$\frac{10,000 \frac{\text{kJ}}{\text{s}}}{\left(46.4 \frac{\text{kJ}}{\text{kg}} \right) (0.84)} = \dot{m} = 256.5 \frac{\text{kg}}{\text{s}}$$

And the mass flow rate is dependent on area of the exit and the velocity of the exit.

$$256.5 \frac{\text{kg}}{\text{s}} = V_{exit} A_{exit} \left(760 \frac{\text{kg}}{\text{m}^3} \right)$$

$$\frac{256.5 \frac{\text{kg}}{\text{s}}}{760 \frac{\text{kg}}{\text{m}^3}} = V_{exit} A_{exit}$$

Since the exit velocity is dependent on the pressure of the line, the 10,000 kilowatt heat release rate can be achieved by many combinations of $V_{exit} A_{exit}$.

Pool Fire Calculations

For the pool fire configuration, the fire will again be considered a cylindrical flame. The shape factors used in the jet/spray fire (see Table A-1) are the same ones used for the

pool fire. However, it is important to establish the orientation of both the flame and the intended target, as these will both vary between the jet/spray and the pool fire.

One consideration that needs to be recognized is the effects a non-circular pan fire would have on the configuration and the heat flux from the fire. A problem could arise when a large pool fire is desired, as the room is only 8 by 12 feet and there needs to be a certain length for the manikin to be able to enter and exit the room.

Table A-3: The Heat Flux Equations for a Pool Fire

Equation	The Terms	No	Ref
$Q = m'' \Delta H_c x_{chem} \pi \frac{d^2}{4}$	Q is the chemical heat release rate (kW) m'' is the mass burning rate per unit surface area (kg/m ² -sec) ΔH_c is the net heat of combustion (kJ/g) x _{chem} is the combustion efficiency d is the pool fire diameter (m)	(0.9)	
$D_{max} = 2 \left(\frac{V_s}{\pi y} \right)^{\frac{1}{2}}$	D _{max} is the maximum pool diameter V _s is the volumetric spill rate (m ³ /sec) y is the liquid pool fire regression rate (m/s)	(0.10)	13
$Q = \rho_L V_s \Delta H_c x_{chem}$	ρ_L is the liquid density (kg/m ³)	(0.11)	
$m'' = m''_{\infty} (1 - e^{-k'D})$	M'' is the mass burning rate per unit surface area (kg/m ² -sec) m'' _∞ is the asymptotic mass burning rate for large pool fires k' is the effective absorption coefficient D is the pool diameter (m)	(0.12)	13
$t_{max} = \frac{0.564 D_{max}}{(gyD_{max})^{\frac{1}{3}}}$	D _{max} is the maximum pool diameter (m) g is the gravitational acceleration (9.81 m/sec ²) y is the pool regression rate (m/s)	(0.13)	13
$H_f = 0.23 \dot{Q}^{*\left(\frac{2}{5}\right)} - 1.02 D$	H _f is the flame height (m) \dot{Q}^* is the non-dimensional heat release rate (kW) D is the fire diameter (m)	(0.14)	13
$E_f = \epsilon \sigma (T_f^4 - T_a^4)$	E _f is the flame emissive power (kW/m ²) ε is the emissivity σ is the Stefan-Boltzmann constant (kW/m ² K ⁴) T _f is the flame temperature (K) T _a is the ambient temperature (K)	(0.15)	13
$\epsilon = 1 - e^{-kL}$	k is the effective emission/absorption coefficient (m ⁻¹) L is the mean equivalent beam length of the flame (m)	(0.16)	13

Since

$$\dot{Q}_{ch} = \dot{m}'' \Delta H_c A x_{chem}$$

$$D_{max} = 2 \left(\frac{V_s}{\pi y} \right)^{\frac{1}{2}}$$

$$\dot{Q}_{ch} = \rho_L V_s \Delta H_c x_{chem}$$

The heat release rate dependent upon the diameter can be calculated. The figure belows show the diameter dependent HRR for various fuels.

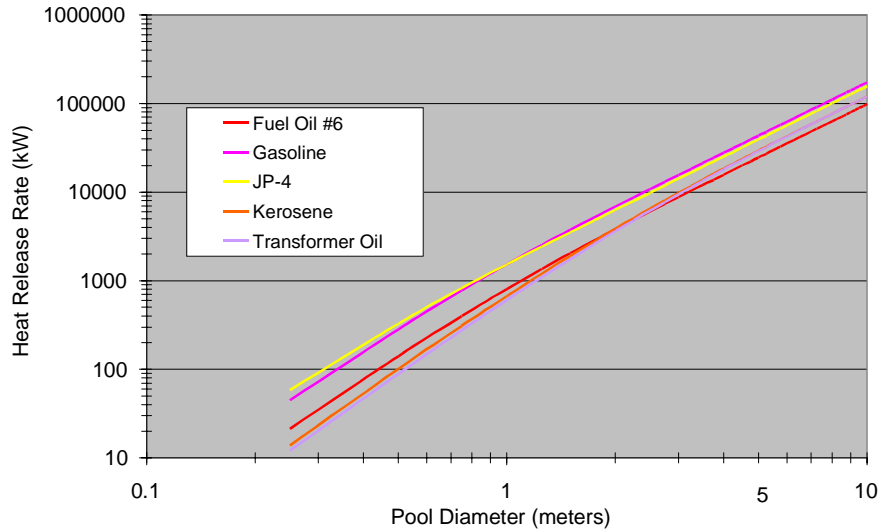


Figure A-1: Predicted Heat Release Rate vs. Pool Diameter

The mass burning rate needed to maintain a pool fire of a given size is then calculated using Babrauskas equations for hydrocarbon fuels. (SFPE HB 3-1)

$$\dot{m}'' = \dot{m}''_{\infty} (1 - e^{-k\beta D})$$

The following graph shows the steady state burning rates of selected fuels that are available onboard a naval vessel.

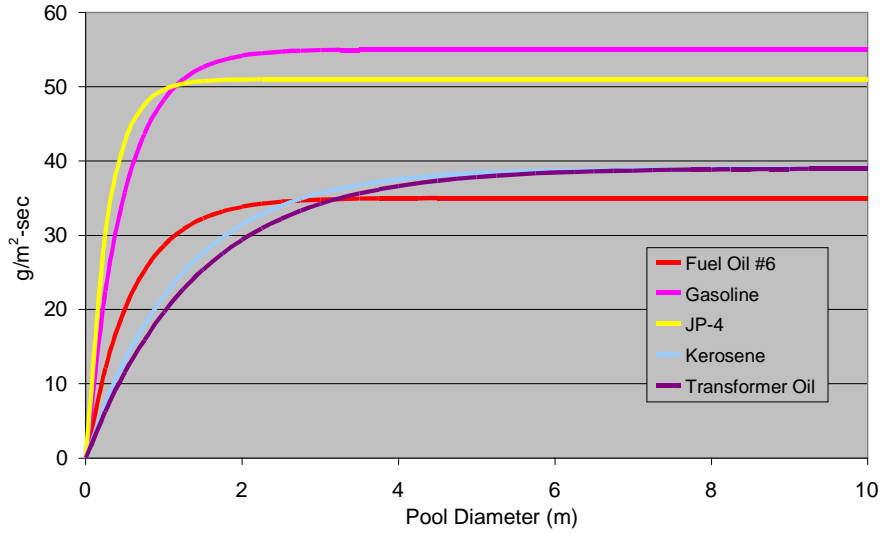


Figure A-2: Pool Fire Mass Burning Rate Per Unit Surface Area

Another consideration for larger pool fires is the growth time of the fire. For small fires, the time to reach steady state is considered small and thus can be neglected. However, in the case of a large pool fire, the time needed to reach steady state could be significant. As in this period of time, one might be able to escape before the room conditions become untenable. Thus the following equation developed by Raj was used to calculate the time needed for a pool fire to reach steady state burning (SFPE HB 3-11).

$$t_{\max} = \frac{0.564D_{\max}}{(gyD_{\max})^{\frac{1}{3}}}$$

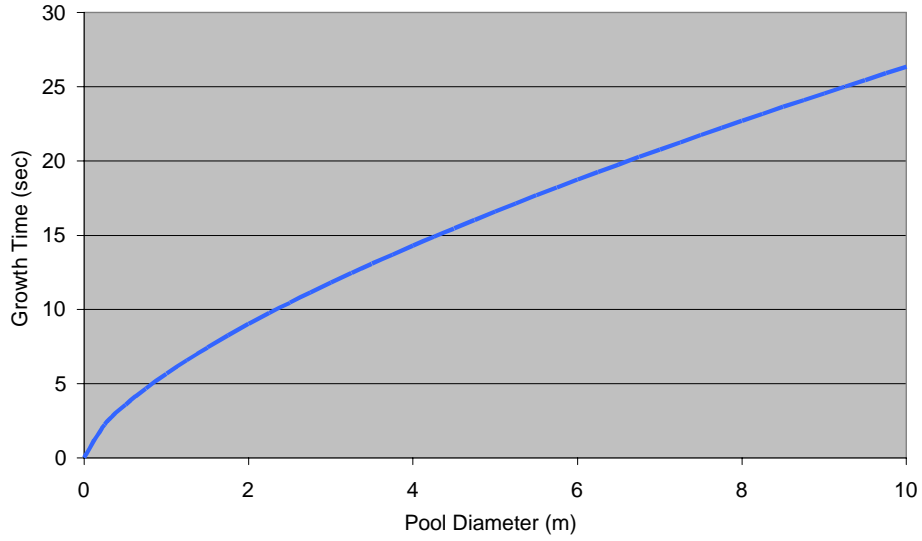


Figure A-3: Pool Fire Growth Time to Peak Heat Release Rate

The Heskestadt flame height correlations (SFPE HB 2-1) were used to determine the flame height of the pool fires of different diameters.

$$H_f = 0.23\dot{Q}^{\frac{2}{5}} - 1.02D$$

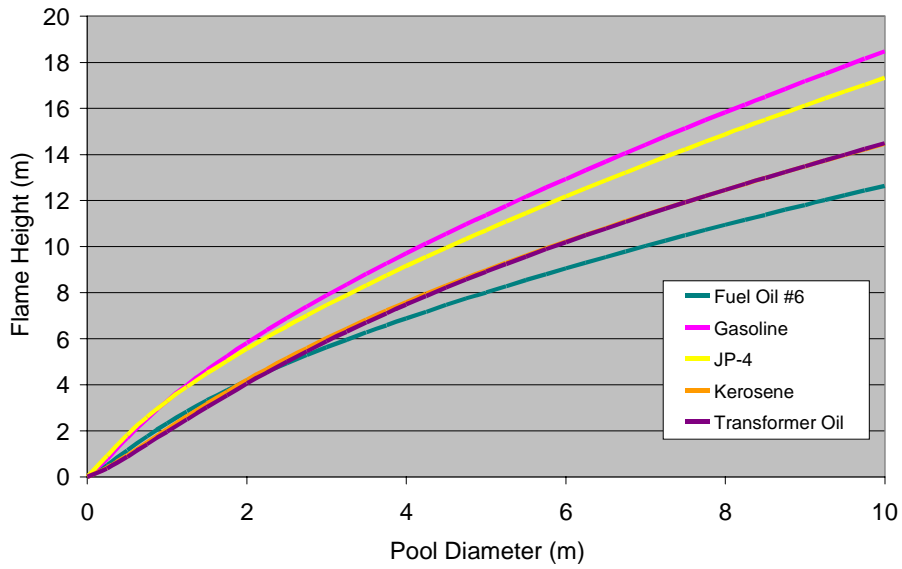


Figure A-4: Pool Fire Flame Heights

Velocity Calculations using pitot tube

$$\text{Air Velocity (V)} = 1096.2 \sqrt{\frac{P_v}{D}}$$

Where P_v = Velocity pressure in inches of water
 D = Air density in lbs / ft³

$$\text{Air Density (D)} = 1.325 \left(\frac{P_b}{T} \right)$$

Where P_b = Barometric Pressure in inches of HG
 T = Absolute Temperature (indicated temp in °F + 460)
 D = 0.075 lbs / ft³ @ 70 °F and 29.9 in of HG

Area of Ductwork (A)

For d = 16 in

$$\text{Area} = \pi r^2 = (\pi d^2)/4 = 64\pi \text{ in}^2 = (4/9)\pi \text{ ft}^2 \sim 1.396 \text{ ft}^2$$

For d = 22 in

$$\text{Area} = \pi r^2 = (\pi d^2)/4 = 121\pi \text{ in}^2 \sim 2.639 \text{ ft}^2$$

Volumetric Rates (V)

$$10,000 \frac{\text{ft}^3}{\text{min}} = \text{The lower limit} \qquad 15,000 \frac{\text{ft}^3}{\text{min}} = \text{The desired air flow}$$

$$\text{Velocity (V)} = \frac{V}{A}$$

For d = 22 in

$$V = 10,000 \frac{\text{ft}^3}{\text{min}} \times \frac{1}{2.639 \text{ ft}^2} = 3,789 \frac{\text{ft}}{\text{min}} \qquad V = 15,000 \frac{\text{ft}^3}{\text{min}} \times \frac{1}{2.639 \text{ ft}^2} = 5,683 \frac{\text{ft}}{\text{min}}$$

Summary Calculations

T (°C)	P _b (HG)	D (lbs/ft ³)	P _v (in)	Velocity (ft/min)	V (ft ³ /min)
20	29.9	0.075	1.80	5,369	14,173
136	29.9	0.054	1.15	5,069	13,383
154	29.9	0.052	1.15	5,179	13,674

Appendix B - Drawings of Traversing Mechanisms

Tracking System

The following section is a summary taken from the technical report on the design and construction of the tracking system. [29]

The manikin travels along a system that is specifically designed for use in this application. This track is a 40 ft. long overhead conveyor system, and consists of a chain, a motor to drive the chain, an enclosure to shield the chain from the heat of the room, and hangers to carry the manikin and the attached thermocouple wires (see Figure B-1 and Figure B-2).

The protective enclosure is 40 feet of Channel beam (C4X5.4, made of ASTM A36 structural steel), divided into three sections of 9 ft., 11 ft., and 20 ft. The 20-foot section is used for the tracking system inside the room, while the 9-foot section is on the outside of the room and holds the motor. The 11-foot section of C-beam is attached to the opposite end of the 20-foot section and is the area where the manikin is prepared for each test. The three sections of track are mounted flush to one another with mounting brackets at the top and bottom of the adjoining beam ends. [29]

The siding of the track is joined to the main C beam with welds. The siding of the track is constructed of lengths of 3/8-inch A36 steel, 2 inches high. This siding, together with the C beam, then acts as a protective shield from the heat of the room (See Appendix A, Figure 3). It was found that further protection can be reached by covering the track with a thin

layer of thermal resistant material, Kaowool. The track is covered with the Kaowool only inside the room, where direct exposure to the hot upper gas layer occurs.

A motor is mounted horizontally, and perpendicular to the outside of the C beams at the start of the 9-foot long section of the track and to the first support just outside the hood. A hole is drilled through the side of the C beam and a drive shaft is inserted through the hole. The motor rotates the drive shaft, which in turn rotates a roller chain sprocket.

A carbon steel single strand ANSI Roller chain wraps around the sprocket, and runs the entire length of the track, wrapping around a free spinning idler sprocket at the opposite end of the track. Smooth bolts with bronze sleeve bearings are inserted through the side of the track every four feet to prevent sagging of the chain.

A hanger is attached to the top length of the roller chain with 1/8 inch set screws. This hanger is used to support the manikin as it travels through the burning room. Similar, smaller hangers travel behind the manikin's hanger, and carry the thermocouple wires that extend from the manikin.

Using a stopwatch, the time it took for the mannequin to travel from one end of the 12 ft. room to the other end was recorded. This was done multiple times. In each case, it took 5.2 seconds for the mannequin to move from one end of the room to the other. Dividing the 12 ft. by 5.2 seconds, the maximum speed of the manikin is 2.31 ft./sec. The speed can

be reduced as necessary by cutting the power to the motor with a variable speed transformer.

Due to the weight and length of the chain used in the conveyor, it is not possible to simply assemble the unit by pulling the ends of the chain tight and connecting them. Therefore, it is necessary to include a means for tightening the chain once the unit is assembled. In addition, chains stretch with exposure to heat and extended use, so this design allows for tuning of the chain as the track is used.

The sprockets at each end of the track were initially placed close enough to each other to allow the chain ends to be connected by hand during assembly, and then moved apart to tighten the chain. This was accomplished by placing the free spinning end sprocket's axle in horizontal slots in the track's sidewalls (See Figure B-3). In this slot the sprocket can be moved closer to or farther from the motor sprocket at the opposite end. The sprocket and axle are adjusted and held in place using screws that run on the outside of the track walls, parallel to the track length. As the screws are tightened, the sprocket is forced away, tightening the chain. The screws must be tightened or loosened together in order to keep the sprocket aligned properly. The beam is constructed with six inches of available adjustment.

The system is mounted inside the room by inserting two, ½ in. high strength (grade 8) steel bolts through the track into the steel frame at the very edges of the modified ATSM Standard Room, above the doorways as well as placing two more bolts at four feet in from

each door. The 9-foot and 11-foot sections of the track that extend out of the room are supported by end-stands on which the track rests. The base of each stand is fitted with adjustable feet, so the stand can be raised or lowered in order to keep the track sections level.

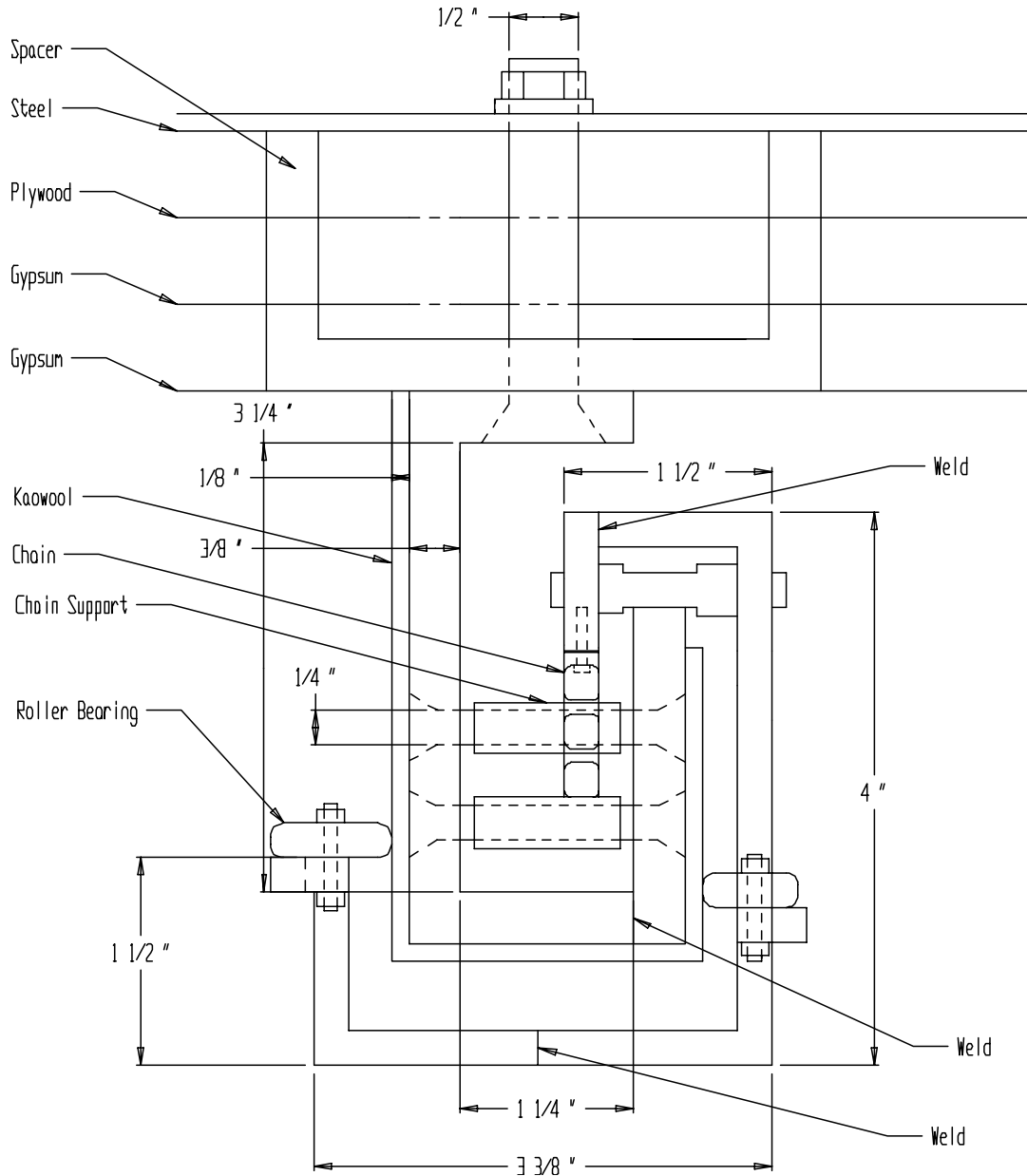


Figure B-1: Carriage Mechanism for Track

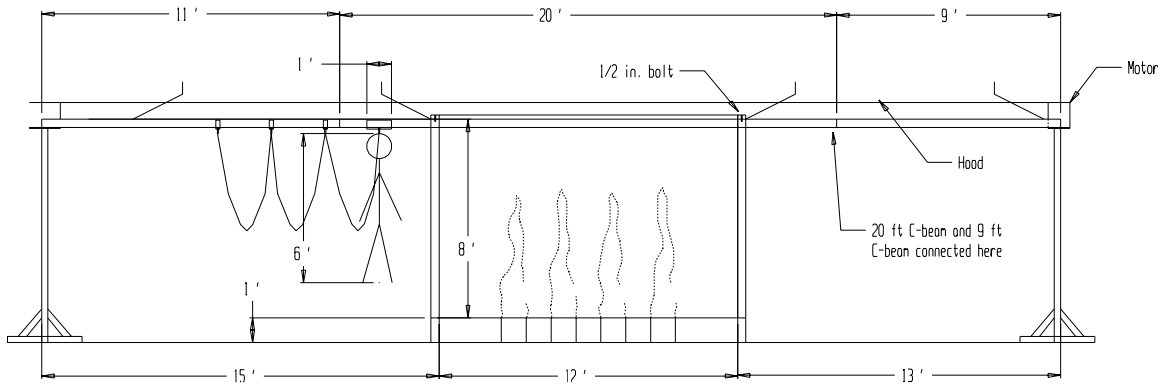


Figure B-2: Track Illustration

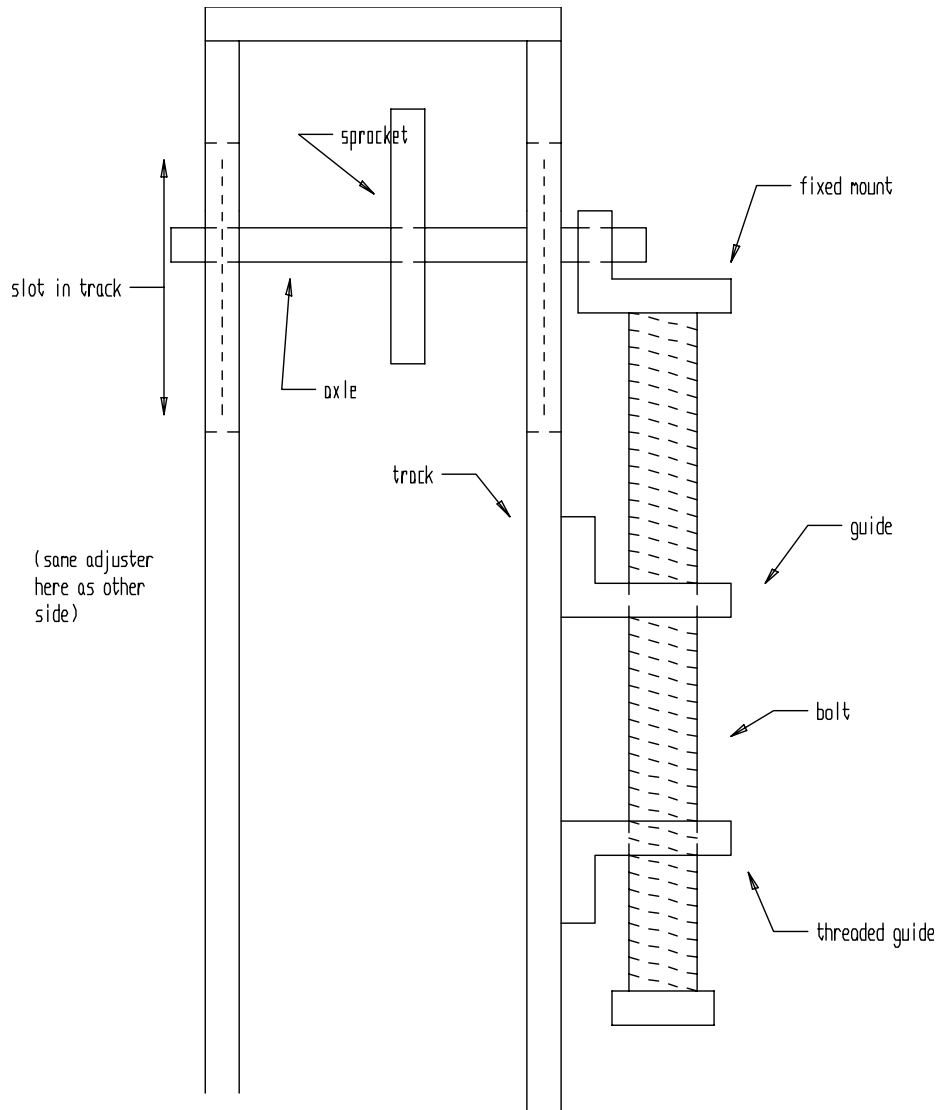


Figure B-3: Chain Tightening Mechanism

Appendix C – Different Burner Configurations

Figure C-1 illustrates several possible burner configurations of which A and B are the standard configuration. These two layouts have the burners pack in tight in either perpendicular with the track (A) or in line with the track (B) and are design to let the 8 burners act as a single burner. These are the simplest approach and provided the most realistic fire. Figure (C) is an example of moving the burners back to remove any flame impingement from the clothing.

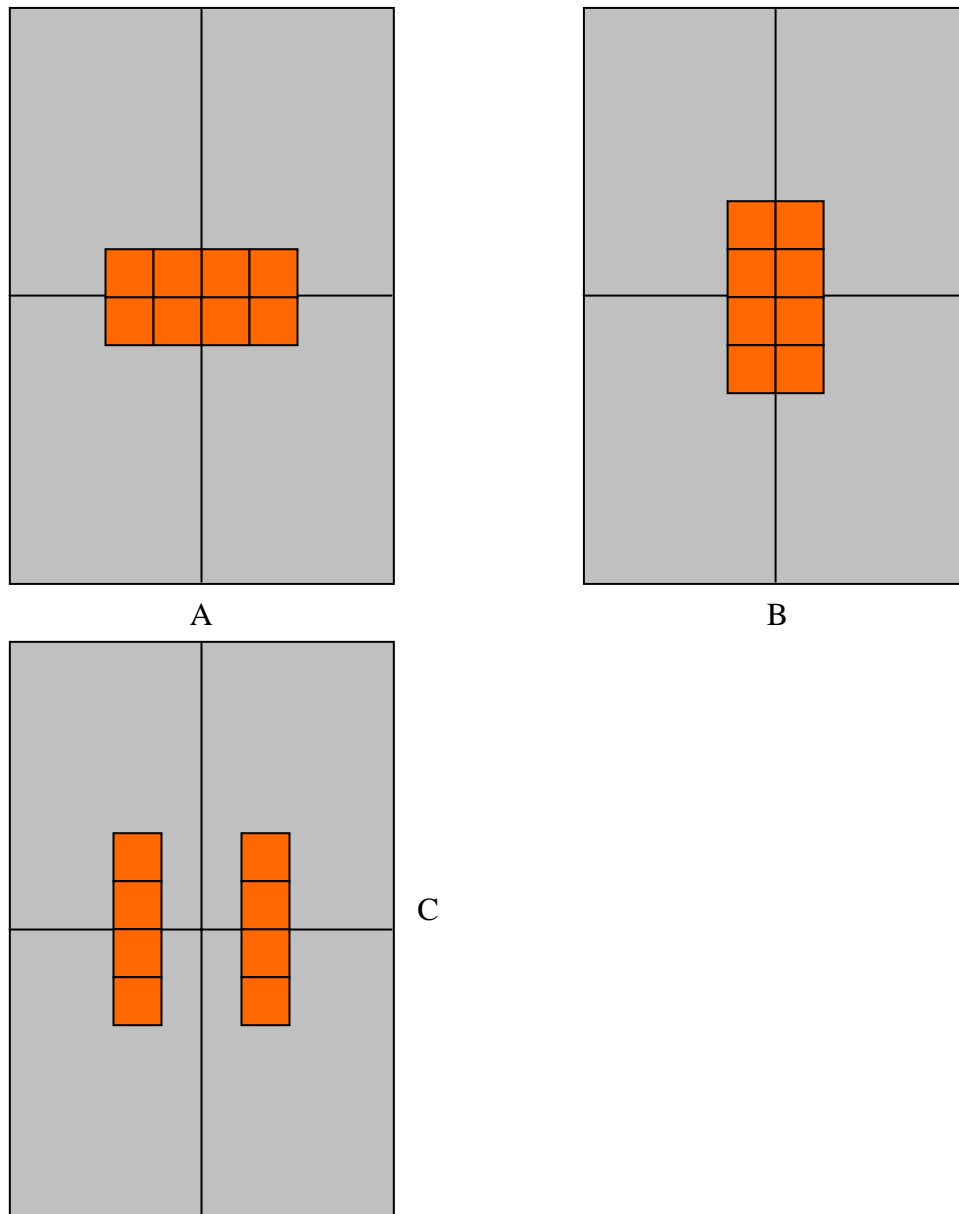


Figure C-1: Different Burner Configurations

Appendix D – Operations and Safety Guide

Volume

1

FIRE TEST FACILITY - ARL BUILDING #11

Operations and Safety Guide

Revision 1.0

FIRE TEST FACILITY - ARL BUILDING #11

Operations and Safety Guide

WPI
Center for Firesafety Studies
100 Institute Road
Worcester, MA 01609
Phone 508.831.5593 • Fax 508.831.5680

Table of Contents

GAS INFORMATION AND SUPPLIER	1
GAS MONITOR / DETECTION	1
TRACK SYSTEM.....	3
ASSEMBLY AND DISASSEMBLY OF TRACK	3
OPERATION OF THE MOTOR.....	3
OVERALL OPERATION OF THE SYSTEM DURING TESTING	4
OPERATORS	4
SAFETY EQUIPMENT	4
VISITORS.....	5
EXITS	5
VAPORIZER (TF-200)	5
OPERATORS	6
OPERATIONS OVERVIEW	6
CONTROL STATION OPERATOR	7
BLOWER & EXHAUST SYSTEM.....	8
SPRINKLER SYSTEM.....	8
DAQ HARDWARE	9
ROOM INSTRUMENTATION.....	9

THE VI INTERFACE	9
APPENDIX E – CHECK LISTS	11
GENERAL INFO.....	12
A: STOP TEST	14
B: SHUTDOWN.....	14

Gas / Fuel Information

The facility uses 400 lbs of liquid propane gas (LPG) and could have up to 800 lbs on site. This is a significant quantity of propane and anyone working in this facility should familiarize themselves with the properties of propane before operating any of the facilities equipment.

Gas Information and Supplier

The Fire Test Facility at ARL is supplied with liquid withdrawal propane tanks from the following supplier:

North East Welding Supply Corp.
31 Sword Street (Auburn Industrial Park)
Auburn, MA 01501
(508) 791-9293

Nitrogen gas is used to purge the propane gas from all the lines as a safety measure. . Approximately 84 CF is used per day and it is recommended to purchase the 115 CF cylinders to prevent the chance of running out of Nitrogen. The Nitrogen supply is received from the same vendor.

Gas Monitor / Detection

The Fire Test Facility has a MSA Ultima Gas Monitor system designed to detect a propane gas leak. It consists of a remote propane sensor, a relay module to provide a local light and horn alarm, and Gas monitor module which will display the propane concentration in percentage of the Lower Explosive Limit (% LEL). If the LEL for a gas was 10% in air and the monitor displayed 50% LEL, then the concentration would be 0.50×0.10 or 5% of the gas in air. It is important to note the gas monitor reading is not the total concentration of the gas in the environment. The system also has an



AC to DC power converter module to provide the necessary 12 Volts DC need to operate the gas monitor and relay modules. .

In addition to the MSA system, a localized hand held gas detector is used in conjunction with soapy water to spot check for leaks with the fittings used in the gas delivery system as well as the burners.

The gas detection system is made up of the following components:

Ultima Power Source – AC to DC Converter	(#815320)
Ultima Relay	(#813703)
Ultima Gas Monitor – Calibrated for Propane	(#H91-702854-010-001)
Ultima Remote Sensor – Calibrated for Propane	
Horn	(Federal 350 – 120V/0.18A)
Alarm	

Experimental Apparatus

Track System

The mannequin travels along a system that is specifically designed for use in this application. This track is a 40 ft. long overhead conveyor system, and consists of a chain, a motor to drive the chain, an enclosure to shield the chain from the heat of the room, and hangers to carry the mannequin and the attached thermocouple wires. The following sections describe the use and maintenance of this tracking system.

Assembly and disassembly of track

During testing, it will be necessary to frequently replace the layers of gypsum wallboard in the Fire Test Facility. Since the track runs along the top of the room, the track needs to be taken down when the wallboard is replaced. To lower the track, all bolts and screws in the track have to be taken out. The track is then lowered slightly to allow room for the insertion of the wallboard.

To lower the track, first remove the third (outer) layer of drywall on the soffits of the room. There will be three holes exposed. Place the 2x4 supports in position with the bolts then place a scrap piece under the track. This allows the bolts that secure the track to be removed. Once all the supporting bolts have been removed one person can lift the track up while the 2x4 spacer is removed. This gives 4 inches of room above the track to reline the room. To replace the track in the test position lift the track up and place the scrap piece under the track to hold it in position while the bolts are being replaced. Remove the braces and store for next time the track needs to be lowered.

Operation of the motor

The track is powered by a 1/3 horsepower AC motor. The electronics for the motor consists of an on/off control and a directional control. The directional control has a forward and backward position. When not running the system, the directional control can be in either position, but the on/off control must be in the off position. To run the system in the forward direction, turn the on/off control to on. Then turn the directional control to the forward position. To stop running the system, the on/off control must simply be turned to off.

To run the system in the opposite direction, the same process as described above must be done, only setting the directional control to backward.

When not in use, the on/off control must not only be in the off position, but the motor must also be unplugged from the outlet. This prevents any accidental running of the system.

Overall operation of the system during testing

The operation of the system is relatively simple. The mannequin is suspended from the hanger. The pole that extends from either side of its head rests in the frame provided by the hanger. The bundle of thermocouple wires, extending from the mannequin, is attached to the wire hangers via hose clamps, and these hangers roll freely behind.

To begin testing, the mannequin must be at the beginning of the track (the end of the 11 ft. piece of track), called the preparation area. The mannequin can be dressed, thermocouple wires attached, and any other preparations made.

The individual operating the system should stand behind the end stand that supports the 9 ft. piece of track (this area is on the opposite end of the track from the preparation area). The motor and its controls are located at this end of the track. The motor controls can then be switched to the forward direction, and then the power turned on. As the mannequin traverses along the track and through the burning room, the operator, along with others present, should observe the system for any problems. Once the mannequin has traveled through the room and approaches the end of the track, the operator should turn off the motor.

The operator should pay full attention to the movement of the mannequin during each test. However, should the operator be unable to stop the mannequin manually when it nears the end of the track, the safety limit-switch will automatically stop the motor. This will ensure that the mannequin does not travel to the end of the track where it will hit the end sprocket, damaging the system. The operator, however, should not depend on this feature, and all efforts should be made to stop the system manually.

To begin a new test, the mannequin must be moved back to the beginning of the track. This can be done by switching the motor setting to reverse and turning the motor on. As with the operation described previously, the mannequin will move to the beginning of the track, and can be stopped manually once there. The free rolling wire hangers, which will have moved due to the previous test will be pushed back to the beginning by the mannequin hanger.

Operators

Only trained individuals are allowed to operate the system. These individuals must have read the operations manual, be well informed of the operation of the system, and be designated by Prof. Jonathan Barnett to operate the system. Only one person is allowed to operate the system at one time.

Safety Equipment

All individuals present at the test site, regardless of whether testing is taking place, must take certain precautions to ensure their safety. All individuals must wear hard hats, safety gloves, safety glasses, and safety shoes at all times when in Building 11. Additionally, when fire tests are being performed, extra precautions must be taken. Safety clothing must be worn by those operating the system, due to the high temperatures present during testing.

Visitors

Visitors of the test site must wear the safety equipment provided at the facility. Additional precautions must also be taken. Visitors will not be allowed to operate any of the systems present at the test site. Also, visitors wishing to view any tests must stand in the designated viewing area at Building 11, behind the mannequin preparation area.

Exits

There are two exits from the facility that are clearly marked. All personnel and visitors should familiarize themselves with these exits before any testing occurs.

Vaporizer (TF-200)

The ThermoFlo vaporizer is designed to vaporize liquid propane. It is a waterbath based, secondary heating design. The coil holding the liquid propane is immersed in a waterbath that is heated via an immersion heater. The heaters and hence the waterbath temperature, are regulated with a programmable controller which constantly displays the actual and setpoint temperature on the face of the control panel. This controller monitors the waterbath temperature via an RTD that is immersed locally in the waterbath.

The control panel also displays status lights for the power, heaters, temperature and two electrical safety devices. These safety devices include a “low water level” switch which insures a minimum water level has been reached. Also, a “high water temperature” switch is pre-set to prevent excessive waterbath temperature. Both of these devices will shut down the system if activated.

Mechanical safety devices include a “liquid carry over float” which prevents liquid propane from exiting the discharge port. The visual “low water level” indicator is an orange ball clearly visible in the site gage when there is adequate water.

A relief valve is set to activate at 250 psi to prevent over pressuring the coil. There is an indicating light that will light if the pressure relief valve activates. Additionally, a temperature gage, which shows the waterbath temperature, is located on the front of the vaporizer.



Technical Specifications for Vaporizer	
Manufacturer	Ely Energy
Type	ThermoFlo Vaporizer
Model	TF 200
Fuel Capacity	120 Gal / hr
Water Capacity	47 gal
Inlet Dimension	¾ in
Outlet Dimension	1 ¼ in
Dry Weight	663 lbs

Operators

There are four persons required to run the facility. These are: Igniter/Fire Operator, 2nd Fire Operator, Fuel Controller, and Safety Officer. The two Fire Operators are responsible for keeping a visual on the fire and to suppress a fire in case of an unexpected event. The Fuel Controller is responsible for running the valves which control the propane throughput. The Safety Officer is responsible for monitoring the fuel tanks for freezing conditions as well as the conditions at the exhaust vent.

All operators should be trained by another experienced operator before running the controls. There are also a set of check list that should be followed for each test which covers the start up phase, the test phase and the shut down phase. Operators should be familiar with the content of this manual in addition to the checklists.

Operations Overview

The heaters are plugged in and turned on, the control panel is turned on and the set point set, then the waterbath heats to the chosen setpoint. The liquid propane is allowed to enter the coil. When the indicator light shows that the vaporizer has reached the setpoint and is ready, the propane is piped into the vaporizer and is heated by the hot water. Thermal energy transfers from the waterbath to the coil, causing the liquid to vaporize. This causes an increase in the propane pressure, which forces some of the liquid back into the bottle. The vapor outlet valve is then opened which allows the propane flow to occur as described below.

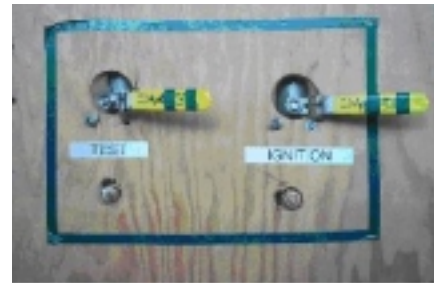
The fuel delivery system is composed of several elements. The fuel source is four 100 lb tanks of liquefied propane gas (LPG) stored in a shed located outside the facility. The four tanks are manifolded together and fed through the wall into the TF200 ThermoFlo Vaporizer. The ¾ in SS hose (silver) connects the propane tank manifold to the vaporizer and the 1 in hose (black) connects the vaporizer to the control station manifold. This manifold separates the propane gas into eight channels corresponding to each burner.

Each one of these eight channels is then split into two sub-channels that have both a needle valve and a ball valve on the front side of the control station. These sub-channels are then rejoined after the valves and connected to the burners. The needle valve on the ignition line is set at minimal flow rate to allow for ignition. This setup allows the operator to safely control the flow while a flame is lit within the room. Once ignition is obtained on all eight burners, the test valve can be used to control the flame during testing.

When testing is complete, the valve is closed and the fire burns out in a few minutes. The control panel and heaters are turned off and the heaters unplugged. The system is nitrogen purged at 20 psi until flameout has occurred on all eight burners. The unit will cool slowly over the next 12 hours.

Control Station Operator

The operator at the control station is responsible for controlling the flow of propane to the burners. During the ignition phase the operator will only open the valves labeled “ignition” until the flames have been established on all eight burners. Once this occurs, the valves label “test” can be opened in any sequence as the current test may prescribe. . In the case of an problem or unexpected event all 8 “test” valves should be turned off and the system should be shutdown normally if possible. Follow the shutdown procedure listed in the checklist.



Blower & Exhaust System

The system is comprised of two 10 ft square exhaust hoods located above each door of the test room. The ductwork for the ventilation system is all 24 gauge and is 16 in diameter from the hood to the union and 22 in diameter from the union to the blower.

The ventilation system is powered by a Buffalo Forge centrifugal blower which is on loan from ARL. This blower has five power settings that are: closed, 25%, 50%, 75%, and fully open. These settings correspond to the position of the exit vents of the centrifugal blower. The complete specifications for the blower are listed in the table to right.

Technical Specifications for Blower	
Manufacturer	Buffalo Forge Company
Type	Centrifugal Blower
Model	Westinghouse Lifeline T
Horse Power	15
Volts	230/460, 3 Ph
Amps	38.6/19.3
RPM	1170
Frame	284T

During the initial warm up phase the blower can be set to 50%, however during a test the setting must be at the 75% open setting to get the required flow setting within the ductwork. The blower should always be closed when turning the power of the blower on or off. Thus to start the blower, make sure the valve is closed, then operate the power button. Once the blower starts up, the valve can be slowly open to the desired setting. Shutdown is the same procedure. Slowly close the valve and once it is fully closed, the power off button can be depressed.

Partial Sprinkler System

As an added precaution a simple partial sprinkler system was design to work as part of the apparatus. The system consists of seven sprinkler heads located directly above the test room. The sprinklers are Standard Response 160°F (k=5.65) Brass upright sprinklers, Firematic Model "U". The system also includes a 2" Model C-700 Positive Displacement flow meter by ABB.

The sprinkler system should be charged every morning and drained every night when freezing is expected. To charge the system, make sure all valves are closed, and then turn the master ball valve to the on position. You will hear the rush of water filling the system and it will take a couple of minutes for the system to fully charge and stabilize. At the end of the day, after the vaporizer has been shut down, the sprinkler system should be discharged. To do this, place the garden hose outside by the drain and close the master ball valve. Then open the garden hose valve and let the system drain. Once the system is complete drained, close the hose valve and coil up the hose.

If the system is going to be shutdown during cold weather for an extended period of time, then the system will have to be completely drained. There is a control valve located outside the facility in the center of a 4 foot diameter pipe. The ball valve must be turned

to the off position (slot parallel to building #11) and then the valve located next to the water meter (in the pit) must be opened and the system allowed to drain.

Instrumentation

DAQ Hardware

The Data Acquisition (DAQ) hardware if from National Instruments and the components are listed below:

- Qty. (1) SCXI-1000 4-slot chassis (Donated)
- Qty. (1) SCXI-1200 12 Bit DAQ Module (#776783-00)
- Qty. (2) SCXI-1102C 32-channel amplifier (#776572-02C)
- Qty. (2) SCXI-1303 32-channel isothermal terminal blocks (#777687-03)
- Qty. (1) SCXI-1100 32-channel amplifier (Donated – Not in use)
- Qty. (1) SCXI-1200 12 Bit DAQ Module (Donated – Not in use)
- Qty. (1) 19” Jack Panel w/ 40 Type K Female Jacks (#19UJP-4-40-K)
- 20 Gauge Shield Thermocouple Wire (#EXPP-K-20-TWSH)

Room Instrumentation

- Qty. (4) Thin-skin calorimeters
- Qty (2) 8’ Temperature Rake (1 in. black steel pipe)
- Type K Insulated Thermocouple Wire (HH-K-24)

The VI Interface

The VI was designed to monitor the room conditions. A separate VI and DAQ system will be used for the mannequin testing and will be provided with the mannequin when testing is underway. The interface for this VI (see Figure below) is set up to allow the user to partition the data file with any comments they wish. This allows for continuous testing to be conducted with out interruption in data. The user can type any comments or notes they wish then press the on/off button in the “Data File” section of the VI and that info will be transcribed into the data file as a marker. The other information is for visual determining the conditions within the room. The alarm LEDs are used to visual represent the outer room temperature and to notify the user when the temperature is approaching the limit for the sprinkler system.

ARL Fire Test Facility

Temperatures

Ceiling Temp. Degree C
Room Temp. Degree C
Ambient Temp. Degree C

Data File

Section Notes

Controls

Power Switch

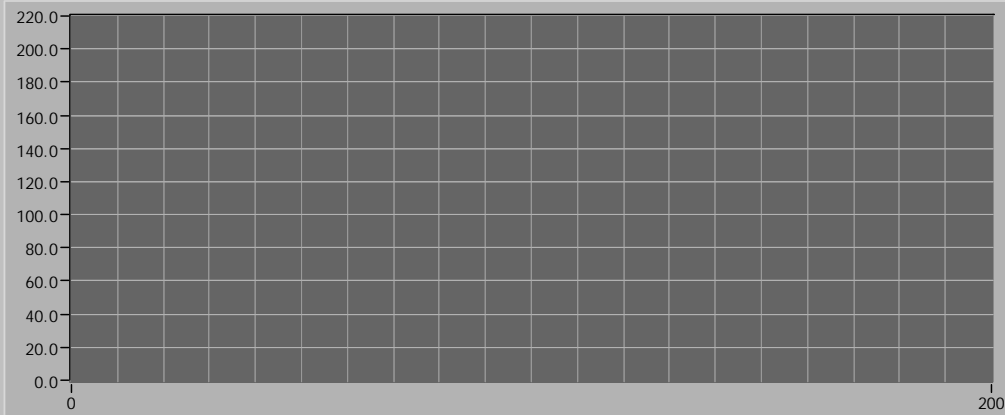
Time

Ceiling Alarm

2nd Alarm

Heat Flux Graph

kW/m²



Appendix E – Check Lists

General Info

Date: _____ Time: _____

Weather: _____

Evening Temp _____

Test Goals: _____

People

Supervisor: _____

Operator(s): _____

Guest/Others: _____

Warm - Up

- Clean combustibles from around test room
All loose paper should be swept up to prevent any fuel from being blown into the room and ignited.
- Check to see if radios are function properly
The three hand radios should be set to the correct channel and testes before any fires are lit.

Pre - Test

- Hook up burners
- Open Overhang Door(s)
- Turn on Fan ($\frac{3}{4}$ mark)
- Turn on water & lay out hose
- Call ADT at (888) 238-2666
Account # (508) 831-5967
Put system on "Test Mode"
- Make sure test room doors open easily
- Ultima Gas Sensor Reading
_____ % LEF
- Leak check @ 30 psi with nitrogen (through Vaporizer)
· Open one at a time: A1, A2, A3 and A4.
· Leak check from bottles to valve B
· Open valves B and C; leak check to controls
· If no leaks, close A1-A4, B, & C
- Run nitrogen through release line
· Open valve A5
· Check flapper, and if opens, close A5
· Check that release light has activated & reset
- Insure heater works before filling Vaporizer with liquid
· Turn on vaporizer control panel. If heater light comes on, then turn off control panel.
· If it doesn't work, then determine problem before continuing.
- Insure liquid inlet valve B and vapor outlet valve C are closed, As well as nitrogen feeds (valves A1-A4)
- Crack one propane bottle and leak check using snoop, nose and gas monitor.
· If no leaks, open fully and leak check.
· If no leaks are detected, proceed to open the three additional propane bottles.
- Open liquid inlet B **SLOWLY** and leave open unless a leak is detected. (**You will hear liquid propane filling the Vaporizer**)
- ** Valve B MUST REMAIN OPEN during the heat up phase ****
- Turn on control panel and adjust set point

- Allow Vaporizer to heat up to set point. · Use gas monitor to leak check while waiting.
 - Keep an eye on temperature also.
 - When both “low water level” and “high water temperature” lights are on and set point is reached, you are ready to test

Test

- Insure ignition source is at burner and burner is at test location.
- Open burner control valve RED 2 – IGNITION, and wait 15-30 second for propane to reach burner. After ignition, open RED 1 – IGNITION and wait for burner to ignite. Proceed through BLUE; GREEN and YELLOW in the same manner. Open only one IGNITION valve at a time.
- Run test

If further tests will be run right away, go to **A: Stop Test**
If done for day, go to **B: Shutdown**

A: Stop Test

- Close all TEST valves (RED, BLUE, GREEN and YELLOW), leaving only the IGNITION valves open to maintain the fire source.

To run another test, go back to **Test**

B: Shutdown

- Close all four propane bottles and let fire burn down
- Purge Vaporizer
 - Make sure ignition source is at burners then open nitrogen at 5 psi. Open valves A1, A2, A3 and A4. Fire size will jump up then proceed to die out. After fire has extinguished, wait 30 second then turn off nitrogen.
 - Close valves A1, A2, A3, and A4

Post - Test

- Shut off heater (by lowering temperature to 30.0 °C)
- Shutoff control panel
- Indicate bottle amount
- Close inlet valve B
- Check visual water gage
- Close outlet valve C
- Close all “Test” valves on control panel
- Insure all bottles are closed
- Turn off hood
- Close propane shed and lock gate
- Call ADT at (888) 238-2666
Account # (508) 831-5967
Take system off “Test Mode”

**** Insure all valves are closed! ****

Post – Test (Winter Complete Shutdown)

- Lay hose to drain outside,
Close water main ball valve
Open hose valve to let system drain.

- After draining, close hose valve
- Recoil hose hang and the hose hook
- Open water pit cover and open valve at base of pit. (It is located just in front of the water meter) and let the remainder of the system drain.
- Close pit water valve
- Close and re-insulated the pit cover
- Close main valve